AIAA

MISSILE SCIENCES CONFERENCE

MONTEREY, CALIFORNIA

29 NOVEMBER - 1 DECEMBER 1988

# VOLUME 10

# NAVY BALLISTIC MISSILE TECHNOLOGY

PAPERS PRESENTED AT SESSION 10

THURSDAY - 1 DECEMBER 1988

# AIAA

# MISSILE SCIENCES CONFERENCE

# MONTEREY, CALIFORNIA

## 29 NOVEMBER - 1 DECEMBER 1988

## VOLUME 10

## NAVY BALLISTIC MISSILE TECHNOLOGY

PAPERS PRESENTED AT SESSION 10

THURSDAY - 1 DECEMBER 1988

Chairman: CAPT John T. Mitchell (USN), SSP

Vice Chairman: Robert Ginn, LMSC

Five papers were submitted for inclusion in Volume 10: All presentation titles and the authors are listed below along with their phone number. A check in the margin denotes that a paper is included in this volume.

✓ TARGET NON-HOMOGENEITY AND EFFECT ON EPW DESIGN


William J. Patterson
Sandia National Laboratories
Penetrator Weapon Development Division
P. O. Box 5800
Albuquerque, NM 87185
Phone: (505) 844-6915

C. Wayne Young
Sandia National Laboratories
9122 - Advanced Projects Division II
P. O. Box 5800
Albuquerque, NM 87185
Phone: (505) 844-4842


✓ ANALYTICAL ESTIMATION OF TRANSIENT STRUCTURAL RESPONSE OF EARTH PENETRATING WEAPONS


Robert J. Kipp
Sandia National Laboratories
Applied Mechanics Division II
P. O. Box 5800
Albuquerque, NM 87185
Phone: (505) 846-3602


✓ EXPERIMENTAL EARTH PENETRATOR RESPONSE DATA ANALYSIS FOR APPLIED FORCE ESTIMATION


Vesta Batemen
Sandia National Laboratories
7542 - Vibration Testing Division
P. O. Box 3800
Albuquerque, NM 87185
Phone: (505) 844-8704




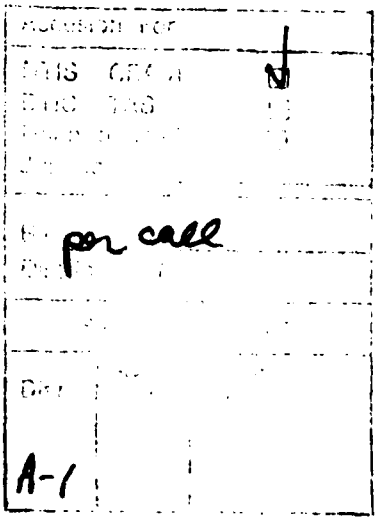

WEIGHT OPTIMIZATION OF EARTH PENETRATING WEAPONS

Ned R. Hansen and Kevin R. Eklund
Sandia National Laboratories
5165 Penetrator Weapon Development Div.
P. O. Box 5800
Albuquerque, NM 87185
Phone: (505) 844-8891
(505) 844-8892

ATTACKING STRATEGIC RELOCATABLE TARGETS:
AN ARTIFICIAL INTELLIGENCE APPROACH

H. W. Egdorf
Los Alamos National Laboratory
Los Alamos, NM 87545
Phone: (505) 667-1087

LTC John Denelsbeck, SACLO
Los Alamos National Laboratory, MS F631
Los Alamos, NM 87545
Phone: (505) 667-3510

SLBM PENETRATION CONCEPT STUDY

Drs. Alfred M. Morrison and Ronald S. Brunsvold
Naval Surface WarfARE Center - K201
Silver Spring, MD 20903-5000
Phone: (202) 394-3894
(202) 394-2082

STRATEGIC MISSILE DESIGN IN RESPONSE TO A
FLIGHT TEST BAN

Bob Dietz
Lockheed Missiles & Space Co., Inc.
Advanced Concepts - 0/81-71, Bldg. 157
P. O. Box 3504
Sunnyvale, CA 94088-3504
Phone: (408) 756-1909

# TARGET NONHOMOGENEITY AND EFFECT ON EPW

C. W. YOUNG

W. J. PATTERSON

NOVEMBER 1988

SANDIA NATIONAL LABORATORIES
ALBUQUERQUE, NM

## Target Nonhomogeneity and Effect on EPW

Most calculations of EPW penetration performance and structural survivability are made using a material model which assumes a homogeneous target. For some calculations that assumption is reasonable, but for many calculations it is unacceptable. Target nonhomogeneity is difficult to handle analytically. An approximate method to account for target nonhomogeneity on EPW lateral and axial loading has been developed.

## EPW Design Considerations

The purpose of the first few slides is to bring the effect of target nonhomogeneity into perspective by briefly considering some of the other factors affecting an EPW design.

Payload - The primary consideration of any EPW is the payload. Nuclear vs. conventional, the size constraints, weight, resistance to shock loads, etc.

There are also delivery system constraints, such as overall weapon weight, length, diameter, cg, etc. Compromises can be made, but in the end, a weapon is only useful when it can be delivered to the target.

The impact conditions are usually more critical to an EPW design than other weapons.

And finally, the target considerations which are covered in the next slide.

# EPW DESIGN CONSIDERATIONS

- PAYLOAD

  NUCLEAR VS. CONVENTIONAL, SIZE, ETC.

- DELIVERY SYSTEM CONSTRAINTS

  WEIGHT, DIAMETER, LENGTH, C.G.

- IMPACT CONDITIONS

  VELOCITY, ANGLE OF ATTACK (AOA), IMPACT ANGLE

- TARGET CONDITIONS

## Typical Target Descriptions

The target set is very important for an EPW. Are the targets point or area targets? How many? Are they well characterized? A detailed description of soil is not necessary for an EPW designed for deep penetration into a variety of geologic materials. Target materials, layering, type, strength, water content, density, and whether it is frozen are usually known.

For concrete, the strength, thickness, and existence of rebar are usually known. Only occasionally will there be information on lateral boundary conditions.

For rock the information usually given is the rock type (granite, basalt, limestone, etc), its strength, density, and perhaps water content. What is really needed is information on weathering, cracks, fissures, bedding planes, etc. These are the things which cause nonhomogeneities, and are the subject of this presentation.

# TYPICAL TARGET DESCRIPTION

- TARGET SET
  POINT OR AREA TARGETS? NUMBER?
  WELL CHARACTERIZED?
- SOIL - DETAILED DESCRIPTION NOT USUALLY NECESSARY
  LAYERING, TYPE, STRENGTH, WATER CONTENT, DENSITY, FROZEN, ETC.
- CONCRETE
  STRENGTH, REBAR, THICKNESS, BOUNDARY CONDITIONS
- ROCK
  - GIVEN
    TYPE, STRENGTH, DENSITY, WATER CONTENT
  - NEEDED
    WEATHERING, CRACKS, FISSURES, BEDDING PLANES, ETC.

## Evaluate Effect of Assuming Homogeneity in Typical Targets

This vugraph addresses the effect of assuming homogeneity in typical EPW targets.

We can usually handle soil nonhomogeneity analytically. In the vertical direction there are soil layers, varying in penetrability by at least a factor of two, but we have material models for this. Even though there are similar variations in penetrability laterally, the variations are gradual and do not cause significant lateral loads.

# EVALUATE EFFECT OF ASSUMING HOMOGENEITY TYPICAL ANALYSIS

## SOIL

- AXIAL - CAN BE HANDLED ANALYTICALLY
- LATERAL LOADING - NO SIGNIFICANT EFFECT

## CONCRETE

- AS AN ENGINEERING MATERIAL
  - * EFFECTS OF REBAR, AGGREGATE, STRENGTH VS. THICKNESS VARIATIONS - RELATIVELY UNIMPORTANT
- AS A TARGET
  - * EDGE EFFECTS - MAJOR IMPORTANCE TO LATERAL AND AXIAL LOADS
  - * SOIL OVER OR UNDER - SECONDARY IMPORTANCE
  - * RUBBLE - IMPORTANT TO LATERAL LOADS

## ROCK - PROPERTIES TAKEN FROM INTACT SAMPLES

- * AXIAL LOADS - CONSERVATIVE APPROACH
- * LATERAL LOADS - VERY NON-CONSERVATIVE

Ft. Riley Road Cut

This slide shows a road cut near Ft. Riley, Kansas. A general geologic description of this area reads something like "limestone, alternating layers of shale, little or no soil overburden, 5 m to water table". It would not be unreasonable to estimate the limestone strength as 8000 psi UNC strength. After drilling and coring this area, the rock strength was found to be 4000 psi to 5000 psi UNC. The problem we face is how to calculate the loads on a penetrator passing through materials like this with layers, voids, cracks, fissures, etc, in all directions.

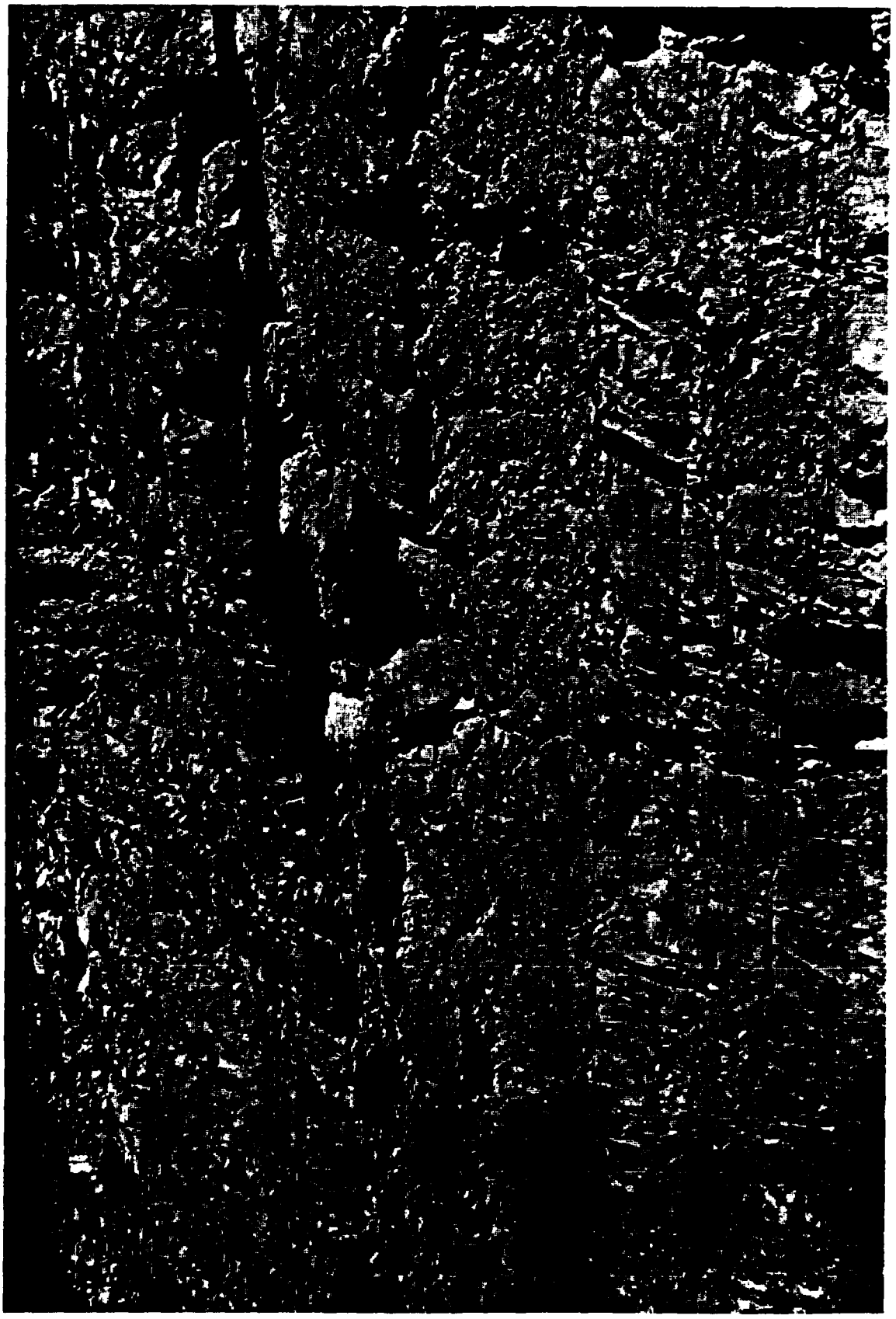

## Data Base

Sandia National Laboratories has an extensive data base of penetration into most earth materials, including rock. Our formal or documented data base includes over 800 selected data points. We have data from over 3000 full scale penetration tests into natural earth and concrete targets, but for various reasons many of these are not included in the data base. There were many duplications, particularly when the data came from demonstration or verification tests of a specific penetrating weapon system. In other cases the test data or target data was incomplete.

The data base was searched for (1) rock, (2) no angle of attack, and (3) normal impact.

Fifty-one tests were found meeting these criteria. If the targets were truly uniform or homogeneous, there should have been no lateral loads on these penetrators. In fact, 21 of these penetrators were bent or broken due to lateral loading. It should be pointed out that our data base is rather strongly biased towards homogeneous targets. Many months were spent looking for the most competent and uniform targets possible.

The obvious conclusion is that if 40% of the EPW's tested in rock have been damaged due to target nonhomogeneity, we must have a method of analysis to include this effect.

# DATA BASE

D-BASE III: OVER 800 SELECTED DATA POINTS

- SEARCHED FOR
  - * ROCK
  - * NO ANGLE OF ATTACK
  - * NORMAL IMPACT
- LOCATED 51 TESTS
  - * THESE SHOULD HAVE HAD NO LATERAL LOADING
  - * 21 OF THESE WERE BENT DUE TO LATERAL LOADING
- CONCLUSION
  - * 40% OF OUR EPW'S ARE DAMAGED DUE TO TARGET NONHOMOGENEITY
  - * METHOD OF ANALYSIS IS NEEDED

## Approaches to Solving Rock Nonhomogeneity Problem

Modeling the target and running a 3 dimensional finite element or finite difference code is one rather obvious method. However, even for homogeneous materials the elastic-plastic models of rock require more work. Also, the randomness of cracks, fissures, etc, make this approach impractical. The effects will vary from insignificant to catastrophic, and it appears to be impractical to guess or estimate what can be considered a typical lateral and vertical profile of these nonhomogeneities.

We chose a quasi empirical method, based on the data base. We know how to calculate loading due to angle of attack, so our approach was to determine an equivalent angle of attack to quantitatively match the effect of nonhomogeneity.

## APPROACHES TO SOLVING ROCK NONHOMOGENEITY PROBLEM

- MODELING
  - * ELASTIC-PLASTIC MODELS OF ROCK REQUIRE MORE WORK
  - * RANDOMNESS OF CRACKS, FISSURES, ETC., MAKES THIS APPROACH IMPRACTICAL
- QUASI EMPIRICAL (BASED ON DATA BASE)
  - * SINCE WE CAN CALCULATE LOADING DUE TO ANGLE OF ATTACK, DETERMINE AN EQUIVALENT ANGLE OF ATTACK TO QUANTITATIVELY MATCH THE EFFECTS OF NONHOMOGENEITY

Combined Effects of AOA and Impact Angle

This slide shows the combined effects of angle of attack and impact angle on lateral acceleration of the penetrator, for different impact velocities. Also shown are the zones where there is no penetrator structural damage, damage, or complete failure. This is for a typical penetrator configuration into rock at a 60° impact angle. We can make a curve of this type for any penetrator configuration and impact angle. This curve is shown only to demonstrate the calculational method in which the equivalent angle of attack is used.

# EXAMPLE OF COMBINED EFFECTS OF AOA AND IMPACT ANGLE

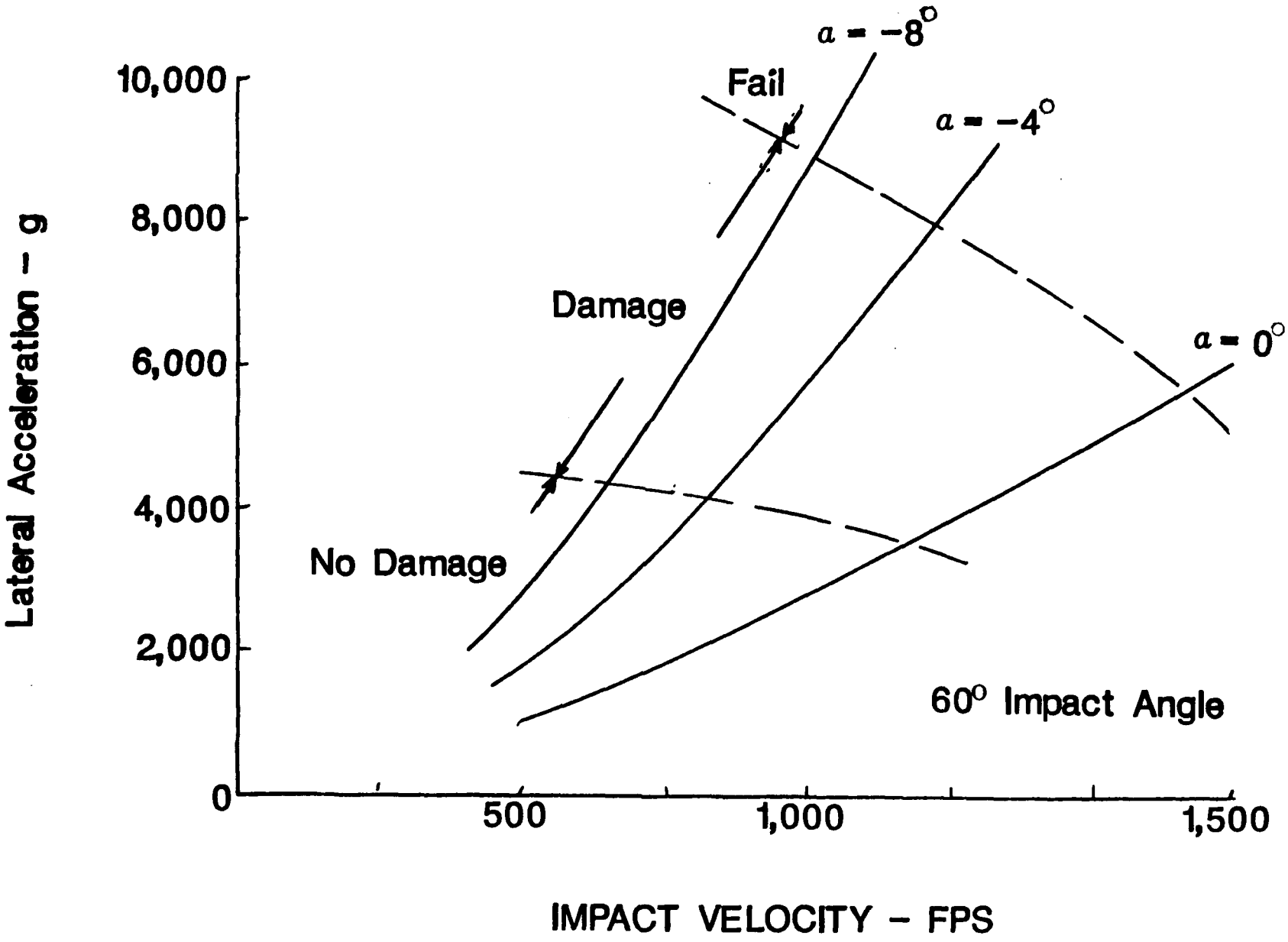

## Determination of Equivalent AOA

Using SAMPLL code, we determined the AOA necessary to damage each of the 21 penetrators damaged during rock penetration tests. Recall that these were normal impacts with no known angle of attack. For each data point the angle of attack was increased until the correct amount of damage would be predicted by the code.

Even though there was a large amount of data scatter, the typical equivalent AOA was found to be 4°. It should be remembered that our data base is biased.

In addition to using the damage criteria to determine an equivalent AOA, data on the trajectory during rock penetration was also used. The equivalent AOA was used in SAMPLL to calculate the final rest position and angle, which was then compared to the measured data. Reasonably good correlation was found, but there were too few data points to consider this as specific verification of the analytical method.

The effects of nonhomogeneity are very random, as one would expect.

# DETERMINATION OF EQUIVALENT AOA

- USING SAMPLL CODE, DETERMINE AOA NECESSARY TO DAMAGE ROCK PENETRATORS AS NOTED IN OUR DATA BASE
- THE TYPICAL EQUIVALENT AOA WAS DETERMINED TO BE 4°
- BASED ON TRAJECTORY DATA IN ROCK, IT WAS ALSO NOTED THAT
  - THE EQUIVALENT AOA CONCEPT APPEARS REASONABLE
  - THE AFFECTS OF NONHOMOGENEITY ARE INDEED VERY RANDOM

## Assumptions for a "Worst Case" Analysis

This slide considers ways to use the equivalent AOA concept in the design of earth penetrators. Remember that there are usually constraints on the overall penetrator weight, length, etc, but we can start with a "worst case" analysis to see if the penetrator will survive. Use the worst case impact angle. Assume the AOA is additive to the impact angle. Assume the equivalent AOA (for target nonhomogeneity) to also be additive. Use the SAMPLL code to calculate the lateral g-level and penetrator survivability.

There will be two possible conclusions from this analysis. First, if the EPW can survive with these assumptions, the the design will be adequate for most impact and target conditions. The word "most" is used because the equivalent AOA is for typical nonhomogeneities, not worst case. We do not have enough data to select an equivalent AOA for 2 sigma or 3 sigma conditions. In practice, there will always be some number of cases of nonhomogeneities that can damage any reasonable penetrator design.

The second, and most likely , conclusion will be that the design is not adequate for the above assumptions, leading to a statistical analysis. That is, even though you cannot survive all possible combinations of impact and target conditions, you design the penetrator to be as rugged as possible and then evaluate its probability of survival.

# ASSUMPTIONS FOR A "WORST CASE" ANALYSIS

- USE WORST CASE IMPACT ANGLE
- ASSUME AOA IS ADDITIVE EFFECT TO IMPACT ANGLE
- ASSUME EQUIVALENT AOA (NONHOMOGENEITY) TO ALSO BE ADDITIVE

## POSSIBLE CONCLUSIONS

1. IF YOU CAN SURVIVE ABOVE ASSUMPTIONS, THE DESIGN IS ADEQUATE FOR MOST CONDITIONS
2. IF THE DESIGN IS NOT ADEQUATE FOR THE ABOVE ASSUMPTIONS, A STATISTICAL ANALYSIS WILL BE NECESSARY

## Statistically Based Design

Rather than use the worst case assumptions, use realistic values for variations of each input parameter. For example, a wind induced angle of attack will usually be random in direction, which should be used in the analysis. Also, target nonhomogeneities are random in direction. In this type of analysis we are considering that the two types of AOA may either be additive, or may tend to cancel each other out. Likewise, the adverse effect of impact angle may be offset by the angle of attack.

This is also the place to consider variations in the target penetrability. There are two types of variations to include in the analysis. If the target is an area target we have to estimate the variability in penetrability of each target layer, and the thickness of each layer, over the areal extent of the target. Secondly, we should place values on the accuracy of the data which led to the estimate of penetrability and layer thickness.

Calculate the probability for a successful penetration for each target on the target list.

Select the number of weapons required to give the desired kill probability. This type analysis is of more use to the weaponeer, even though it can be useful as a design tool also.

# STATISTICALLY BASED DESIGN

- USE REALISTIC VALUES FOR VARIATION OF EACH INPUT PARAMETER
- CALCULATE $P_K$ FOR EACH TARGET
- SELECT NUMBER OF WEAPONS REQUIRED TO GIVE DESIRED $P_K$

NOTE: THIS TYPE ANALYSIS IS OF MORE USE TO THE WEAPONEER, EVEN THOUGH IT CAN BE USEFUL AS A DESIGN TOOL

V-Gamma Plot, Weathered Rock

This slide gives a specific example of how we use some of the concepts that have been discussed to design a strategic penetrator. The penetrator weighs about 1,000 lbs, with a body diameter of about 12 inches. The target set includes soil, concrete, weathered rock, and frozen soil.

This first slide shows what combinations of impact velocity and impact angle will lead to a successful penetration into a weathered or low strength rock. This is not a statistically based analysis. A 2° angle of attack was assumed to be additive to the impact angle. The effects of target nonhomogeneity on axial penetration is automatically included in the value for penetrability. The solid line outlines the window of impact conditions which should lead to a successful penetration. Using only the solid line it would appear that in this rather soft target the penetrator is considerably stronger than necessary. However, looking at the dashed line we see a smaller operational window. The dashed line is for the same rock, but with an added 4° angle of attack for nonhomogeneity. The dashed line is a much more realistic description of the target and acceptable impact conditions.

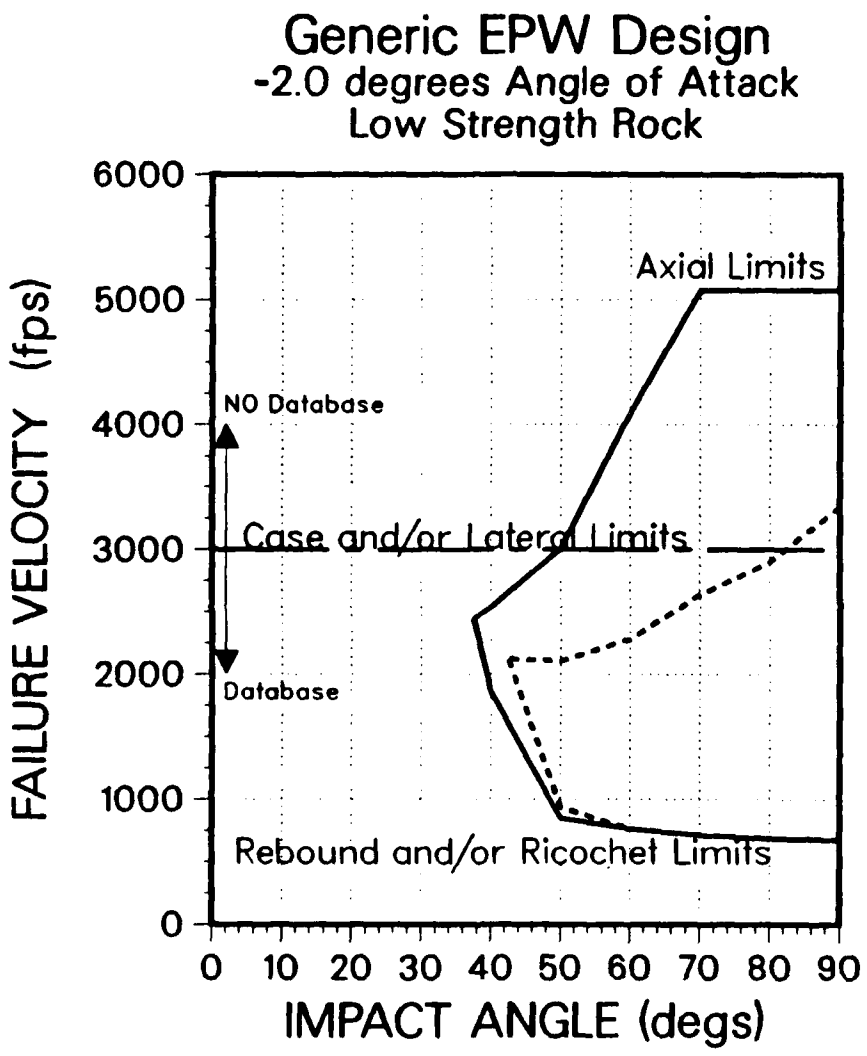
Generic EPW Design
-2.0 degrees Angle of Attack
Low Strength Rock
FAILURE VELOCITY (fps)
6000
5000
4000
3000
2000
1000
0
Axial Limits
NO Database
Case and/or Lateral Limits
Database
Rebound and/or Ricochet Limits
0 10 20 30 40 50 60 70 80 90
IMPACT ANGLE (degs)

V-Gamma Plot, Medium Strength Rock

This slide is the same as the last one, except the target is medium strength rock (about 10 000 psi UNC). The solid line outlines the acceptable impact conditions, without considering nonhomogeneity. It is this line that may lead people to conclude that the penetrator is overdesigned, and that the overall penetrator weight could be reduced. The dashed line shows a much smaller, and more realistic, operational window. The debate as to how much weight can be removed from the penetrator case continues, but we recognize that the statistical approach must now be applied. This curve shows that the probability exists that a lighter penetrator will encounter unacceptable target conditions.

In conclusion, our method of including target nonhomogeneity in the analyses is approximate, but it does match the data base. Using this method does not guarantee that a penetrator design will handle all target nonhomogeneities, but it will increase confidence in the penetrator designs.

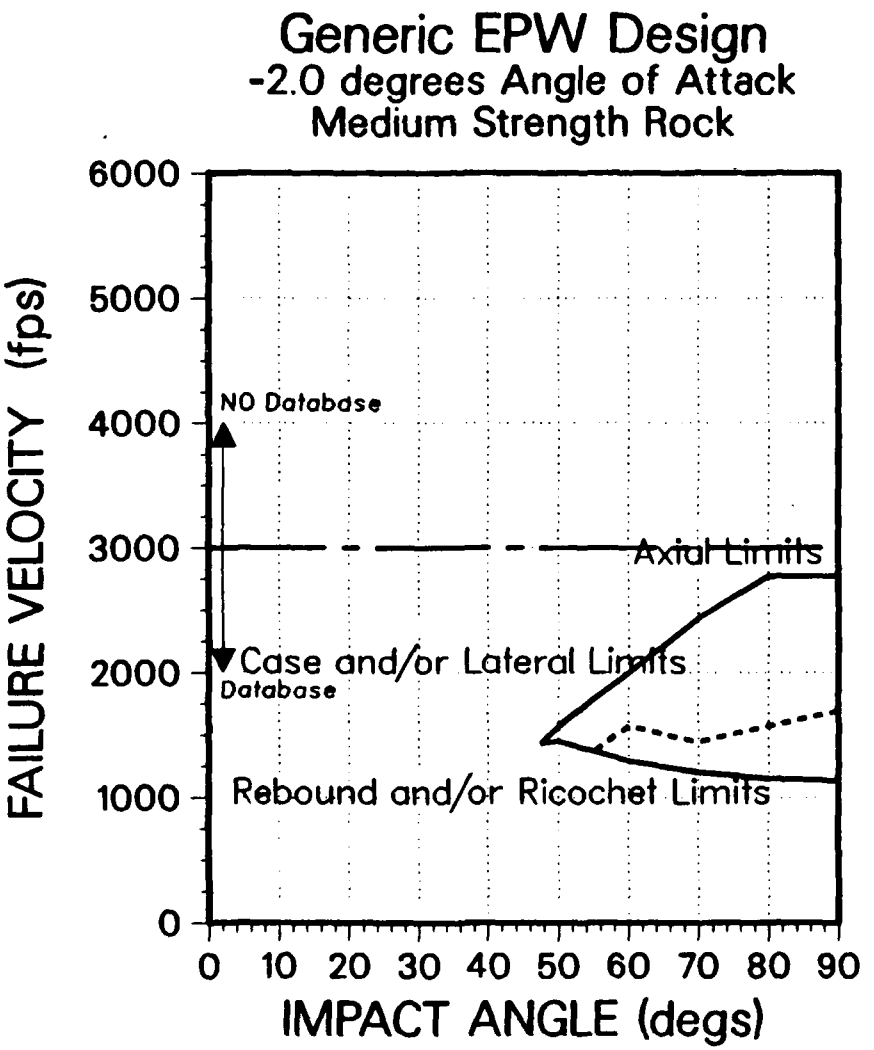
Generic EPW Design
-2.0 degrees Angle of Attack
Medium Strength Rock
FAILURE VELOCITY (fps)
6000
5000
4000
3000
2000
1000
0
NO Database
Axial Limits
Case and/or Lateral Limits
Database
Rebound and/or Ricochet Limits
0 10 20 30 40 50 60 70 80 90
IMPACT ANGLE (degs)

SAND88 1634A

To be presented at AIAA Missile Systems Missile Sciences Conference.
Monterey, CA November 28 - December 1, 1988

# Analytical Estimation of Transient Structural Response of Earth Penetrating Weapons and Comparison with Laboratory and Field Test Data

Robert J. Kipp
Applied Mechanics Division II

Sandia National Laboratories
Albuquerque, New Mexico

Applications of analytical techniques for predicting response of Earth Penetrator Weapons (EPWs) during severe penetration events include evaluating EPW capabilities and determining the desirability or feasibility of design modifications. Analysis can also enable a "balanced design" to be achieved, which is an EPW design where no structure or component has significantly less capability to survive prospective penetration events than other structures or components of the penetrator. To be useful in these applications, the analytical technique should be able to determine stresses in the EPW case as well as the shock environment at locations of components which must survive the penetration event. An analytical technique is being used at Sandia that utilizes cavity expansion load models to determine time- and spacially- dependent axial and lateral forces on a rigid body penetrator that are then applied to a detailed structural model of the EPW. Case stresses and component shock environments are thus estimated for various penetration target and event parameters.

Transient lateral load-induced phenomena, such as component lateral accelerations and case bending stresses, are extremely important in the determination of EPW capability and yet are very difficult to characterize and quantify. Recently, data systems have become available which are enabling the simultaneous acquisition of axial and lateral accelerations and case strains during actual penetration events with a high degree of dependability. This now allows meaningful comparisons with analytical predictions of structural response, including lateral load-induced phenomena. The accuracy of the structural models can be verified independent of the penetration load uncertainty through comparison with data from laboratory modal and shock tests that have been performed on field test configuration penetrator units. The internal structures included in these units are rather complex and significantly affect the response of the penetrator to time-dependent loads.

This paper discusses the the analytical technique used in penetration analysis, presents results that have been useful in determining EPW capability and achieving a balanced design, and discusses efforts to reconcile the analytical response predictions with available laboratory and field test data.

# ANALYTICAL ESTIMATION OF TRANSIENT STRUCTURAL RESPONSE OF EARTH PENETRATING WEAPONS AND COMPARISON WITH LABORATORY AND FIELD TEST DATA

Robert J. Kipp
Applied Mechanics Division II

Sandia National Laboratories
Albuquerque, New Mexico

Annotations for enclosed view foils (as numbered):

1. Title. This presentation discusses several topics: 1. a methodology by which transient structural response of an earth penetrating weapon (EPW) is calculated; 2. an application of this methodology in which the structural capability of an EPW was determined, and a corresponding worst-case component environment analytically defined; 3. efforts to validate the accuracy of the analytical technique; and 4. some insights regarding earth penetration phenomena gleaned from analyses and testing.

2. Illustrates methodology of earth penetrator analytical technique. Axial and lateral force-time histories are obtained from cavity expansion load models assuming a rigid penetrator (top). These are applied to a structural model of penetrator (bottom). Shell, solid, beam, and lumped mass elements are used to model the case and internals. The lateral forces are modeled as acting at discrete locations along the penetrator.

3. Examples of target material models used in cavity expansion code GNOME to predict loads during penetration. The target material is assumed to be either spherically expanding or radially (cylindrically) expanding away from the invading surface. These kinematic assumptions permit calculation of the penetrator/target interaction without the need to discretize the target into finite elements. Bottom part of foil illustrates available constitutive models for target material.

4. Comparison of analytical predictions of axial deceleration in the component region (aft end) of the penetrator assuming it is a rigid body (dash) and a flexible structure (solid) for an impact of 1500 fps into Sidewinder tuff (a moderate strength rock).

5. Comparison of analytical predictions of lateral acceleration in the warhead region (mid-station) of the penetrator assuming it is a rigid body (dash) and a flexible structure (solid) for an impact of 1500 fps, +2 degree angle of attack, 20 degree from vertical angle of impact, into Sidewinder tuff.

6. Same as 5 but for component region. Compare with 5 to show variation of lateral acceleration with longitudinal location. Note also the lateral acceleration values are significantly higher than axial for this event.

7. Same as 6 but for +4 degree angle of attack instead of +2. Compare with 6 to show high degree of sensitivity of lateral acceleration to angle of attack.

8. Structural model of baseline penetrator WR design. Structural effects of internals have been included in case elements. The weak spot is the

analytically determined region of highest stress in the case for a class of penetration events. The case is thin and the internals are not stiff at this location.

9. Magnitude of analytically predicted maximum total stress at the weak spot in baseline design weapon case for a penetration event of 1500 fps, +2 degree angle of attack, 20 degree from vertical angle of impact. The total stress includes axial and bending stress. The maximum value is near the 200 ksi yield strenth of the case material. Permanent deformation of the case is not predicted for this event.

10. Same as 9 but for +4 degree angle of attack instead of +2. The maximum stress value predicted by the linear elastic structural model far exceeds the yield of the material, and permanent deformation of the case is indicated for this penetration event. Compare with 9 to envelope predicted structural capability of baseline design.

11. Analytically predicted lateral shock spectra in component region for events discussed in 9 and 10. Result of this effort was to analytically determine structural capability of penetrator case and then make initial analytical specification of worst-case component shock environments.

12. Analytically predicted axial shock spectra in component region for same penetration events. Compare with 11 to show lateral shock environment is much more rigorous than axial.

13. Illustration of field test configuration showing model of penetrator, location of strain gages on inside of case, and schematic of Davis gun which shoots penetrator into target. This was a virtually normal event, with no angle of attack and only 2 degrees from vertical angle of impact.

14. Axial deceleration data from field test. As this data was hand-digitized, it is inappropriate to infer frequency content from this plot. The "lock-in" phenomenon is evidenced at time 0.050-0.051 sec, and is caused by some combination of structural response of the penetrator and elastic response of the target as the penetrator suddenly comes to rest. No attempt is made to model the "lock-in" phenomenon in these analyses.

15. Analytically predicted axial deceleration for field test event assuming rigid body penetrator.

16. Analytically predicted axial deceleration for field test event using structural model of flexible penetrator. Note reasonably good correlation between analysis and data for initial rise time and peak value. Zero time is arbitrary.

17. Axial stress (strain) data from field test. The two lines represent results from two gage pairs; the degree of correlation between the two pairs is indicative of high quality data. The rapid fall-off at time 0.002 sec is due to the flared aft end of the penetrator contacting the target and reducing axial stress.

18. Analytically predicted axial stress (strain). Note reasonably good correlation between analysis and data for initial rise time and peak value. The effects of the flared aft end were not considered in the analysis.

19. Bending stress (strain) data from field test. Note the magnitude of bending stress is comparable to the axial for this event. As this was a virtually normal impact event, significant bending stress was was not expected. Note also that the subsequent peak value at time 0.0075 sec is at a different planar orientation than the first peak value.

20. Analytically predicted bending stress (strain) assuming 1 degree angle of attack. Analysis did not predict significant bending stress for the event as tested.

21. Analytically predicted rigid body axial decelerations for a penetration event comparing results for a solid concrete target with a layered concrete target one foot thick above soft soil. This is for a different penetrator configuration than previously discussed.

22. Axial deceleration data from field test into a one foot thick layered concrete target at 670 fps for comparison with 21. Again zero time is arbitrary, and the data has been hand-digitized. The degree of correlation between the prediction and data is encouraging and indicates this analytical technique is applicable for penetration into layered targets.

23. Illustration of laboratory shock test setup for applying controlled high-level axial and lateral forces to an instrumented penetrator.

24. Axial strain from axial laboratory shock test (solid) and from analytical prediction (dash). Top graph is for original (unreconciled) structural model; bottom graph shows improvement in correlation between test data and prediction after analytical structural model was reconciled by adjusting damping coefficient.

25. Bending strain from lateral laboratory shock test (solid) and from analytical prediction (dash). Top graph is for original (unreconciled) structural model; bottom graph shows improvement in correlation between test data and prediction after analytical structural model was reconciled by adjusting lateral damping coefficient and effective stiffness of internal joints. View foils 24 and 25 illustrate desirability and feasibility of reconciling analytical structural models with pertinent laboratory data.

26. .Conclusions summary.

# ANALYTICAL ESTIMATION OF TRANSIENT STRUCTURAL RESPONSE OF EARTH PENETRATING WEAPONS AND COMPARISON WITH LABORATORY AND FIELD TEST DATA (U)

(AIAA-88-C-1061)

Robert J. Kipp

Applied Mechanics Division II

Sandia National Laboratories

Albuquerque, New Mexico

AIAA Missile Sciences Conference, Nov. 29 - Dec. 1, 1988

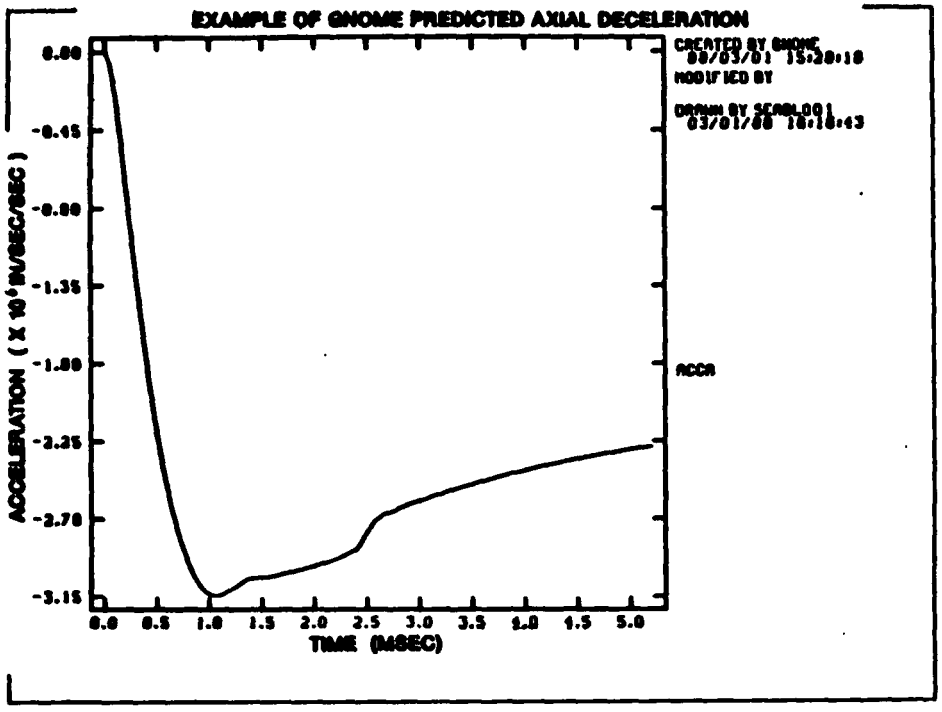
EXAMPLE OF GNOME PREDICTED AXIAL DECELERATION
CREATED BY GNOME
MODIFIED BY
DRAWN BY SCARLOCK
ACCR
ACCELERATION ( X 10⁶ IN/SEC/SEC )
TIME (MSEC)

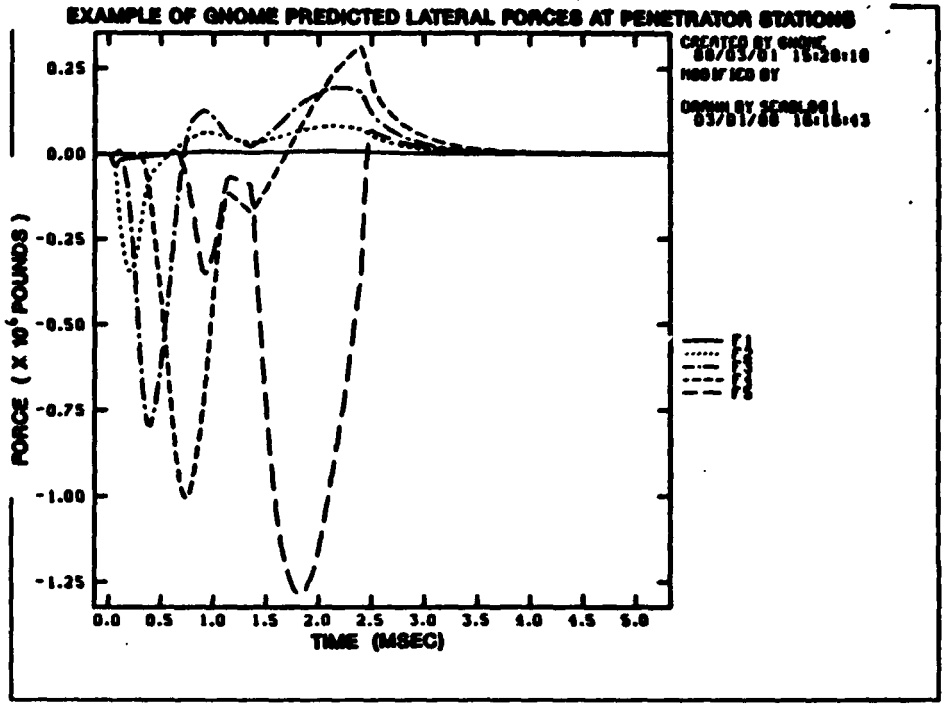
EXAMPLE OF GNOME PREDICTED LATERAL FORCES AT PENETRATOR STATIONS
CREATED BY GNOME
MODIFIED BY
DRAWN BY SCARLOCK
FORCE ( X 10⁶ POUNDS )
TIME (MSEC)

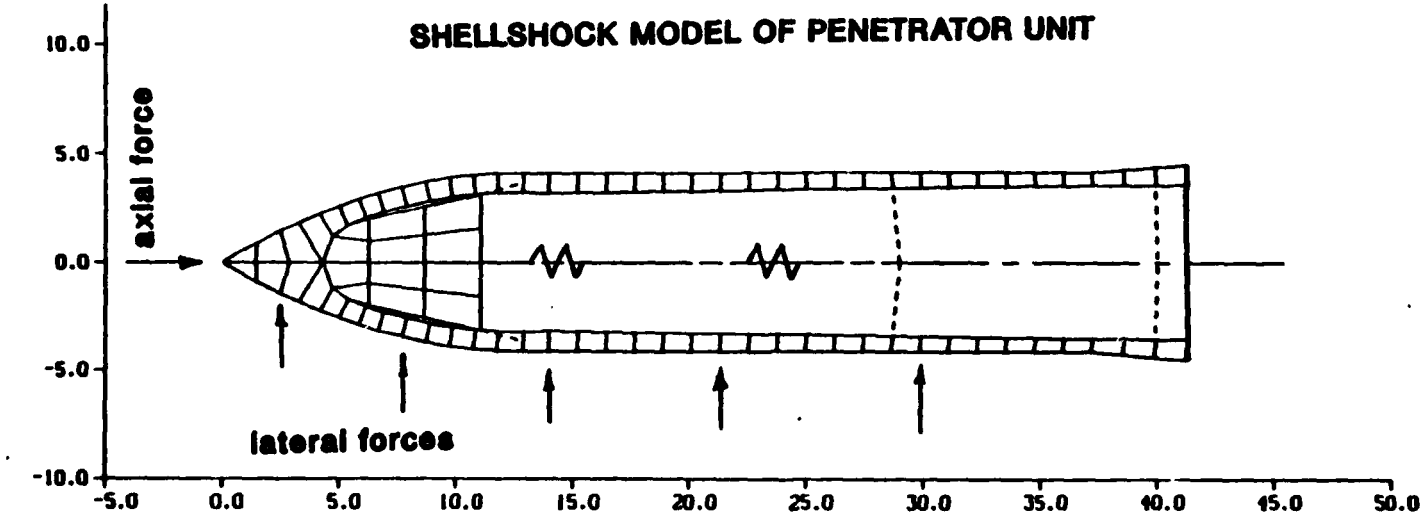
SHELLSHOCK MODEL OF PENETRATOR UNIT
axial force
lateral forces

# GNOME Material Models

## SIG1
spherical

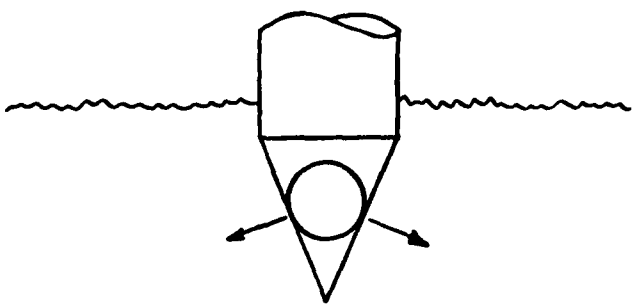

## SIG3
cylindrical

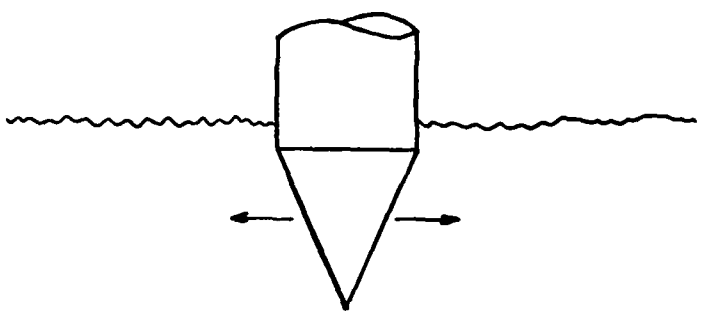

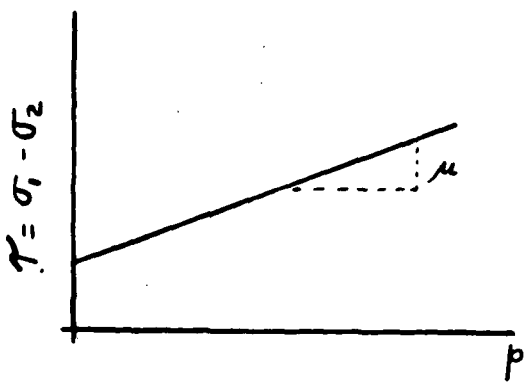


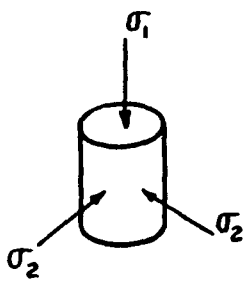


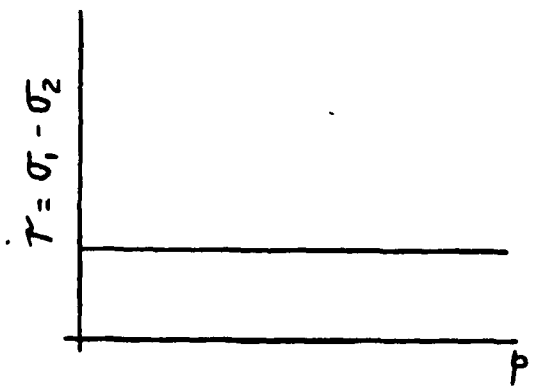

## PREDICTED AXIAL ACCELERATION IN WEAPON COMPONENT REGION BL1500

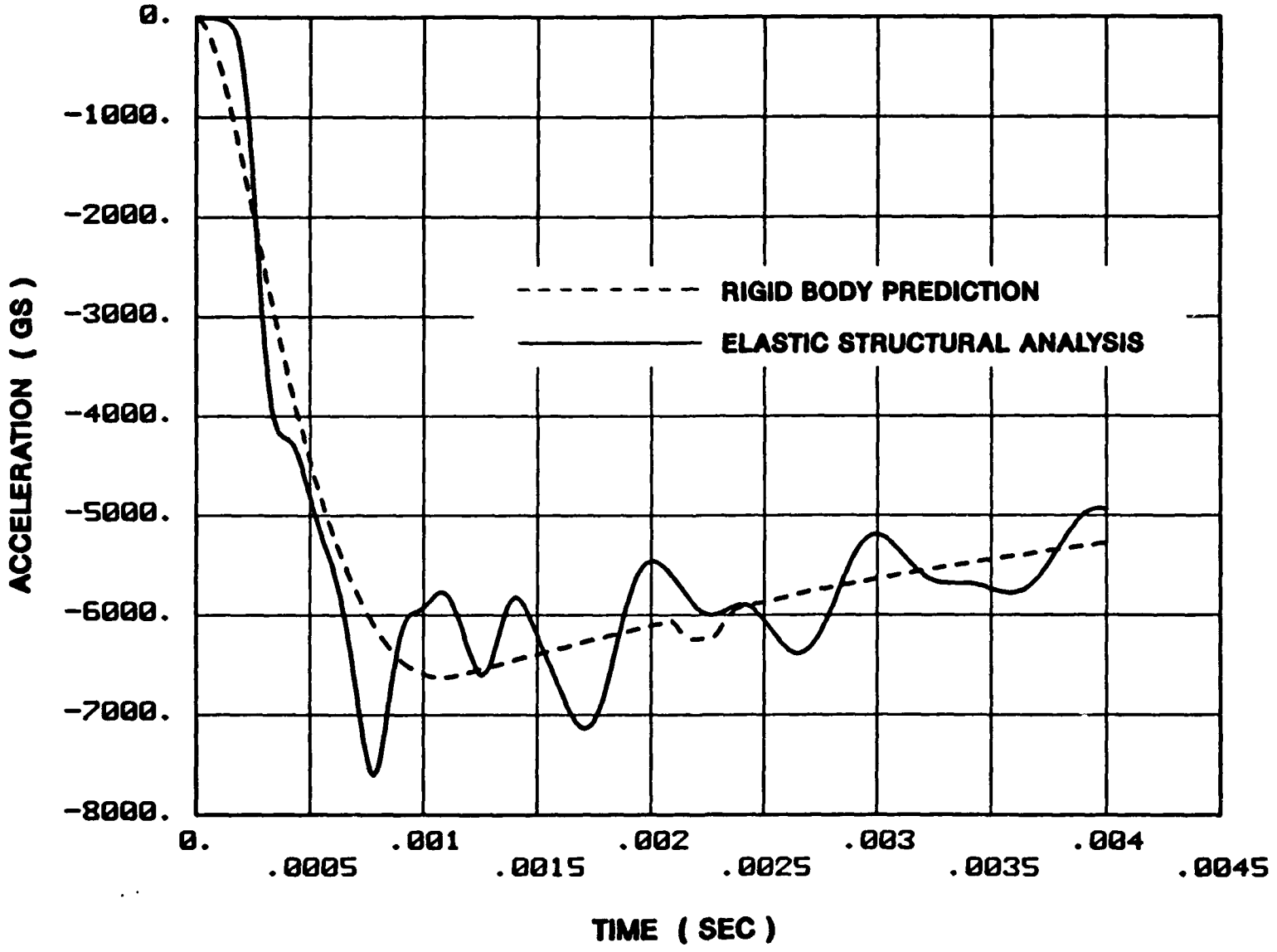

## PREDICTED LATERAL ACCELERATION WARHEAD REGION 1500 2 20

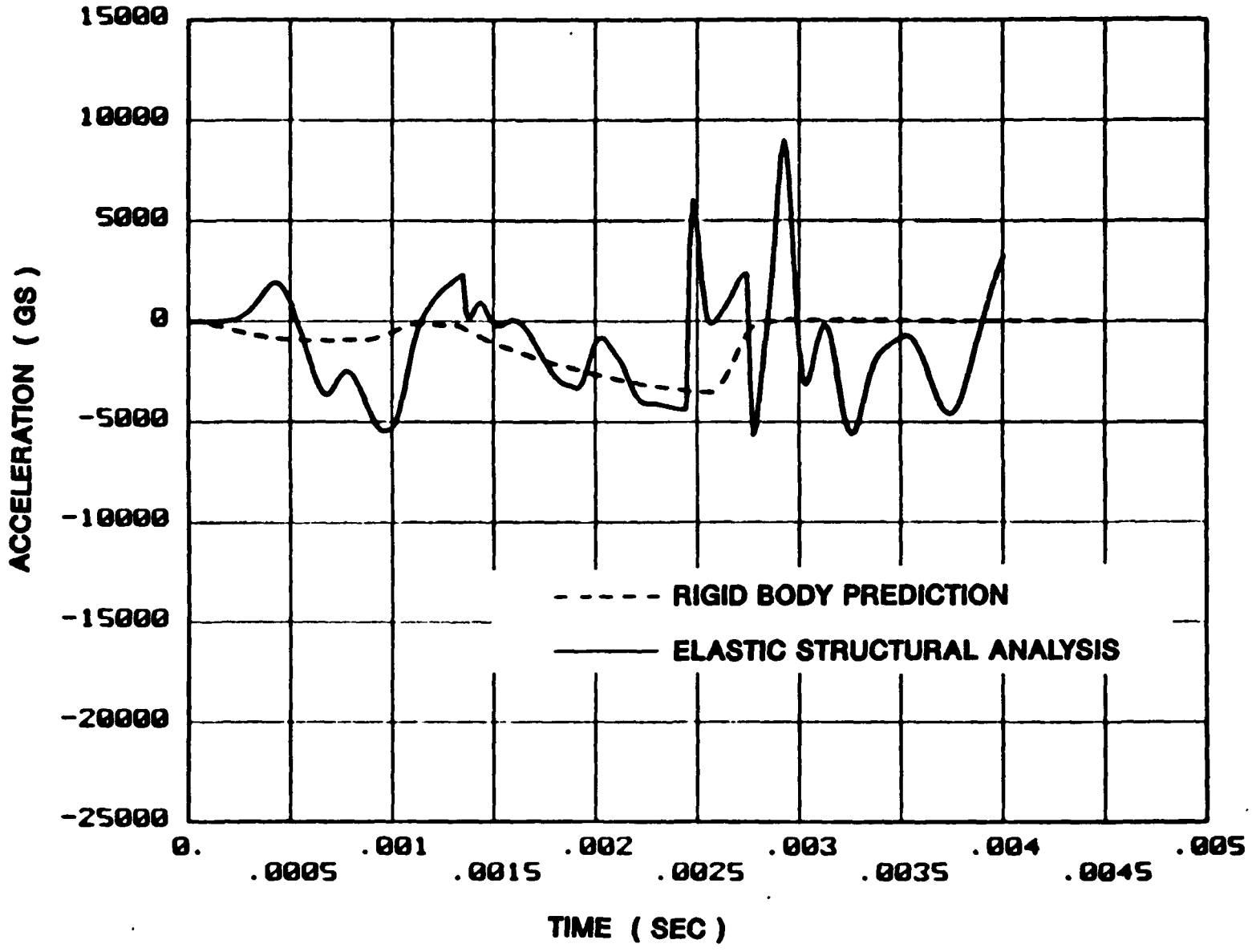

## PREDICTED LATERAL ACCELERATION COMPONENT REGION 1500 2 20

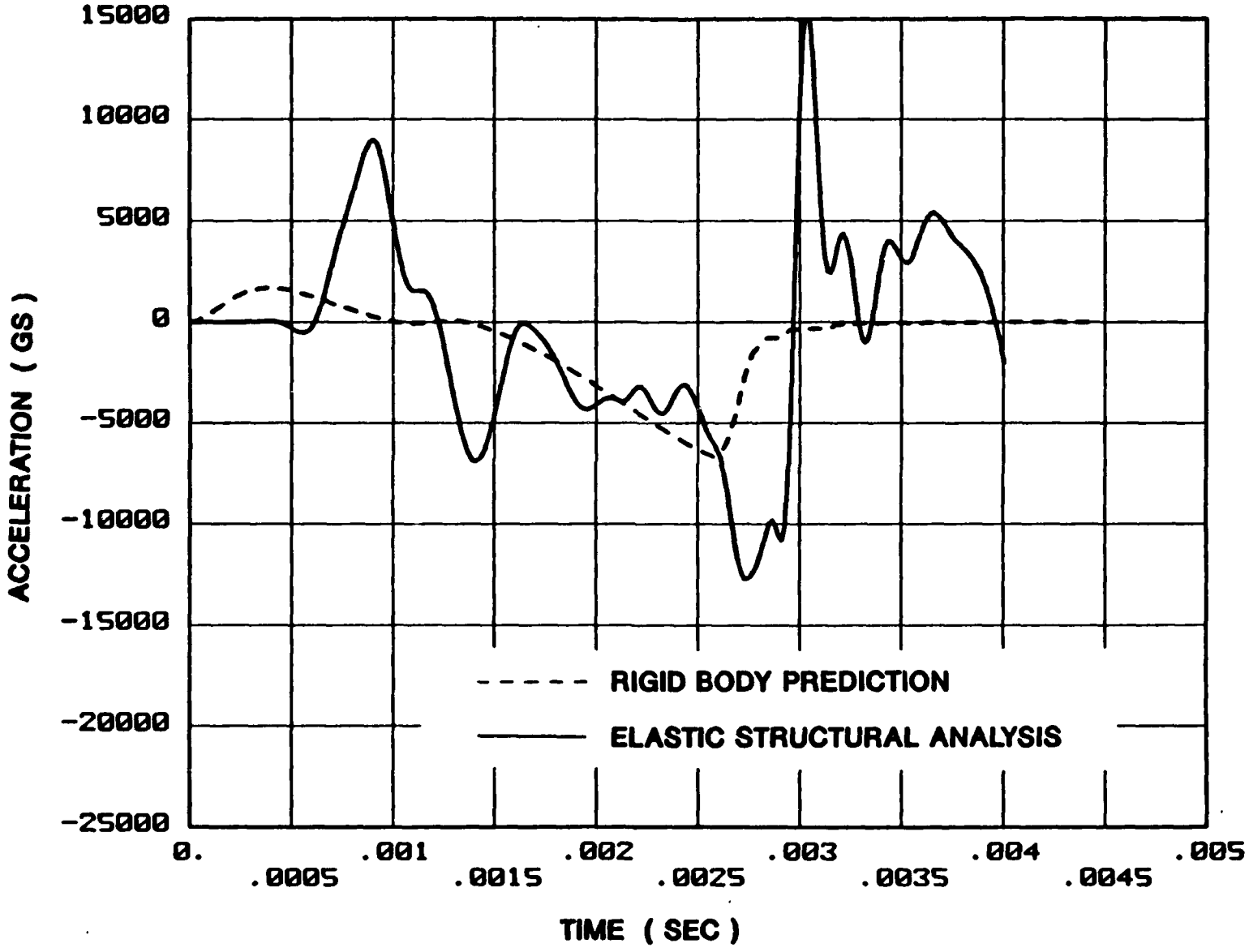

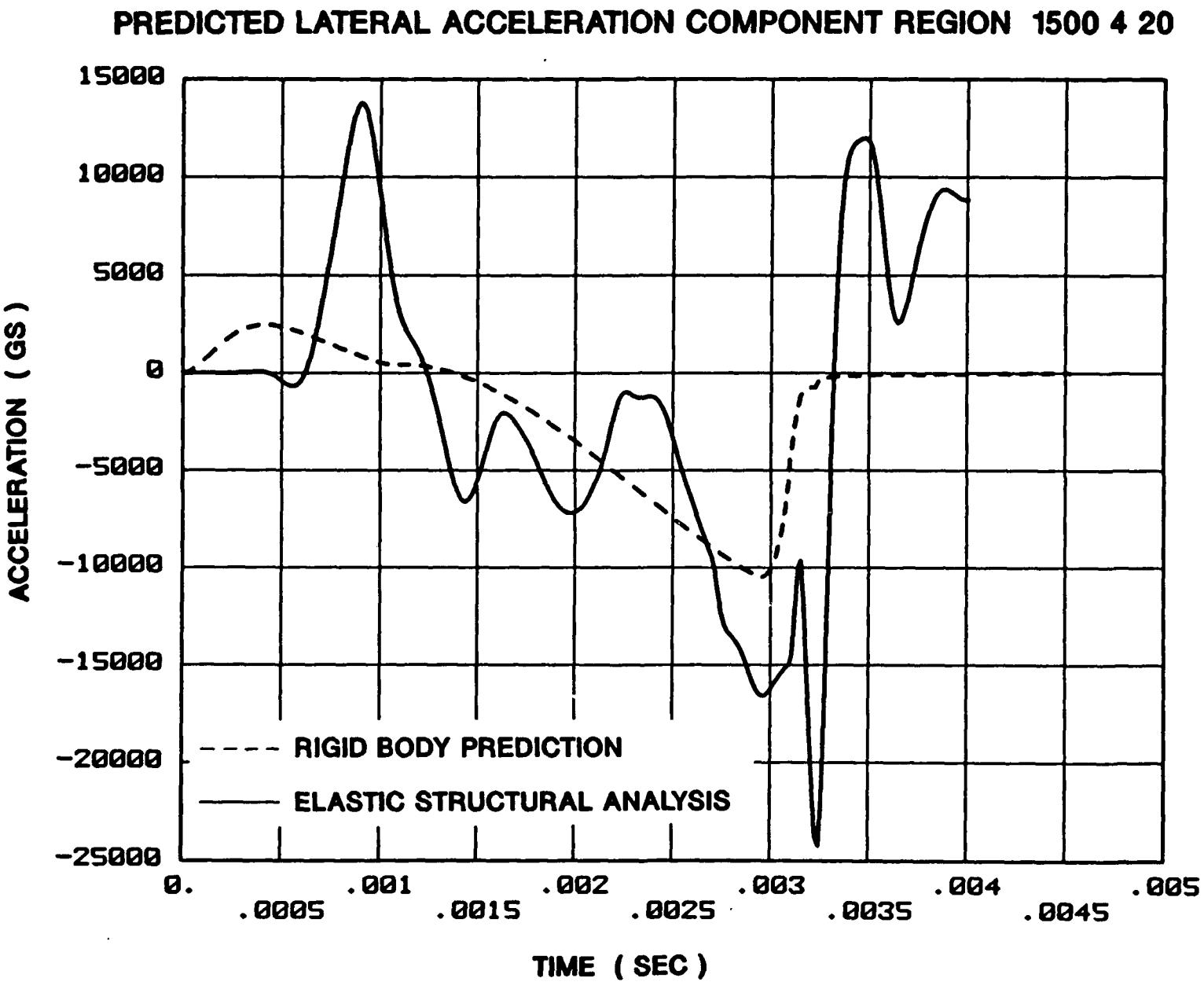
PREDICTED LATERAL ACCELERATION COMPONENT REGION 1500 4 20
15000
10000
5000
0
-5000
-10000
-15000
-20000
-25000
ACCELERATION ( GS )
0.
.0005
.001
.0015
.002
.0025
.003
.0035
.004
.0045
.005
TIME ( SEC )
RIGID BODY PREDICTION
ELASTIC STRUCTURAL ANALYSIS
GRAFAID 2.1 22-NOV-1988 15:31

# SHELLSHOCK Model of Baseline WR EPW

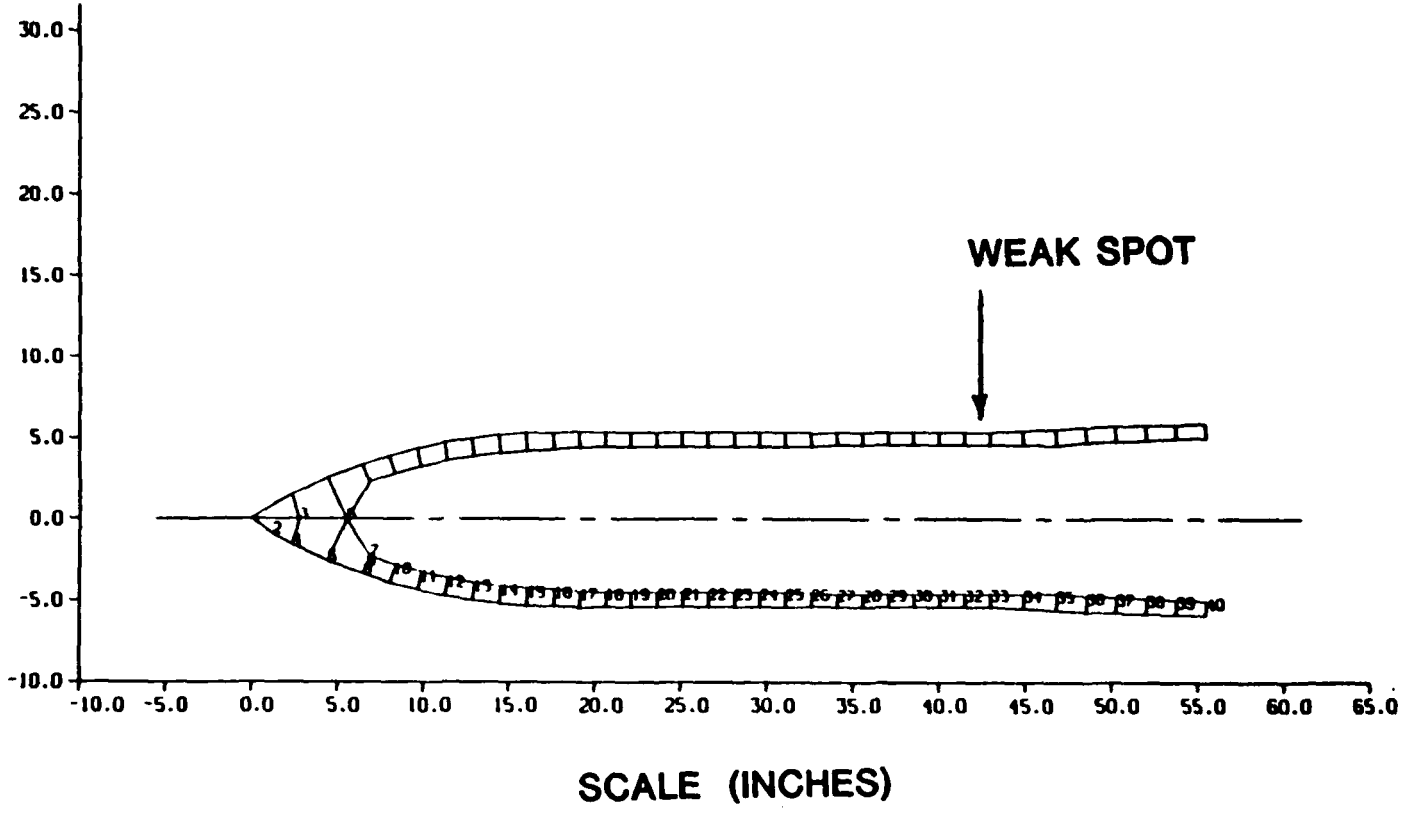

## PREDICTED TOTAL STRESS MAGNITUDE IN CASE AT WEAK SPOT 1500 2 20

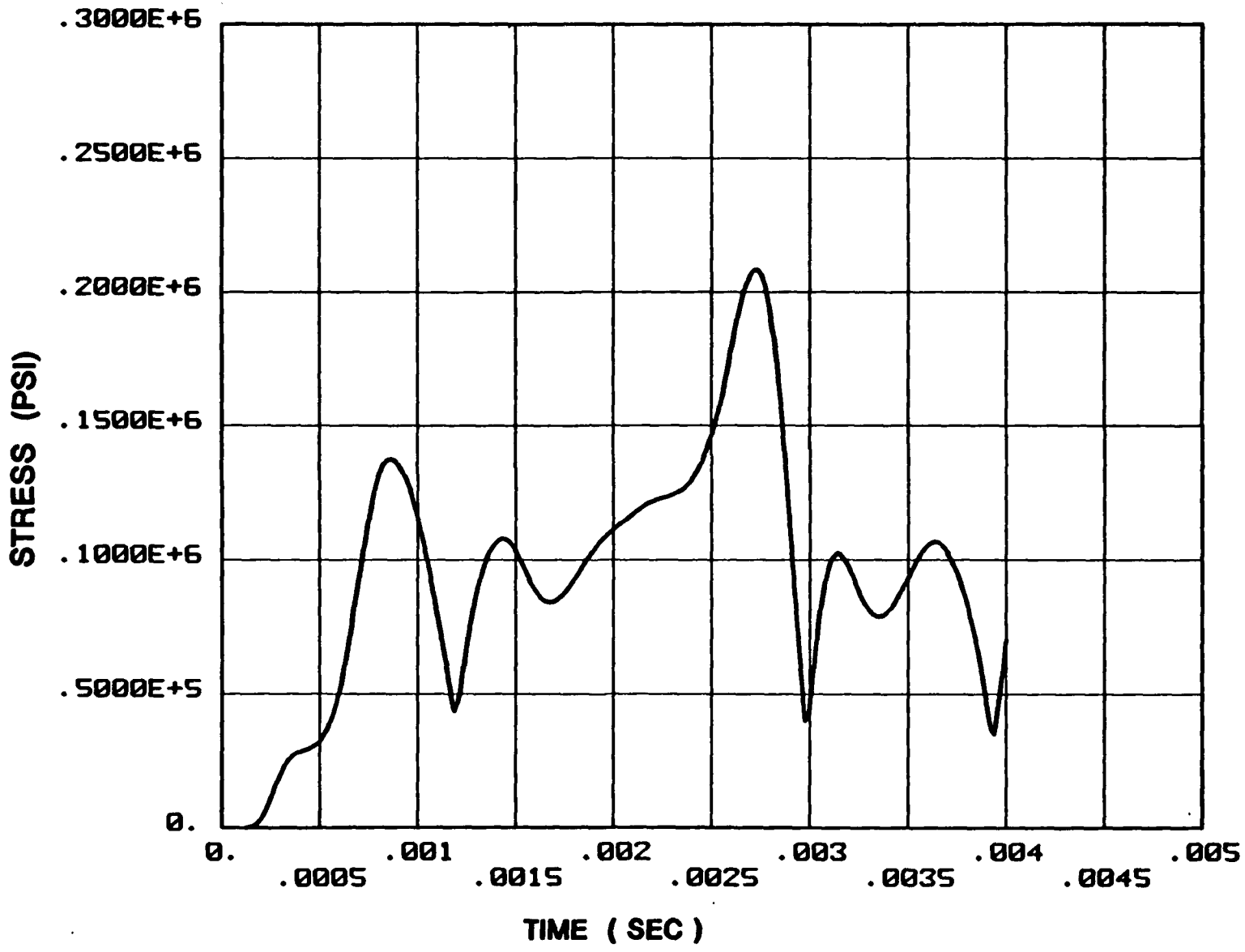

## PREDICTED TOTAL STRESS MAGNITUDE IN CASE AT WEAK SPOT 1500 4 20

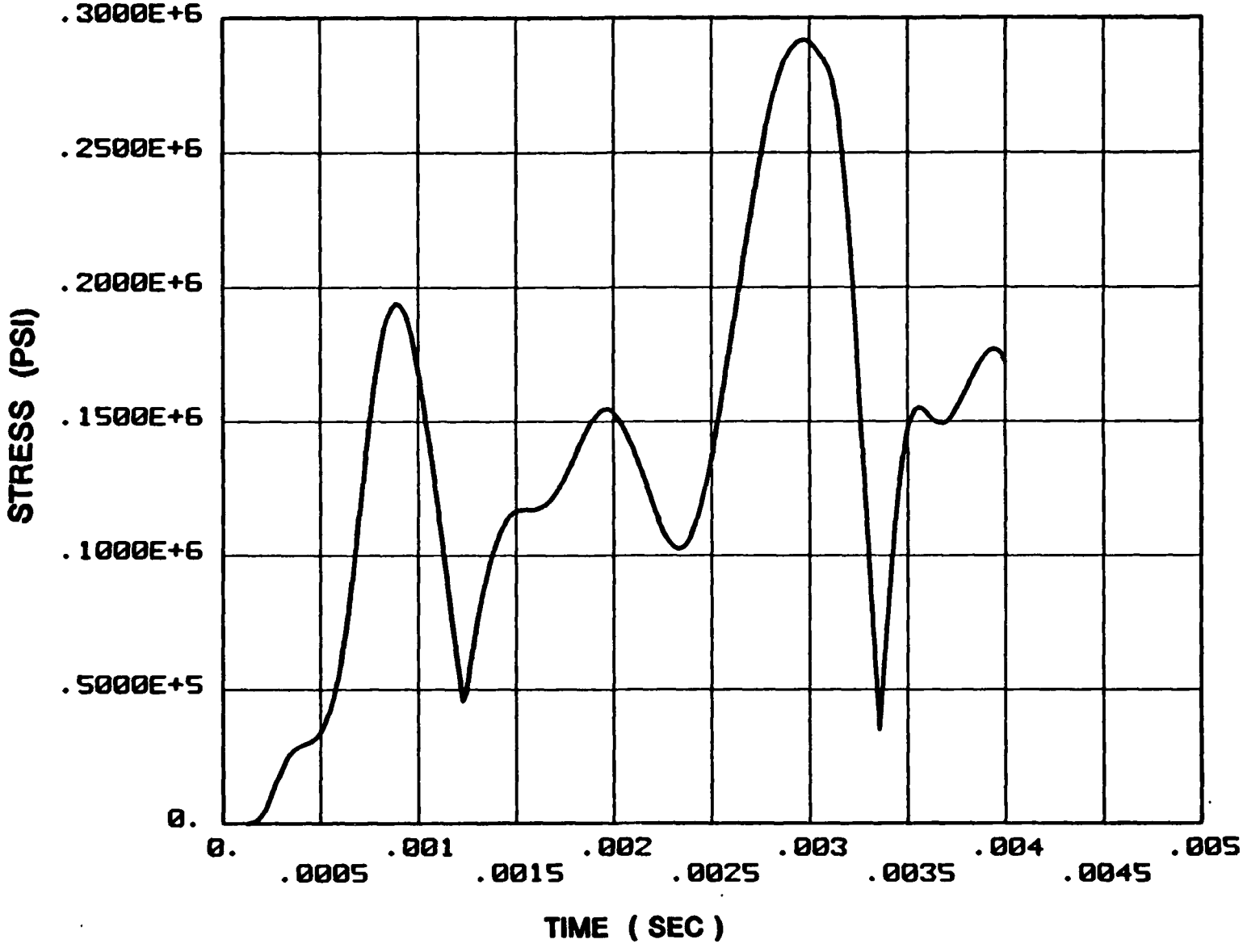

## LATERAL SHOCK SPECTRA FOR COMPONENT REGION 1500 FPS 20 AOI

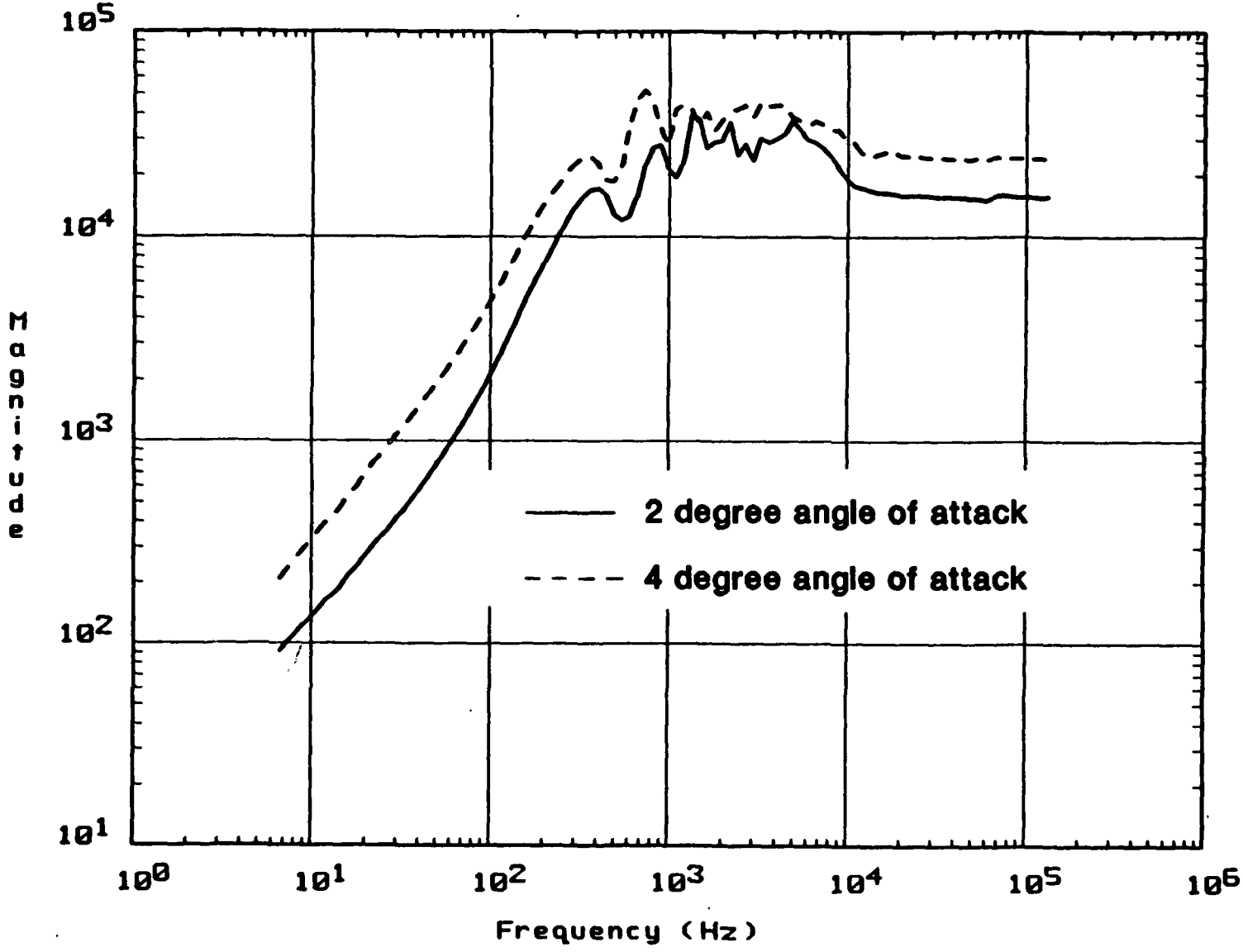

## AXIAL SHOCK SPECTRUM FOR COMPONENT REGION 1500 FPS

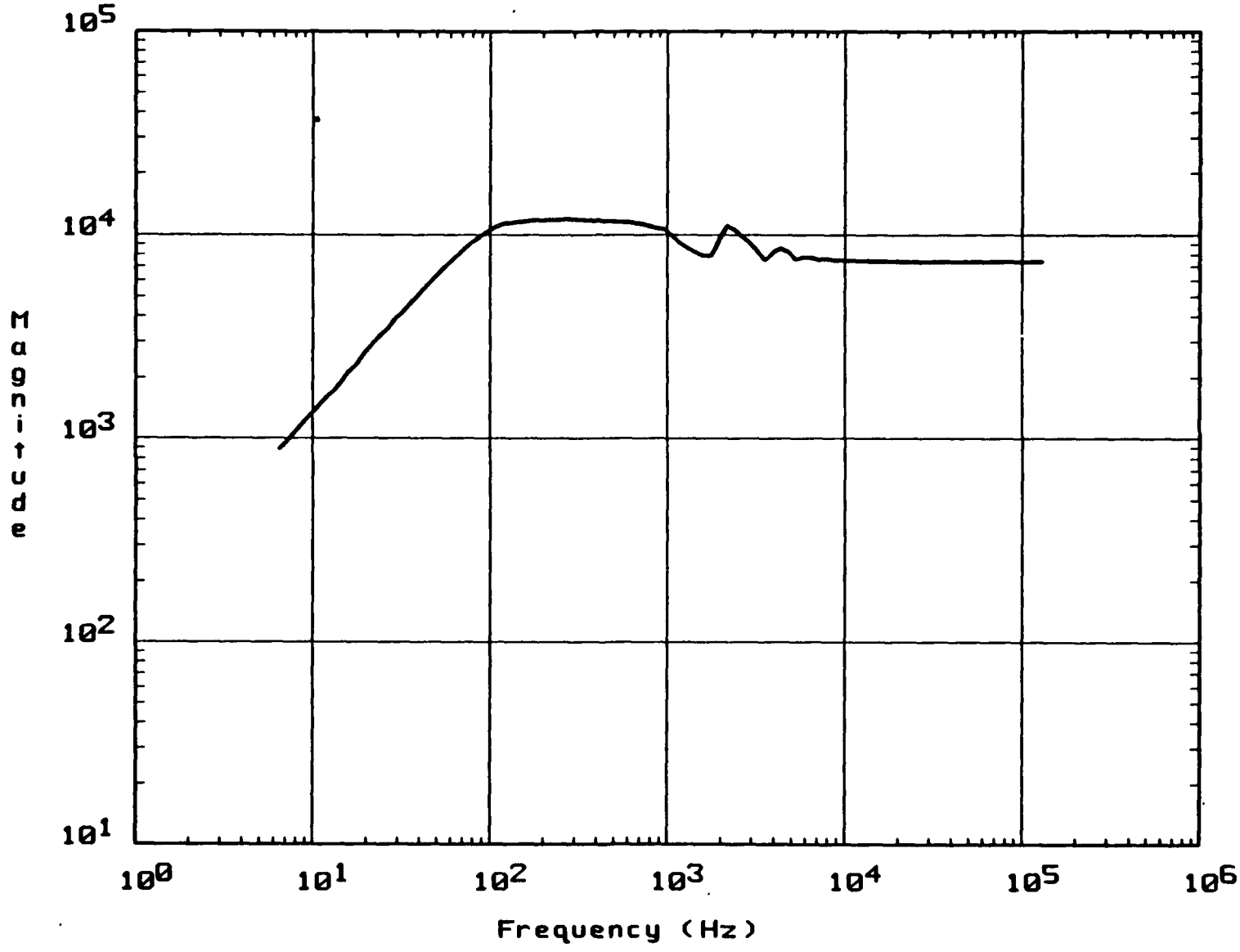

# STRAIN GAGED PENETRATOR FIELD TEST

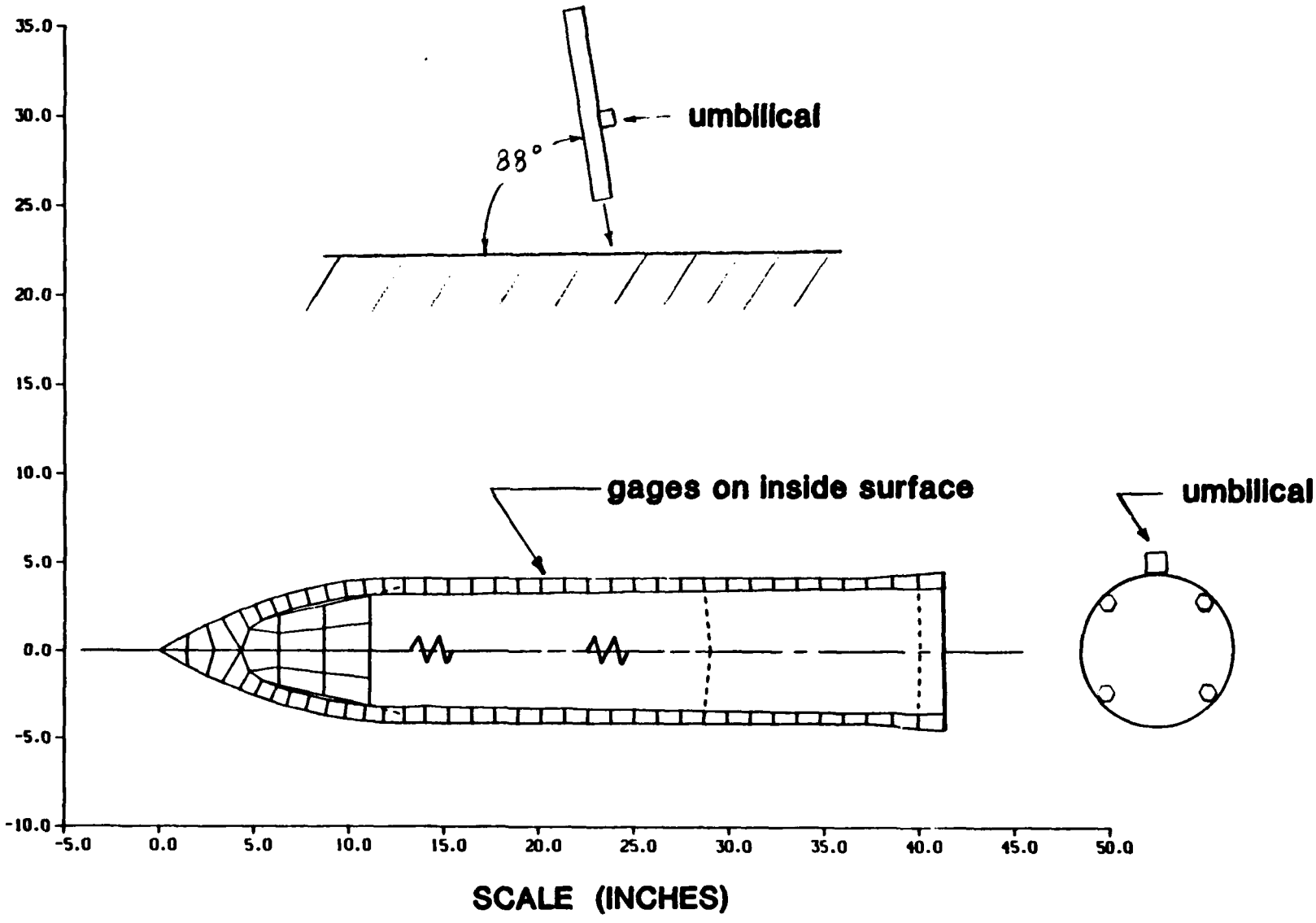

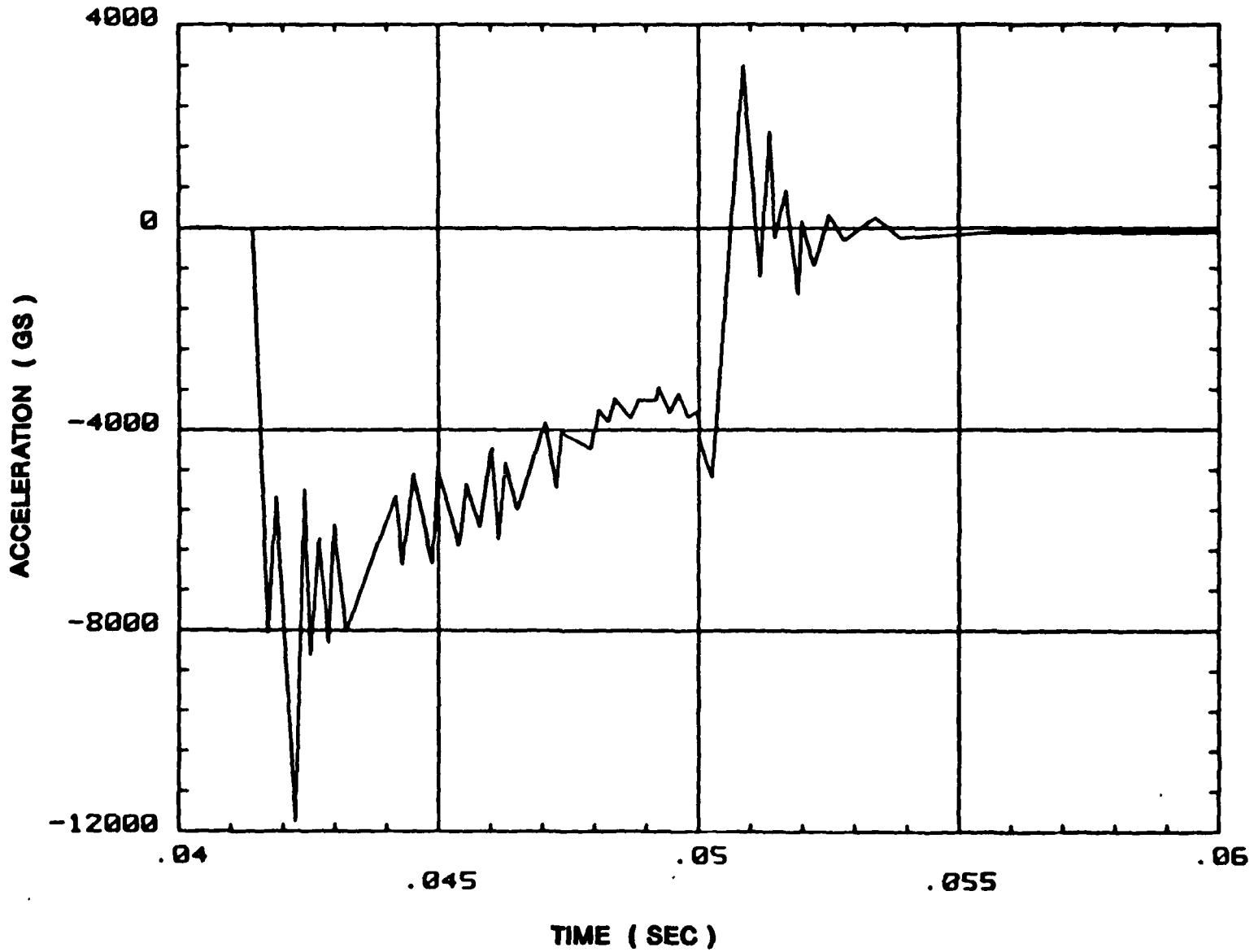


Measured Axial Acceleration vs Time for SEPW-9

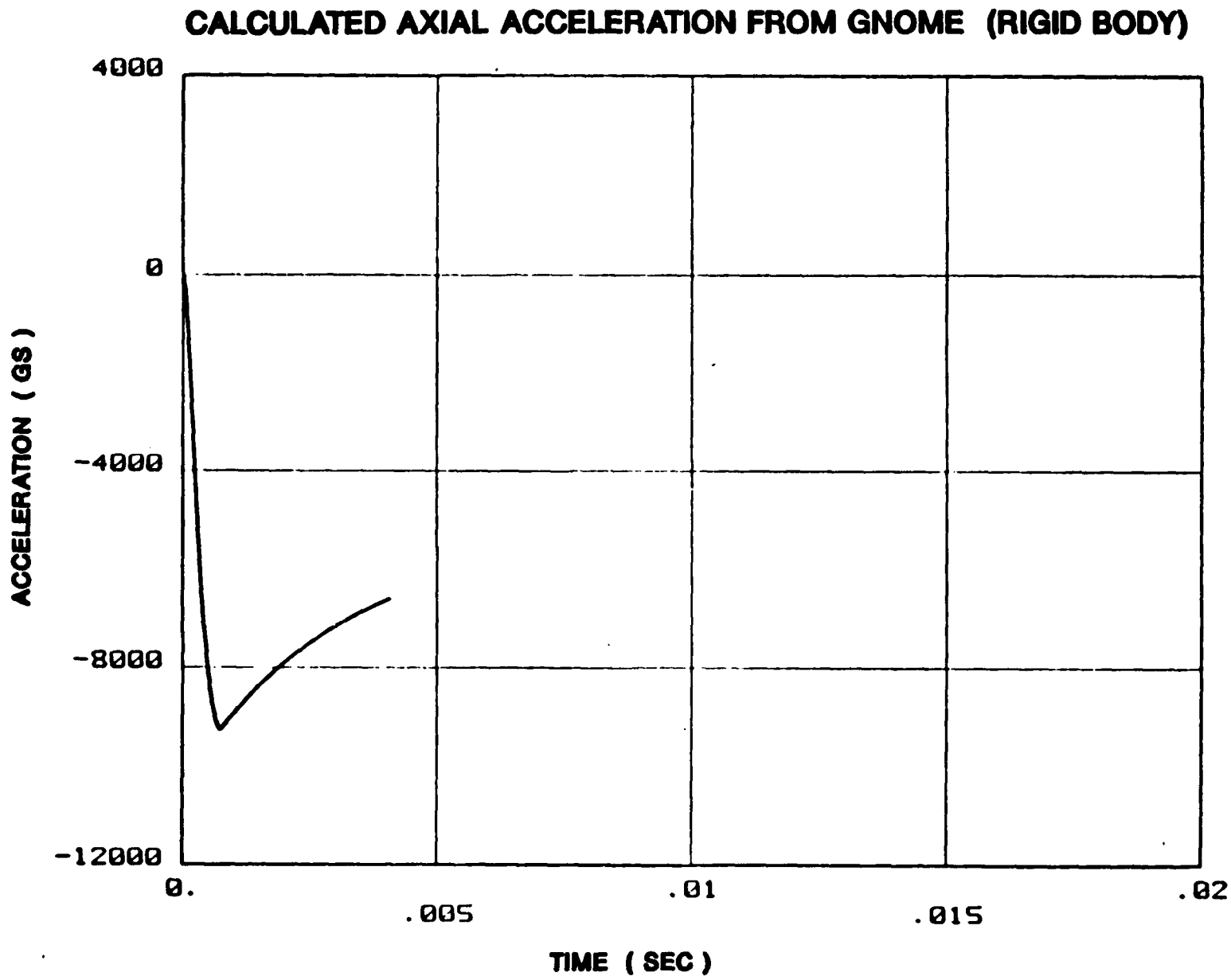
CALCULATED AXIAL ACCELERATION FROM GNOME (RIGID BODY)
4000
0
-4000
-8000
-12000
ACCELERATION ( GS )
0.
.005
.01
.015
.02
TIME ( SEC )

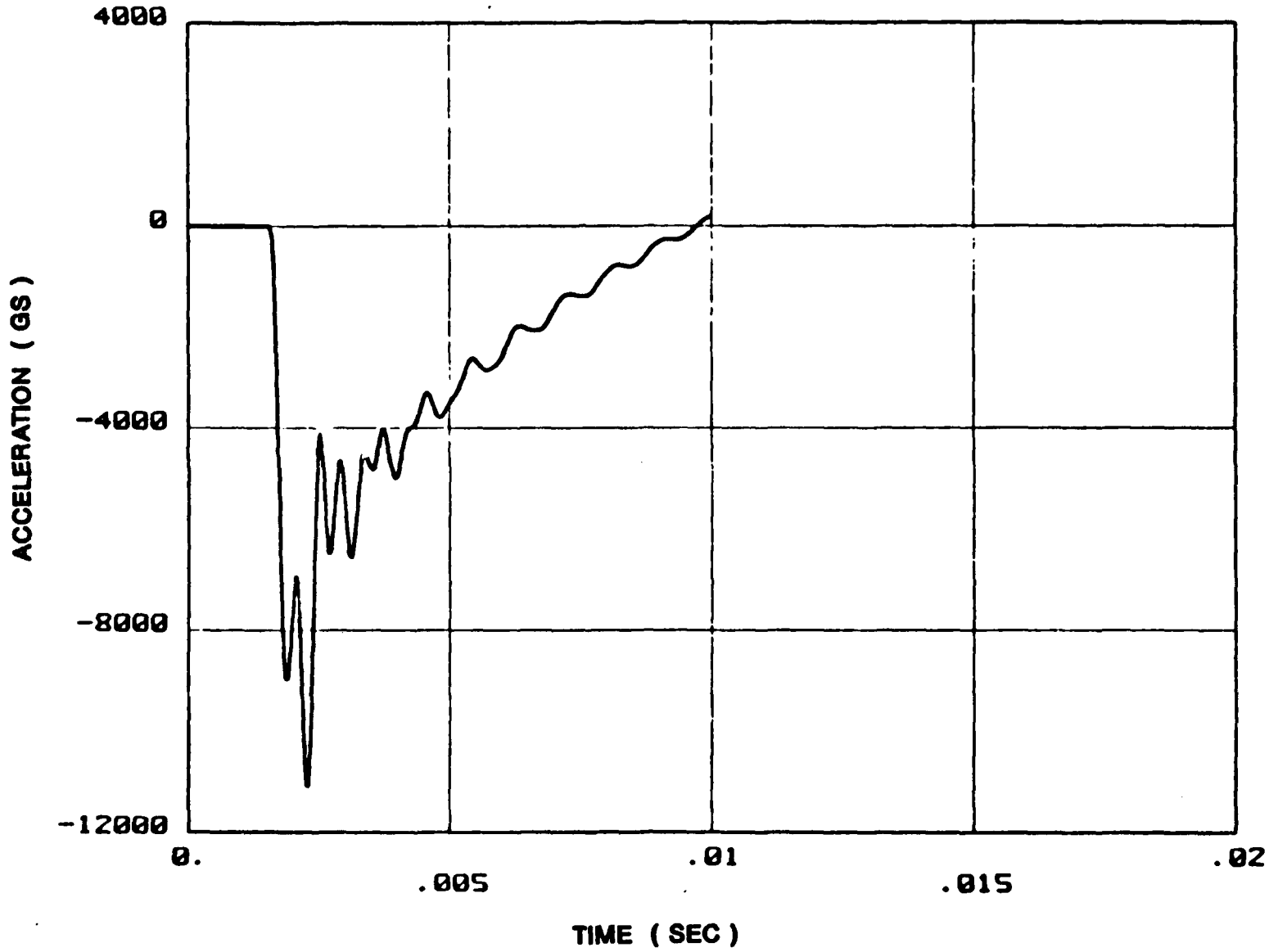


Calculated Axial Acceleration from GNOME and SHELL SHOCK

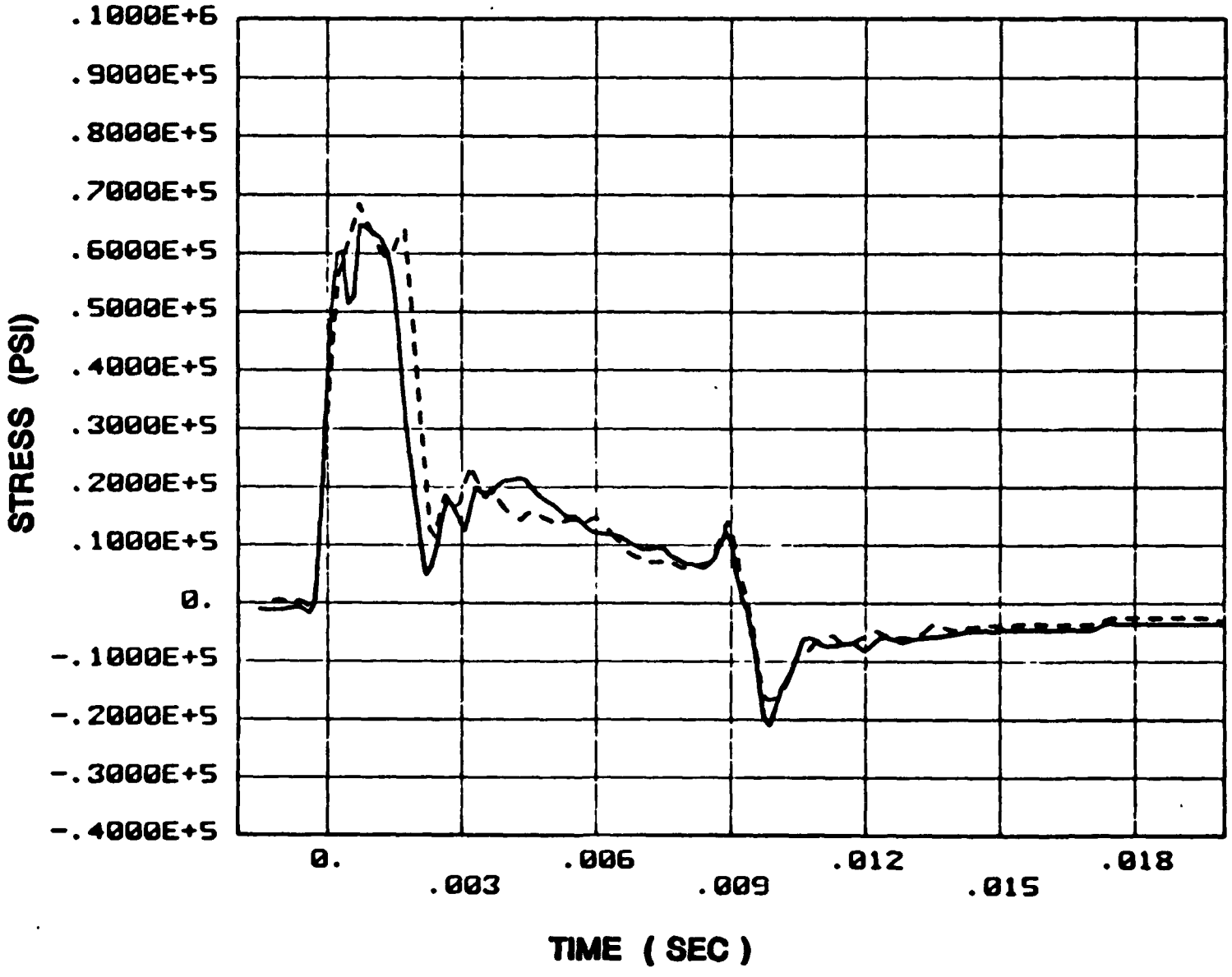


Measured Axial Stress vs Time from Two Strain Gage Pairs

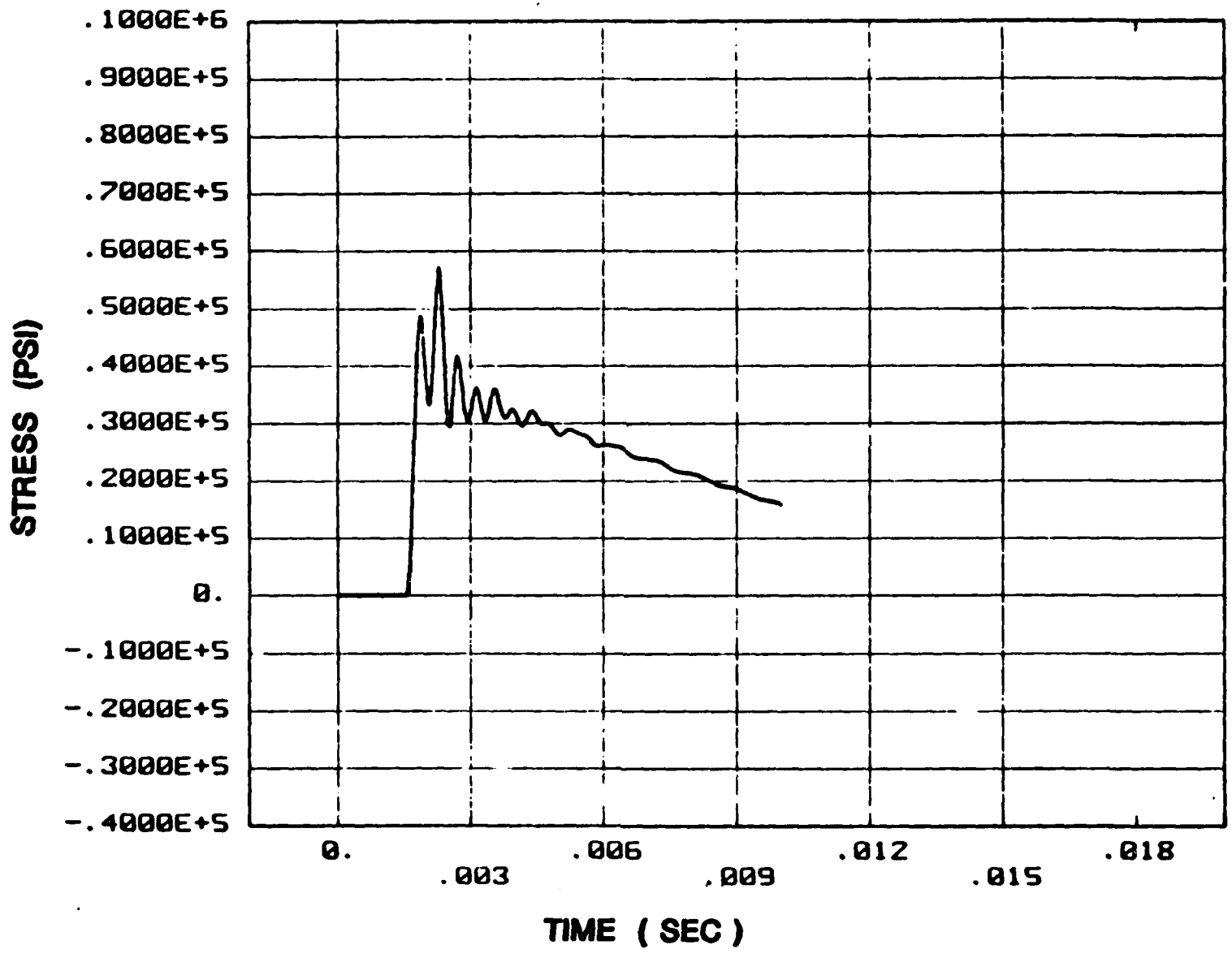


Calculated Axial Stress from GNOME and SHELLSHOCK

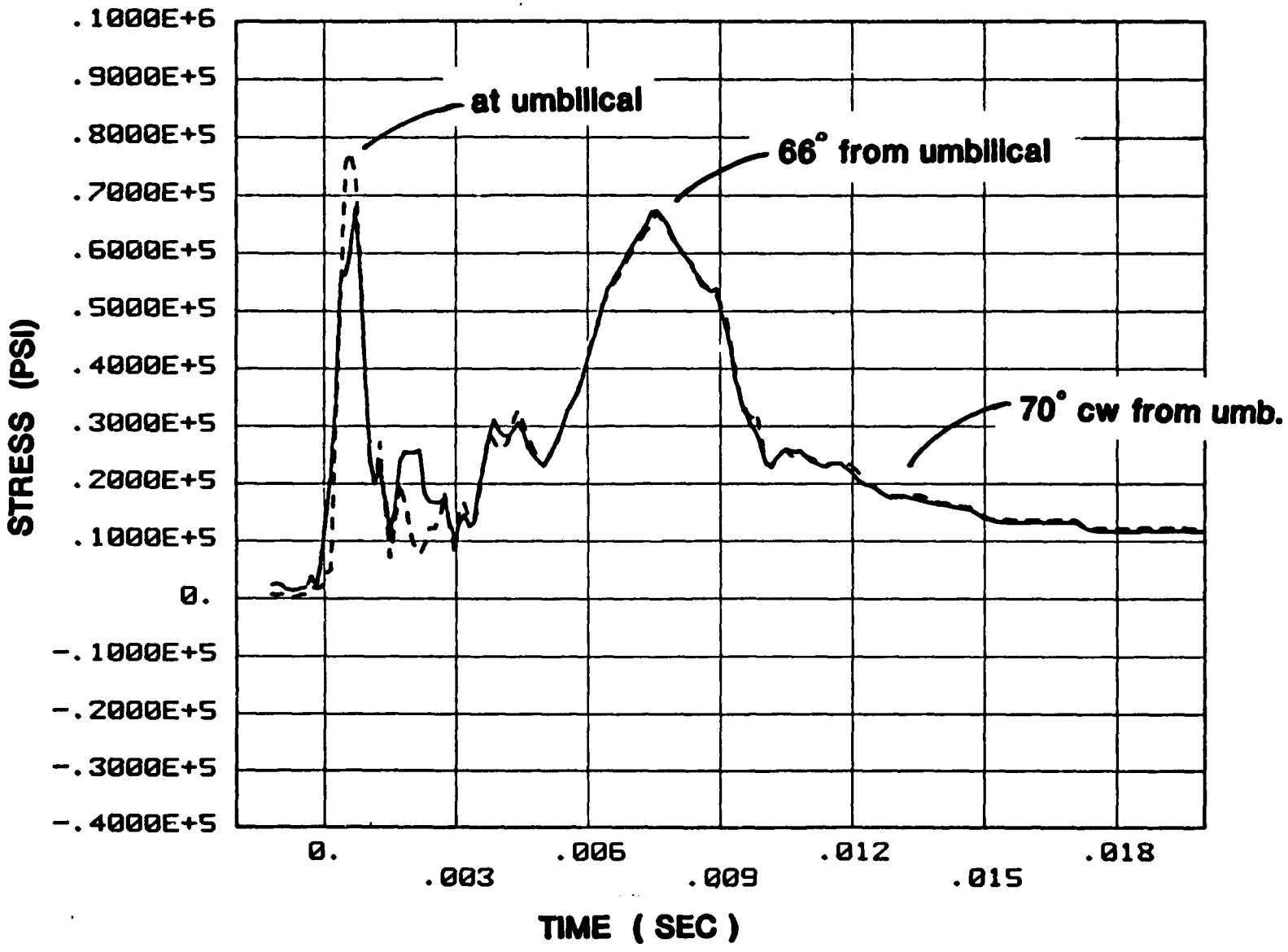


Measured Maximum Bending Stress vs Time from Two Gage Pairs (Irrespective of Orientation)

## CALCULATED BENDING STRESS ASSUMING 1° ANGLE OF ATTACK

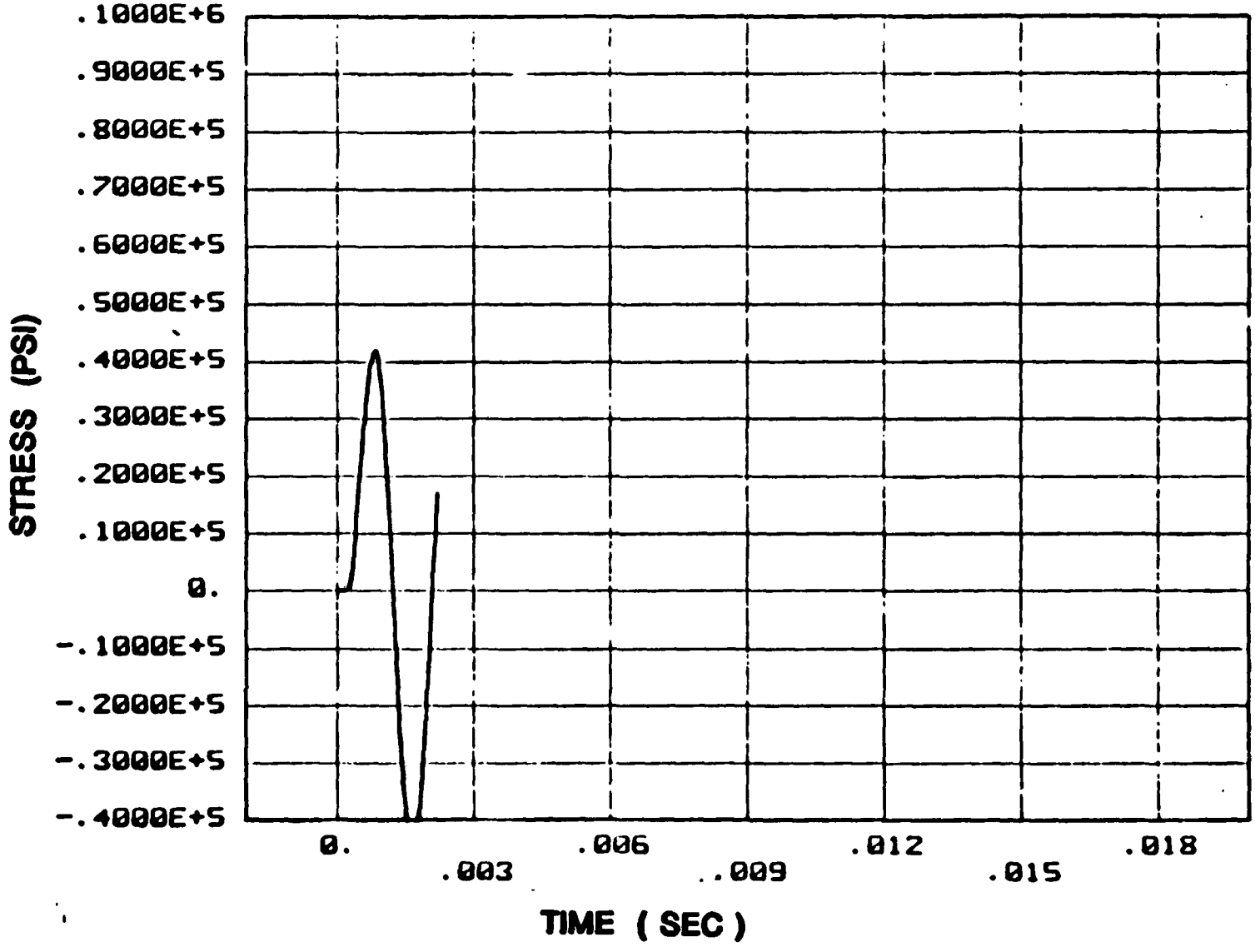

## GNOME PREDICTED RIGID BODY AXIAL DECELERATION FOR LAYERED CONCRETE TARGET

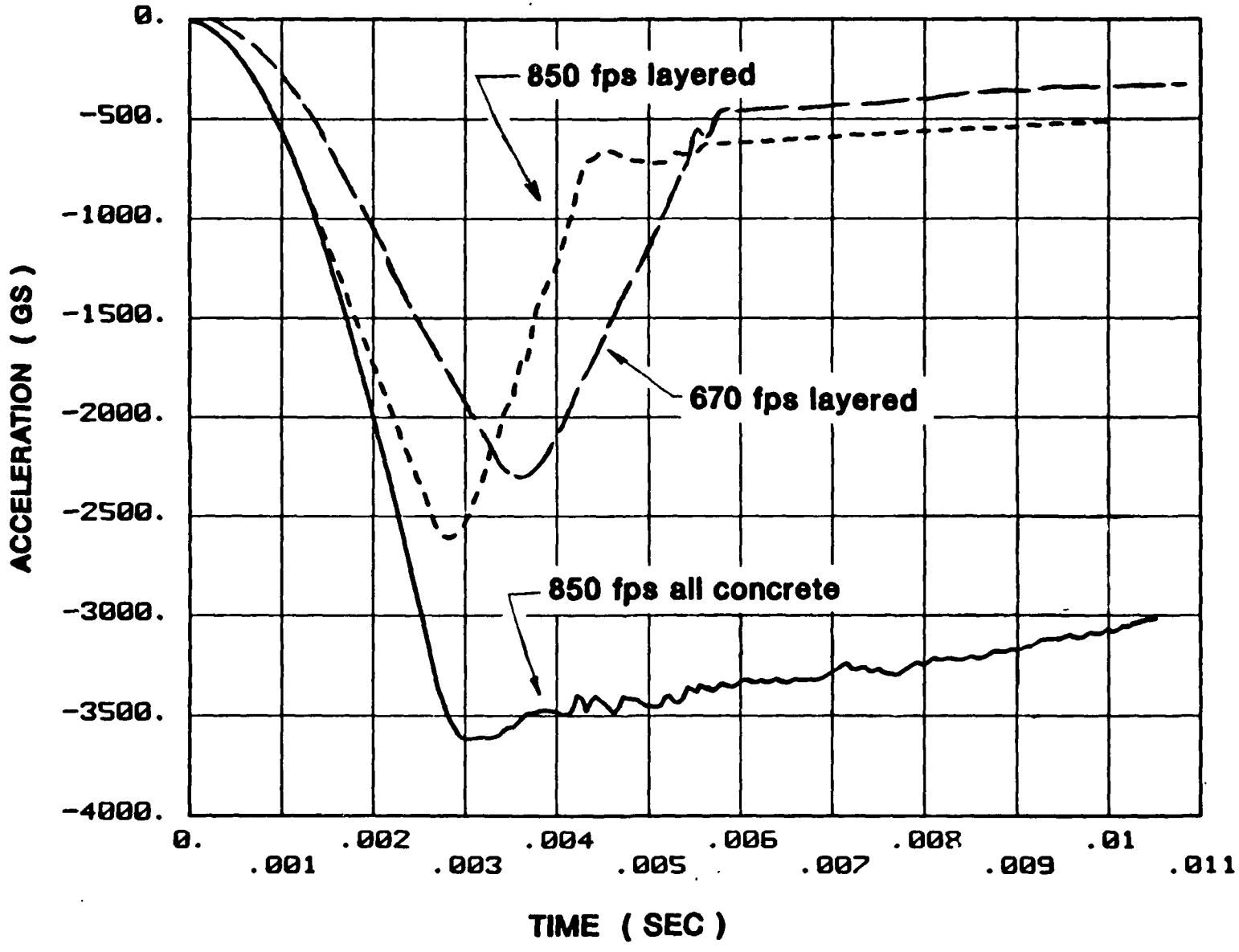

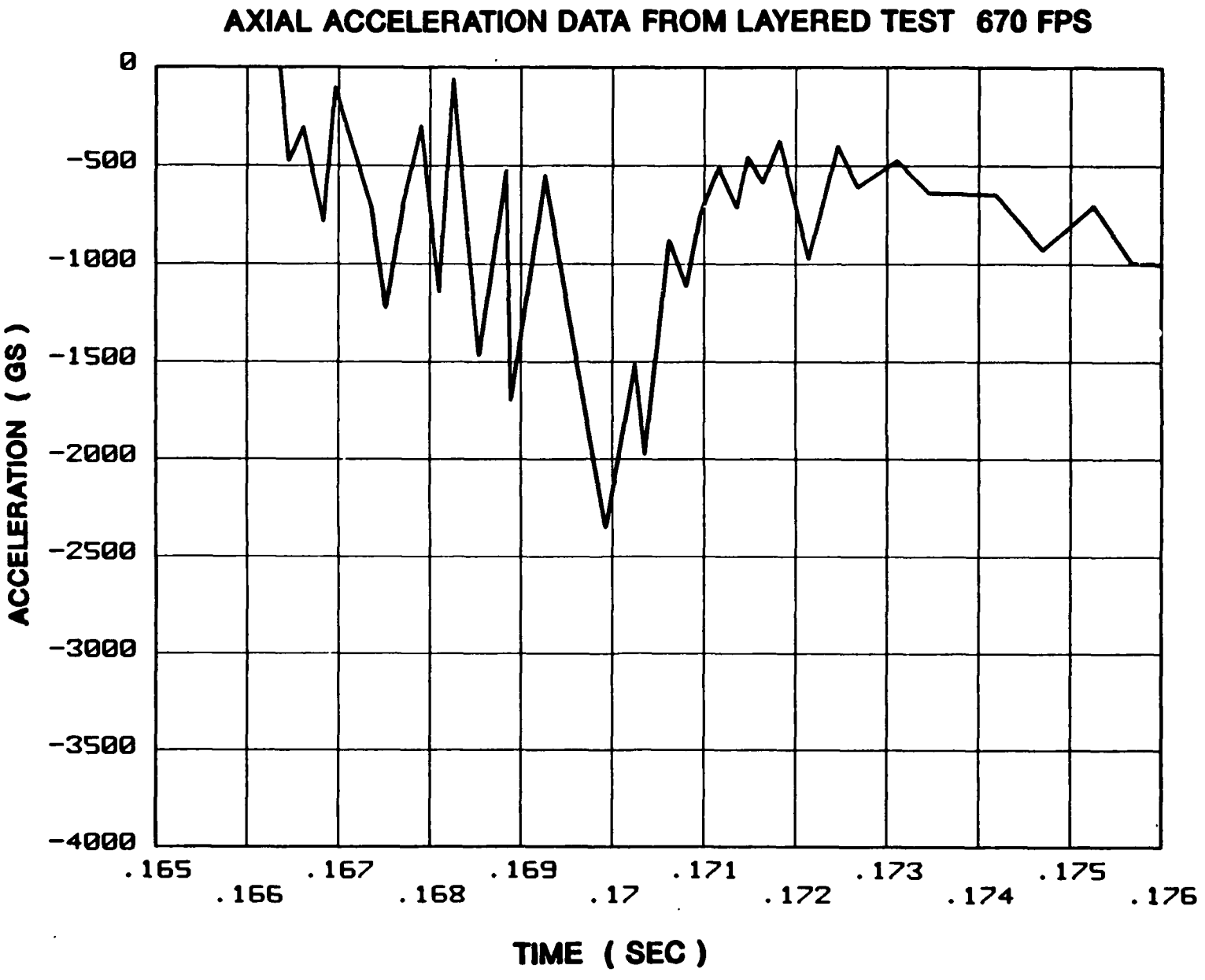
AXIAL ACCELERATION DATA FROM LAYERED TEST 670 FPS
ACCELERATION ( GS )
0
-500
-1000
-1500
-2000
-2500
-3000
-3500
-4000
.165
.166
.167
.168
.169
.17
.171
.172
.173
.174
.175
.176
TIME ( SEC )
GRAFAID 2.1 12-FEB-1988 16:12

# REVERSE HOPKINSON BAR TEST CONFIGURATION

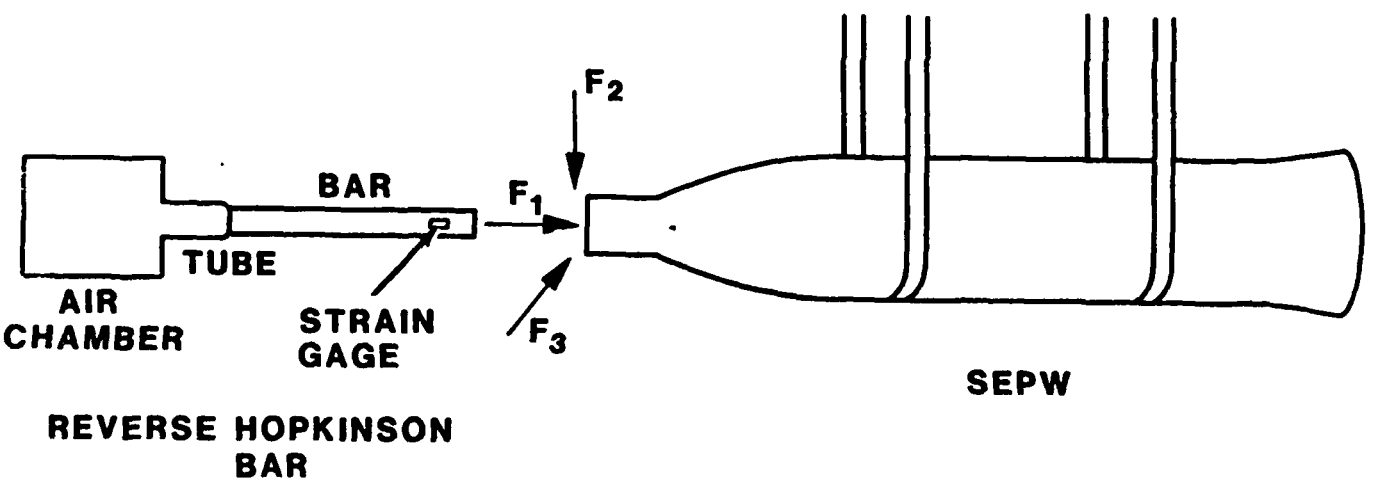

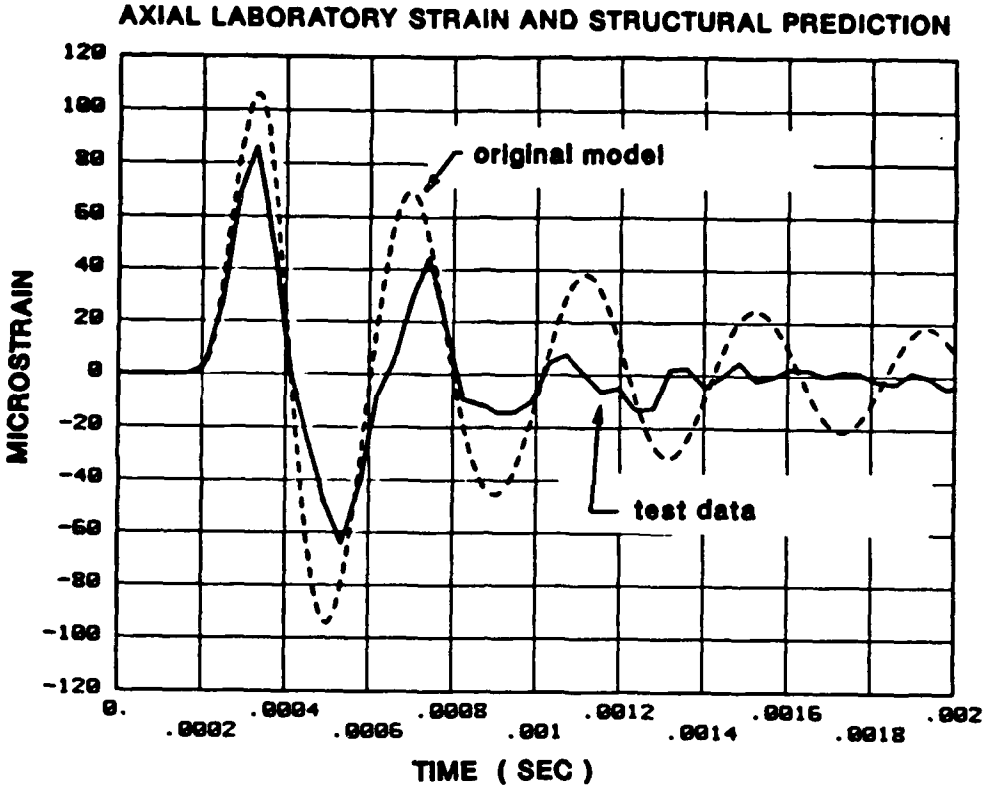
AXIAL LABORATORY STRAIN AND STRUCTURAL PREDICTION
MICROSTRAIN
120
100
80
60
40
20
0
-20
-40
-60
-80
-100
-120
original model
test data
0.
.0002
.0004
.0006
.0008
.001
.0012
.0014
.0016
.0018
.002
TIME ( SEC )

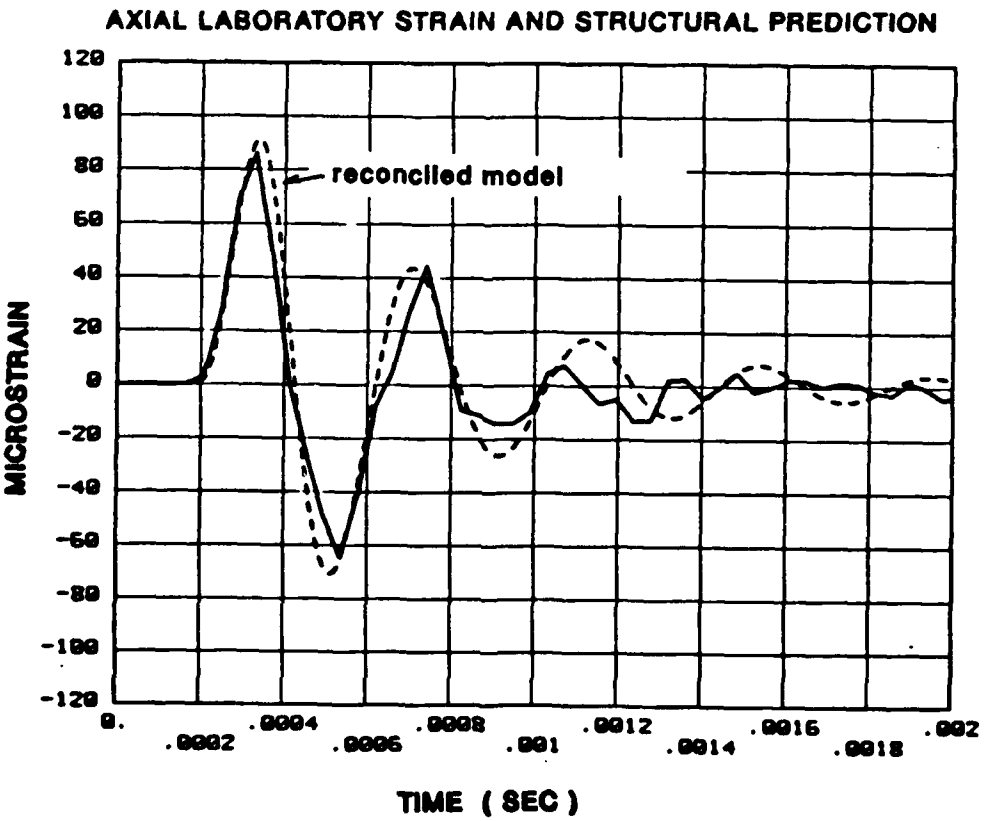
AXIAL LABORATORY STRAIN AND STRUCTURAL PREDICTION
MICROSTRAIN
120
100
80
60
40
20
0
-20
-40
-60
-80
-100
-120
reconciled model
0.
.0002
.0004
.0006
.0008
.001
.0012
.0014
.0016
.0018
.002
TIME ( SEC )

BENDING LABORATORY STRAIN AND STRUCTURAL PREDICTION

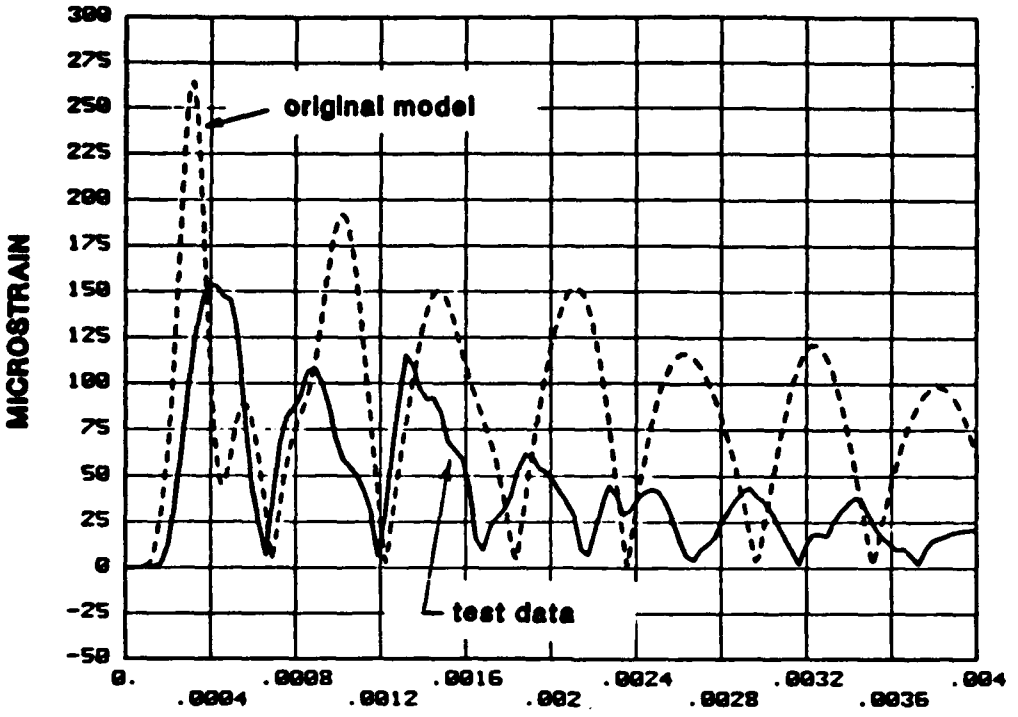


BENDING LABORATORY STRAIN AND STRUCTURAL PREDICTION

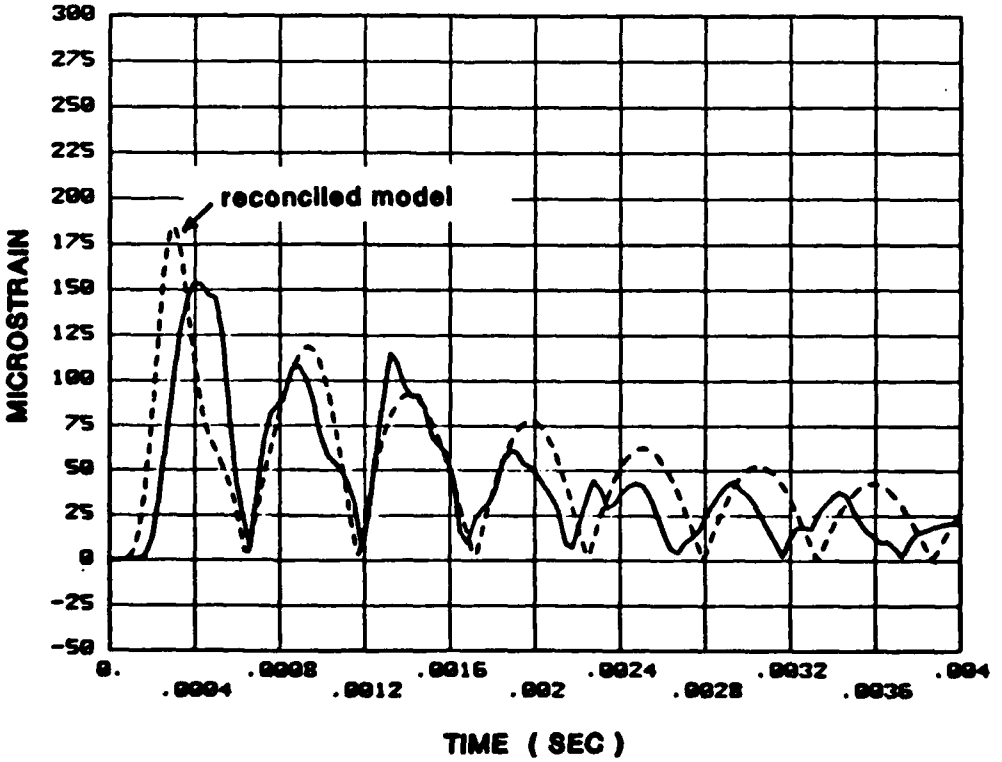

# CONCLUSIONS

1. Analytically estimated structural capability of earth penetrator designs, including composite case, and corresponding worst-case shock environments

2. Demonstrated ability to obtain relevant penetrator structural response data in field- and laboratory-test conditions which can be used to validate analytical predictions

3. Demonstrated effectiveness of using lab data in improving structural models of earth penetrators, including lateral response aspects

# EXPERIMENTAL EARTH PENETRATOR RESPONSE DATA ANALYSIS FOR APPLIED FORCE ESTIMATION

VESTA I. BATEMAN

SANDIA NATIONAL LABORATORIES

Sandia National Laboratories

SAND88-1608

# EXPERIMENTAL EARTH PENETRATOR RESPONSE DATA ANALYSIS FOR APPLIED FORCE ESTIMATION

by

Vesta I. Bateman
Vibration Testing Division
Sandia National Laboratories
Albuquerque, NM

## ABSTRACT

Penetrator response measurements for an experimental earth penetrator are made on the inside of the penetrator case with strain gages. The penetrator structural characteristics are measured with the strain gages in response to a high-level point force generated by a Reverse Hopkinson Bar Technique, developed at Sandia. The Reverse Hopkinson Bar Technique uses a steel bar propelled from an air gun to generate the force input to the penetrator. The force can be reproduced with repeatable characteristics which allows averaging of the response data. The penetrator was excited in both the axial and lateral directions with the Reverse Hopkinson Bar Technique so that both axial and lateral impulse response functions may be calculated from the response data.

Since response measurements are made at only one axial location on the penetrator case, the force estimation method is restricted to the solution of the basic measurement convolution integral,

$$y(t) = \int_0^t h(t) f(t-\tau) d\tau \qquad (1)$$

where y is the measured field response, h is a characterization of the penetrator structure in the form of impulse response, and f is the force which caused that response. The force is generated by explosively propelling the penetrator into a target such as rock. The solution to the convolution integral is a

deconvolution problem which employs a discrete form of equation (1) transformed into the frequency domain as

$$\underline{Y} = \underline{HF} \tag{2}$$

The measured field response may be resolved into a vector of axial and lateral components, so equation (2) may be solved for the force vector of two penetration forces as

$$\underline{F} = \underline{H}^{-1}\underline{Y} \tag{3}$$

where H is a ~~2x2~~ 3x3 matrix of impulse responses which have been transformed into the frequency domain as frequency response functions.

Although the force estimation from equation (3) appears straightforward, there are several problems which arise in its calculation; these problems will be illustrated and discussed in the paper. The axial force estimates will be compared to what is considered to be the rigid body force which is a technique also used to estimate the axial penetration force from measured response data. An evaluation of the force estimation will be made as well as recommendations for future measurements to allow better estimates of the field penetration force environment.

VG-1: Title Viewgraph

The material is this presentation is unclassified.

# RECONSTRUCTION OF DYNAMIC STRUCTURAL INPUTS FROM MEASURED DATA

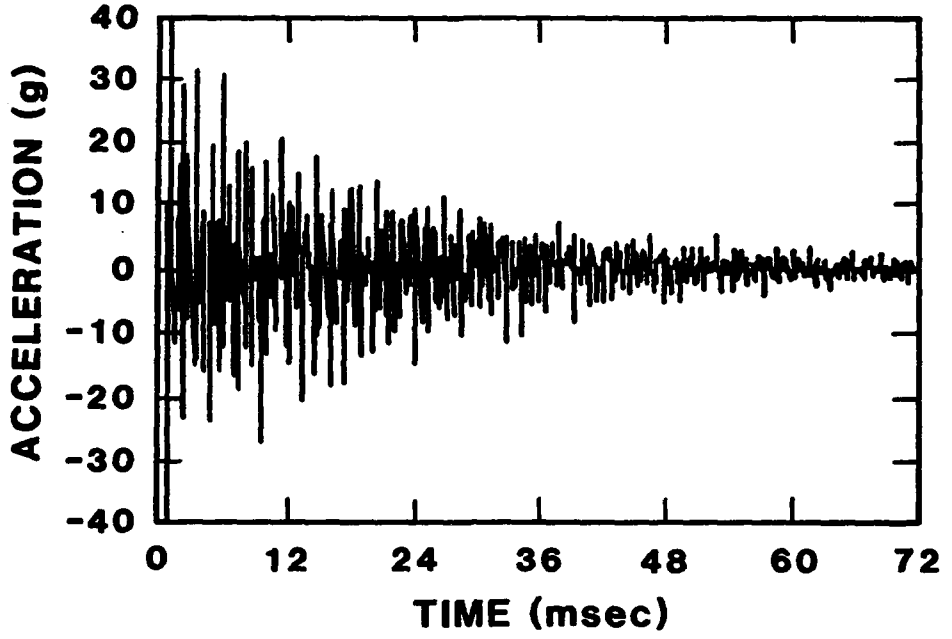


MEASURED RESPONSE FOR A BAR

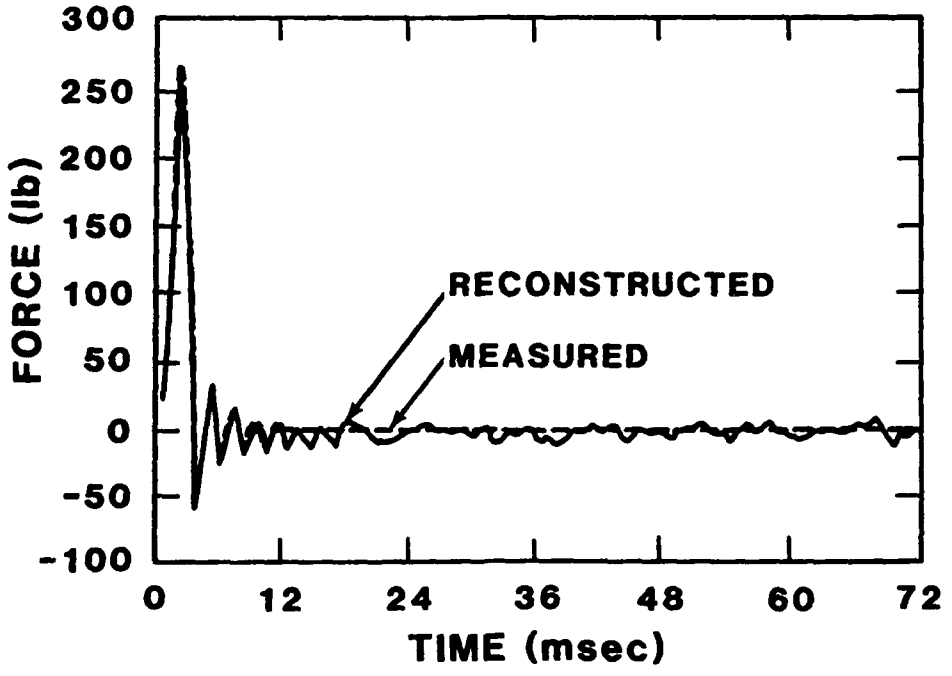


ESTIMATED FORCE AND MEASURED FORCE APPLIED TO A BAR

Sandia National Laboratories

VG-2: Reconstruction of Dynamic Structural Inputs from Measured Data

To demonstrate the general force reconstruction problem, an acceleration measurement from a uniform bar is shown in the top graph. The bar was excited in the axial direction with an instrumented hammer which is typically used for modal analysis. The excitation force cannot be inferred from the acceleration response shown. The bottom graph shows the measured force from the instrumented hammer compared to a reconstructed force which was estimated with a deconvolution technique that is presented in the following viewgraphs.

# PURPOSE OF FORCE ESTIMATION WITH DECONVOLUTION TECHNIQUE

- PROVIDE A POTENTIALLY BETTER FORCE ESTIMATE WITH GREATER FREQUENCY CONTENT

- VERIFY PREDICTED FORCES FROM COMPUTER CODES

Sandia National Laboratories

VG-3: Purpose of the Force Estimation with Deconvolution Technique

There are two reasons to estimate or reconstruct dynamic forces from measured structural response data of penetrator field tests. The first reason is to extend the frequency content in the force estimate. The penetrator structure used for the field test has 20 structural modes in the frequency range of 0-4 kHz which restricts the estimate of rigid body motion to at least one-half the frequency of the first mode at 728 Hz or about 400 Hz. Consequently, if the force is estimated by the equation Force = mass x acceleration, then the acceleration measurement must be filtered to 400 Hz and determines the frequency content in the force. A potentially better estimate of the force can be made by removing the structural response from the data so that the correct rise time and frequency content in the force is preserved. A second reason to reconstruct forces from measured structural response data is to verify computer codes which model both the penetrator structural response and the predicted force environment. The computer codes can then be used to predict structural response for penetration environments not tested.

# ULTIMATE GOAL

**BASIC MEASUREMENT PROBLEM:**

$$\underline{y}(t) = \int_0^t \underline{h}(\tau)\,\underline{f}(t-\tau)\,d\tau$$

**WHERE:**

- $\underline{y}(t)$ — **IS A VECTOR OF MEASURED RESPONSES,**
- $\underline{h}(t)$ — **IS A MATRIX OF IMPULSE RESPONSE FUNCTIONS, AND**
- $\underline{f}(t-\tau)$ — **IS A VECTOR OF FORCES APPLIED TO THE SEPW**

Sandia National Laboratories

VG-4: Ultimate Goal

The ultimate goal of the force reconstruction technique used is to solve the basic measurement convolution integral shown in the time-domain here.

# BLOCK DIAGRAM OF CONVOLUTION IN THE FREQUENCY-DOMAIN

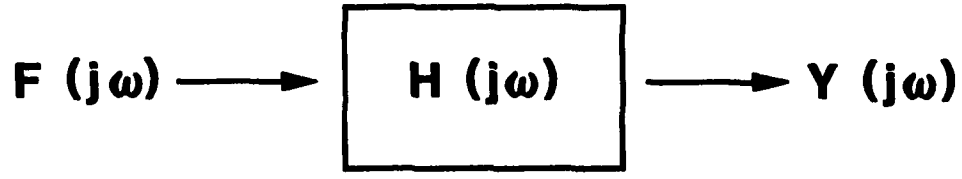


F (jω) = THE FOURIER TRANSFORM OF THE EXCITATION FORCE;

Y (jω) = THE FOURIER TRANSFORM OF THE MEASURED RESPONSE; AND

H (jω) = COMBINED INSTRUMENTATION AND STRUCTURAL FREQUENCY RESPONSE FUNCTION

Sandia National Laboratories

VG-5: Block Diagram of Convolution in the Frequency-Domain

The deconvolution problem was implemented in the frequency-domain where the convolution integral becomes a multiplication of the Fourier transform of the excitation force and the combined instrumentation and structural frequency response function. The frequency response function must be inverted and multiplied by the Fourier transform of the measured response in order to reconstruct the force that caused that response. It is convenient to work in the frequency-domain for structural deconvolution problems because the frequency content of each quantity is easy to identify.

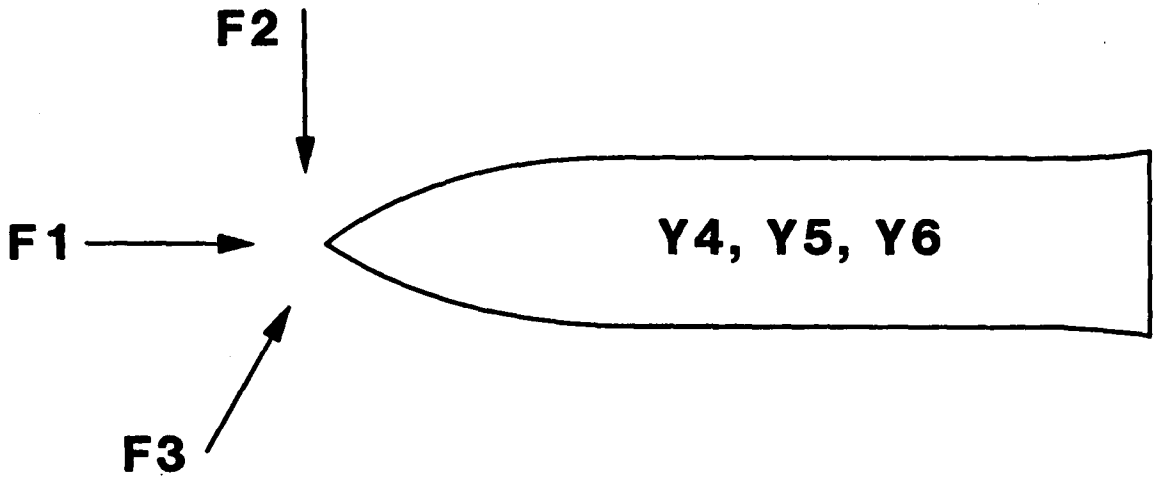


## GENERAL FORMULATION:

$$\begin{bmatrix} Y4 \\ Y5 \\ Y6 \end{bmatrix} = \begin{bmatrix} H14 & H24 & H34 \\ H15 & H25 & H35 \\ H16 & H26 & H36 \end{bmatrix} \begin{bmatrix} F1 \\ F2 \\ F3 \end{bmatrix}$$

**AND SOLVE FOR THE FORCE VECTOR BY A PSUEDO-INVERSE TECHNIQUE.**

Sandia National Laboratories

VG-6: Force Reconstruction by a Deconvolution Technique for an Experimental Penetrator

The deconvolution technique as applied to an experimental penetrator is shown. A matrix of frequency response functions was measured in the laboratory from the application of three orthogonal forces to the penetrator nose. These frequency response functions were combined with the responses measured in a field test at Tonopah Test Range, GM118. In the GM118 field test, the 370 lb-pentrator was fired in a Davis Gun shot into Antelope Tuff at about 2000 fps at a 60 degree impact angle and a 0 degree angle of attack. For this test, the penetrator was instrumented with four strain gages at one axial location (about 23 in from the nose) on the interior of the case and with one axial accelerometer located in the data cannister (about 16.5 in from the nose). From the field data, three orthogonal forces (one axial and two lateral) were reconstructed with the strain gage data and an axial force was reconstructed from the accelerometer data. The two axial forces exhibit unique characteristics derived from the type of measured response used for their reconstruction and will be compared; the two lateral forces are the first lateral forces reconstructed from penetrator data. The application of the force reconstruction technique requires both high-quality laboratory measurements of the frequency response functions and high-quality field test penetrator response data. The outstanding quality of the penetrator field data available from Sandia's instrumentation systems allow the opportunity for force reconstruction.

# REVERSE HOPKINSON BAR TEST CONFIGURATION

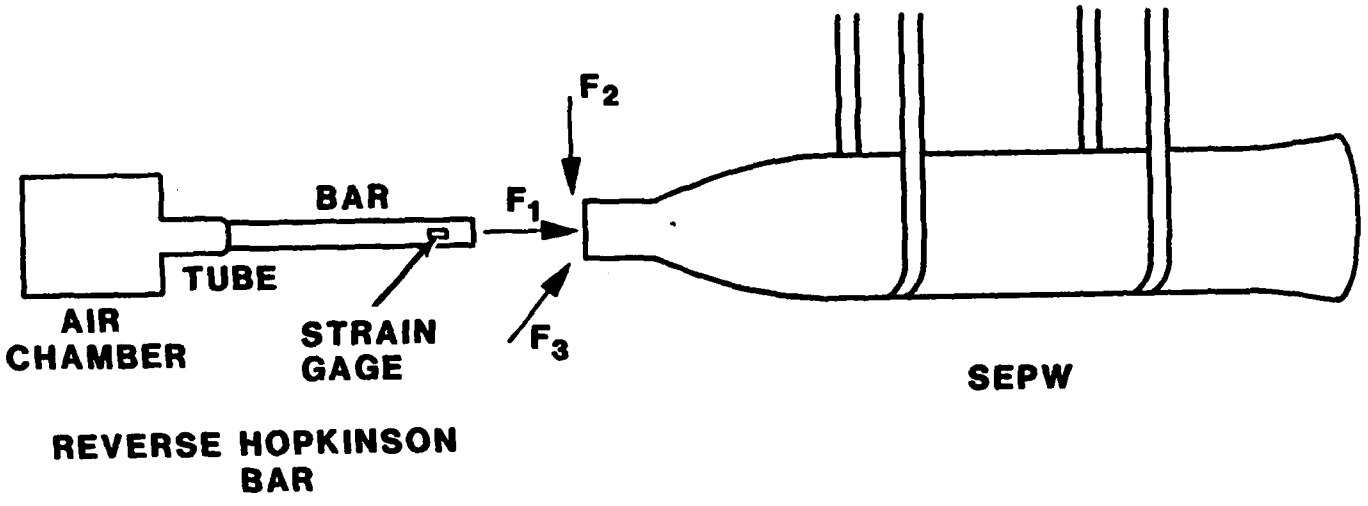


Sandia National Laboratories

VG-7: Reverse Hopkinson Bar Test Configuration

The combined instrumentation and structural frequency response functions were measured in a laboratory test which employed the Reverse Hopkinson Bar test technique that was developed in Sandia's Shock Lab to generate high amplitude forces. The forces generated were 100-160 klbs and were applied to the Strategic Earth Penetrator Weapon in the three orthogonal force directions shown. For this test, the penetrator retained the snub-nose which is removed in the last machining process of the case so that a flat surface was available for the three orthogonal impacts. The Reverse Hopkinson Bar consists of a bar which is accelerated by a pressurized air chamber down a tube to impact the test structure. If certain conditions are met, the force generated by the bar has a duration governed by the bar length and an amplitude proportional to the bar velocity. The bar used here had a 1 in diameter and a 10 in length, so the forces applied to the bar were nominally about 100 micro-seconds long. The forces applied in the lateral direction were longer in duration and lower in amplitude because of reflections generated in the 2 in diameter, 1.75 in long snub nose. The penetrator was supported in a free-free boundary condition by the nylon straps shown.

# REVERSE HOPKINSON BAR FORCE INPUT

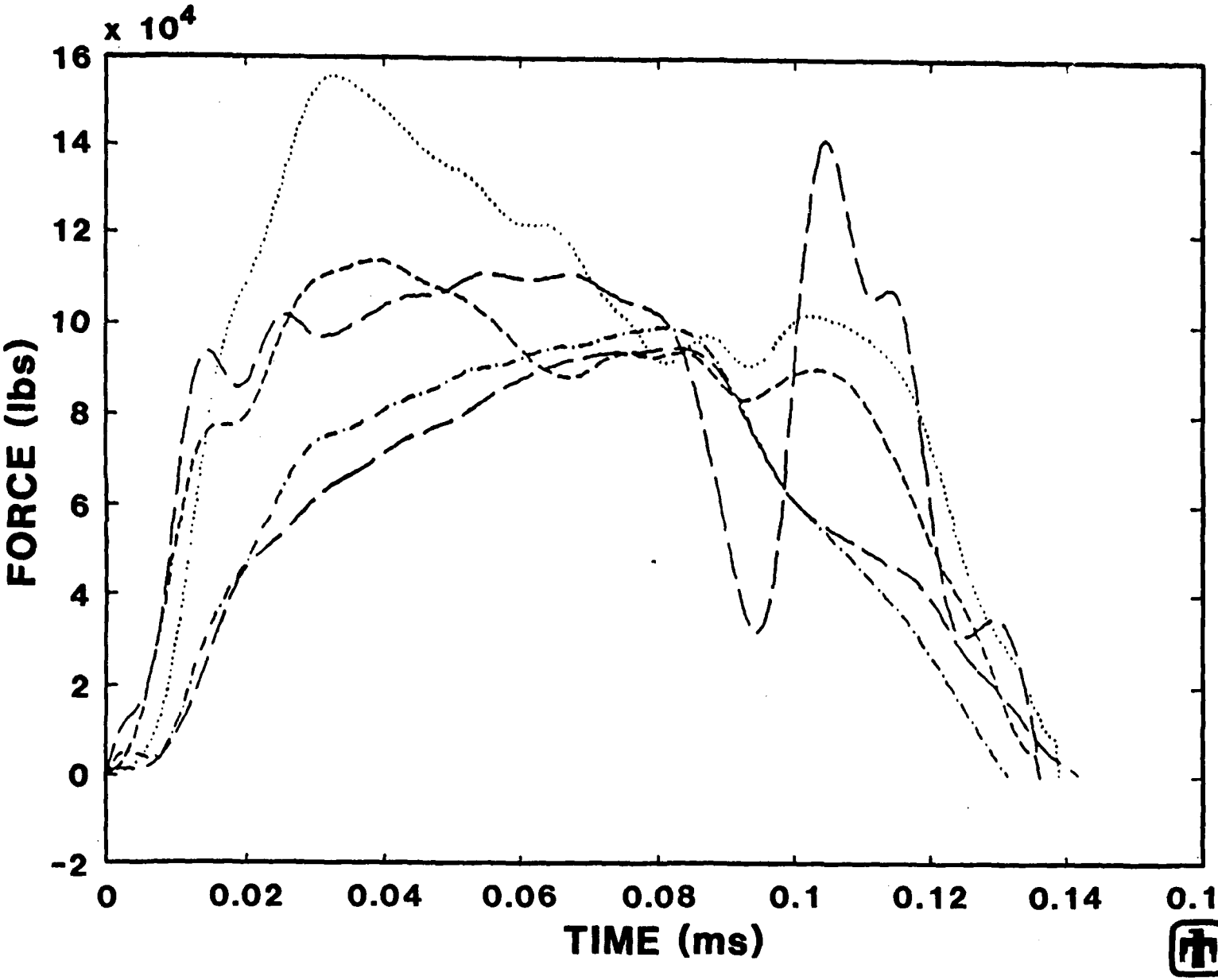


Sandia National Laboratories

VG-8: Reverse Hopkinson Bar Force Input

The five forces applied to the SEPW in the axial direction are shown. Five forces were also applied for each of the two lateral directions. The multiple force and excitation measurements for each orientation allowed the calculation of the frequency response functions by an averaged ratio of the cross-correlation between the force and the response to the auto-correlation of the force.

# SEPW RESPONSE TO REVERSE HOPKINSON BAR FORCE INPUT

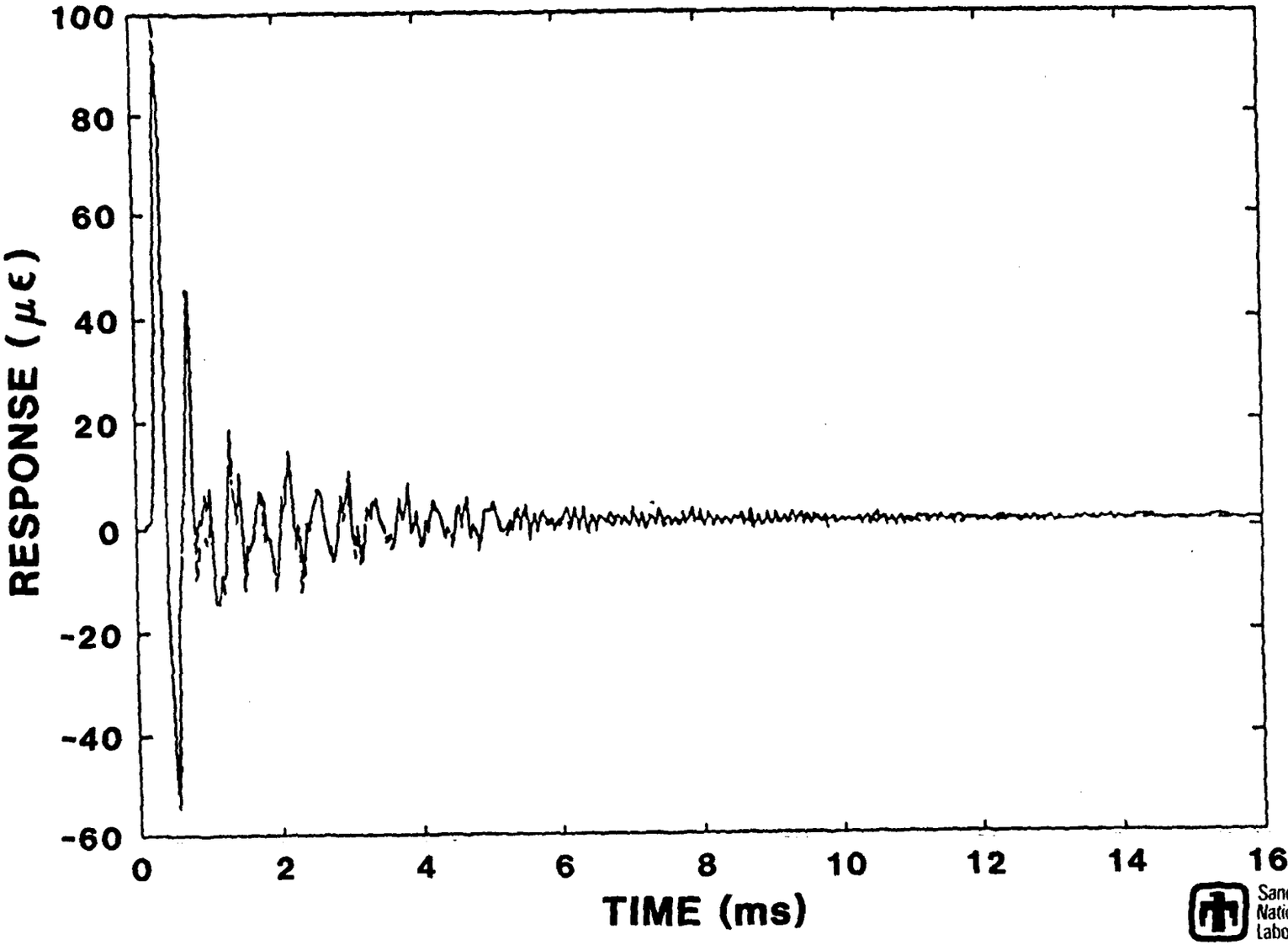


Sandia National Laboratories

VG-9: SEPW Response to Reverse Hopkinson Bar Force Input

A typical response of the penetrator to a force input is shown in the time-domain. The response was sampled at 24255 Hz and filtered with a four-pole, high-pass, analog Butterworth filter whose cut-off frequency was 4800 Hz.

# GM118 MEASURED ACCELERATION

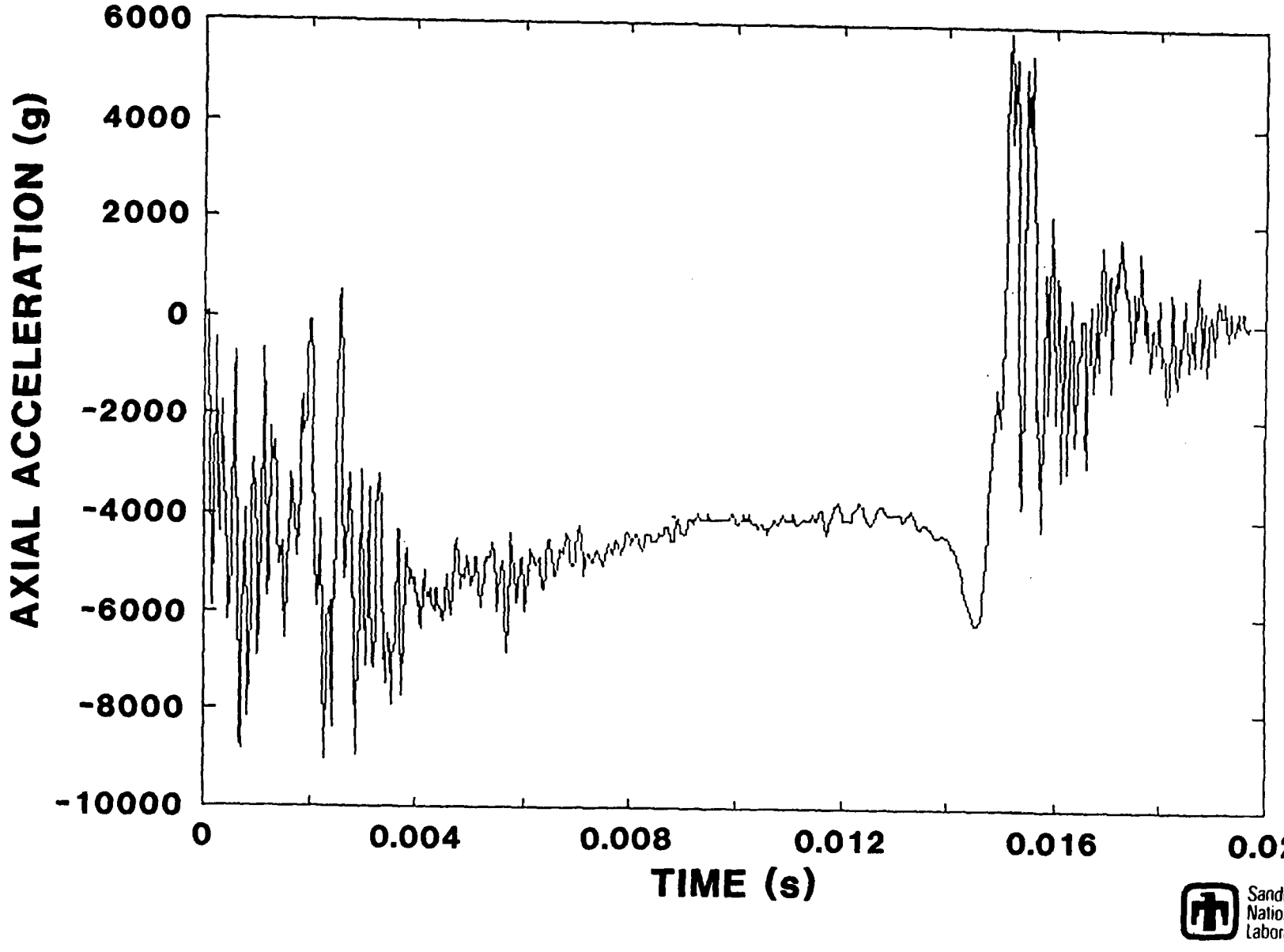


Sandia National Laboratories

VG-10: GM118 Measured Acceleration

The axial acceleration measured in the data cannister is shown. The accelerometer response is also used to trigger the data cannister. This data, as well as the other data measured during the field test, was sampled at 34426 Hz and was analog filtered by a 4-pole, high-pass, analog Butterworth filter whose cut-off frequency was 9600 Hz.

# GM118 AXIAL FREQUENCY RESPONSE FUNCTION (3 kHz)

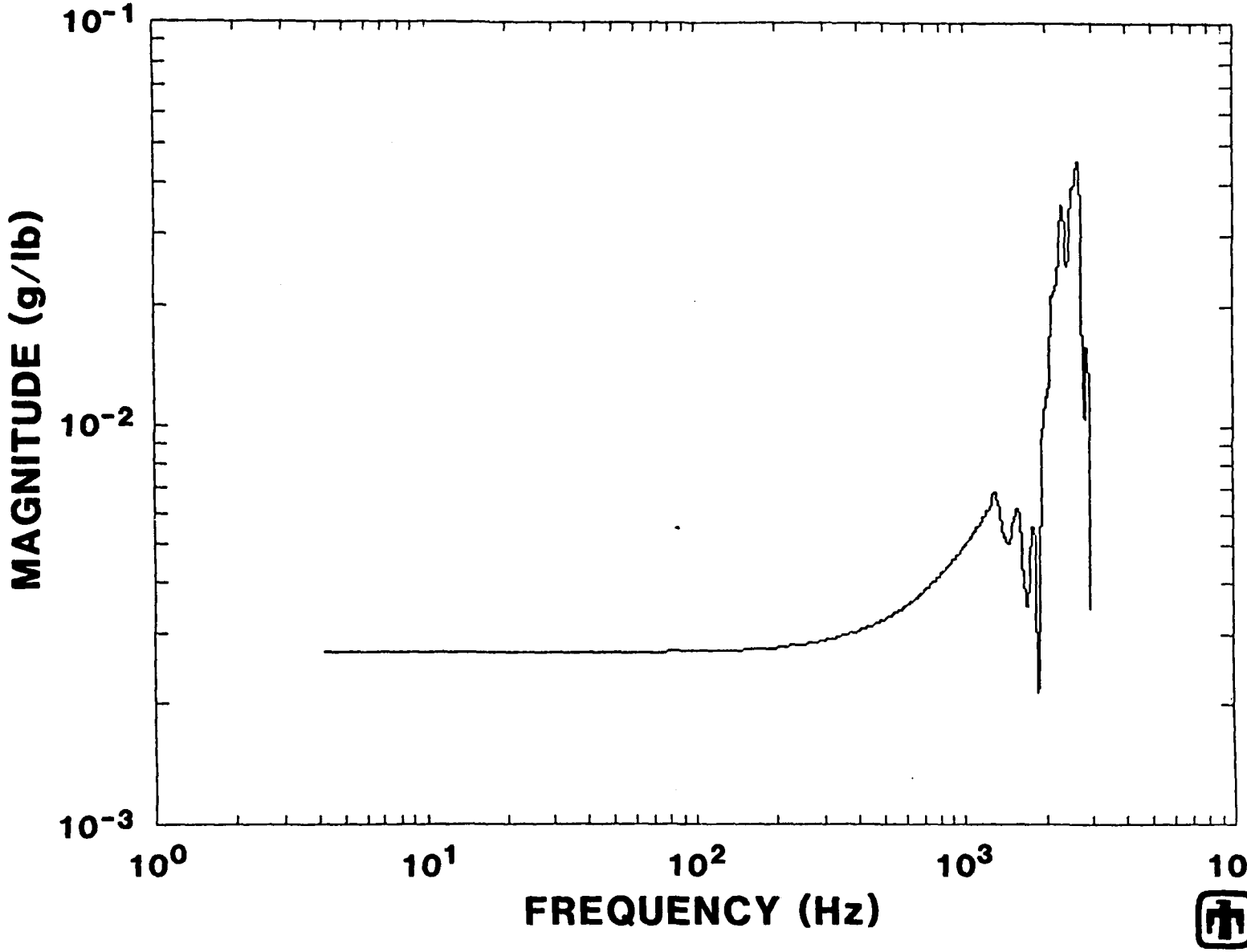


Sandia National Laboratories

VG-11: GM118 Axial Frequency Response Function (3 kHz)

This axial frequency response function was calculated from the Reverse Hopkinson Bar data and includes the first system axial mode at 1800 Hz and the first case axial mode at 2456 Hz. The function is unique to the GM118 configuration for SEPW and was truncated at 3 kHz because of noise which contaminated the force reconstruction result.

# GM118 FORCE RECONSTRUCTED FROM AXIAL ACCELERATION

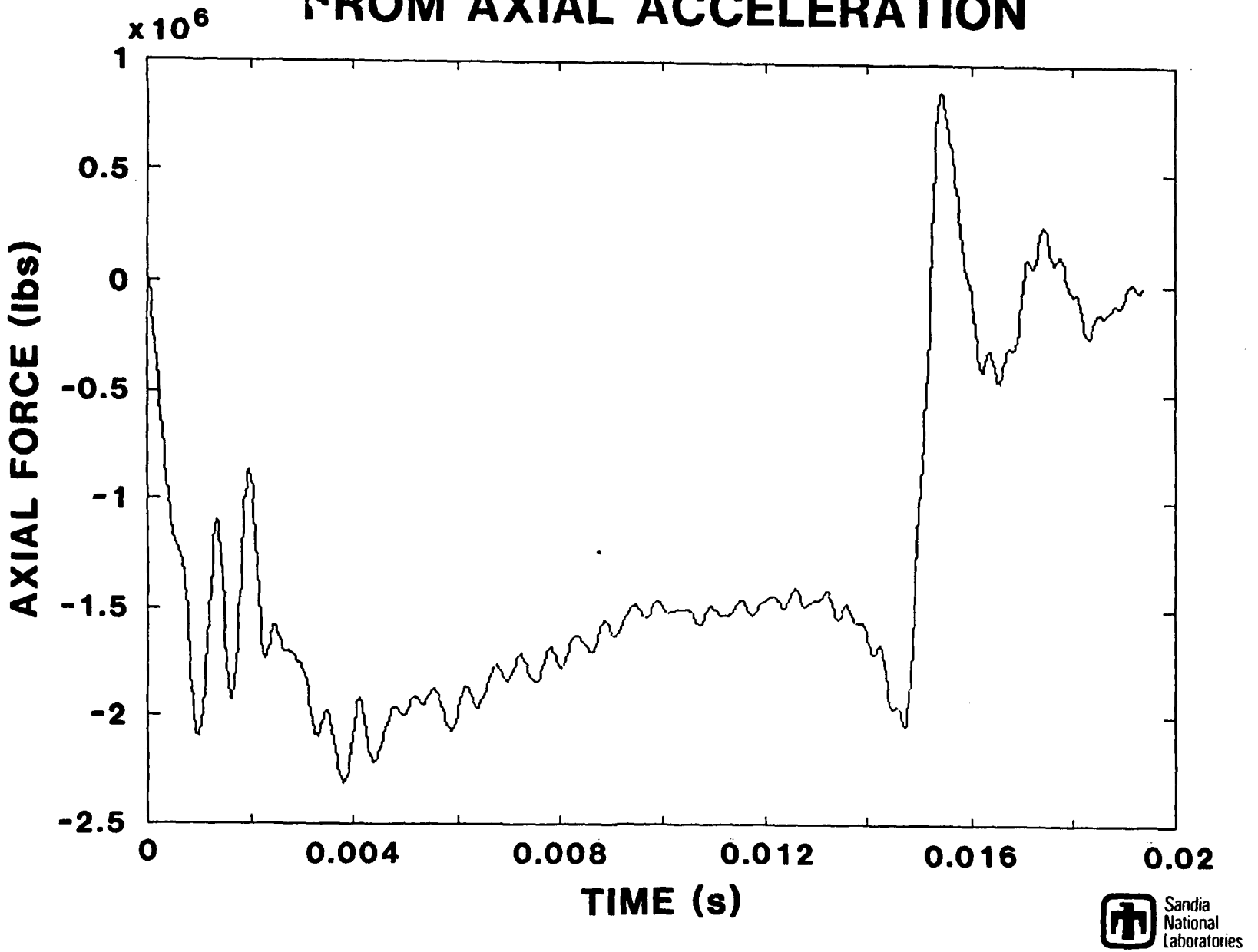


Sandia National Laboratories

VG-12: GM118 Force Reconstructed from Axial Acceleration

This force represents the sum of the forces from the nose and tail force and yields the correct velocity when derived from a momentum principle.

# FREQUENCY RESPONSE FUNCTIONS FOR AXIAL INPUT FORCE

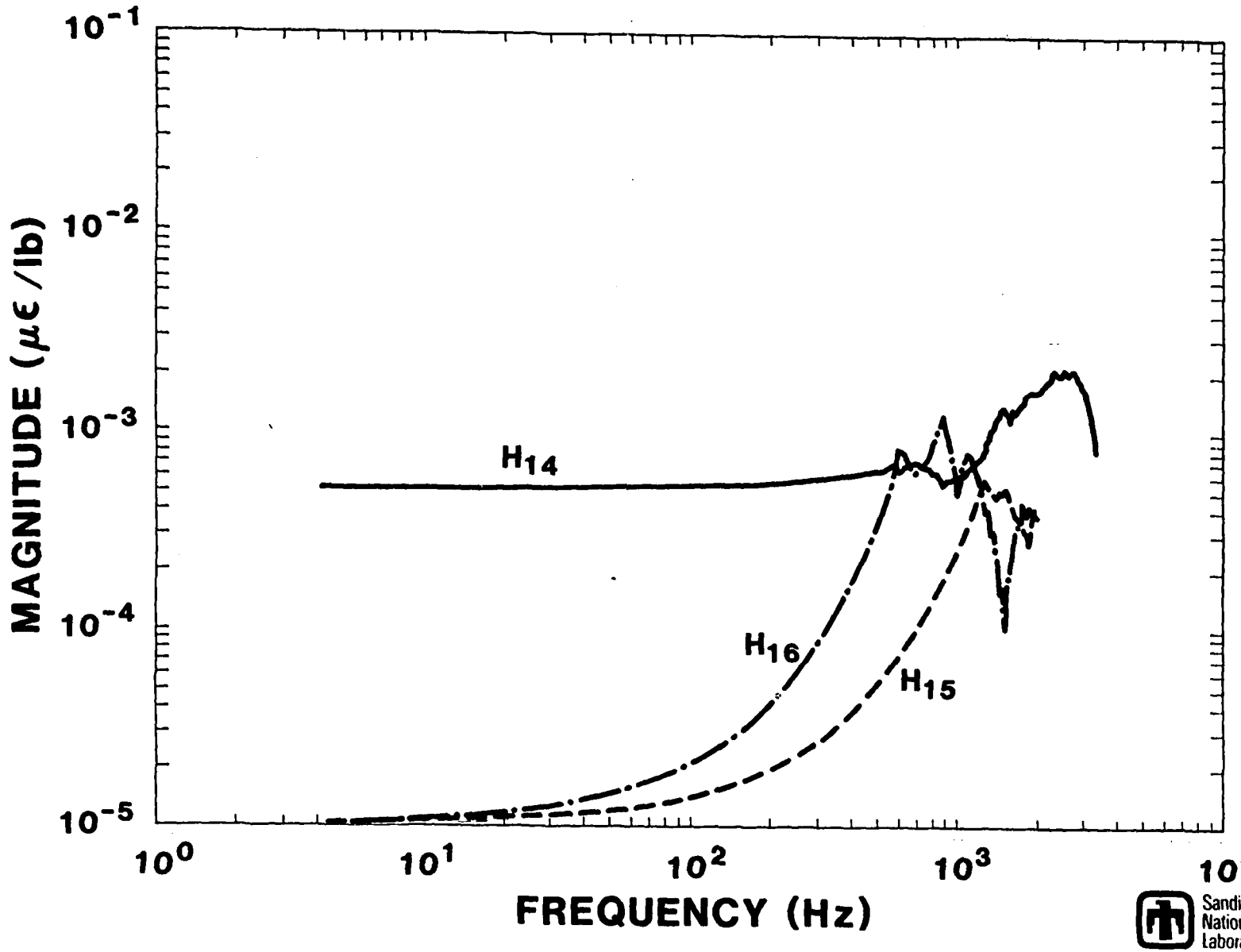


Sandia National Laboratories

# FREQUENCY RESPONSE FUNCTIONS FOR LATERAL (02) INPUT

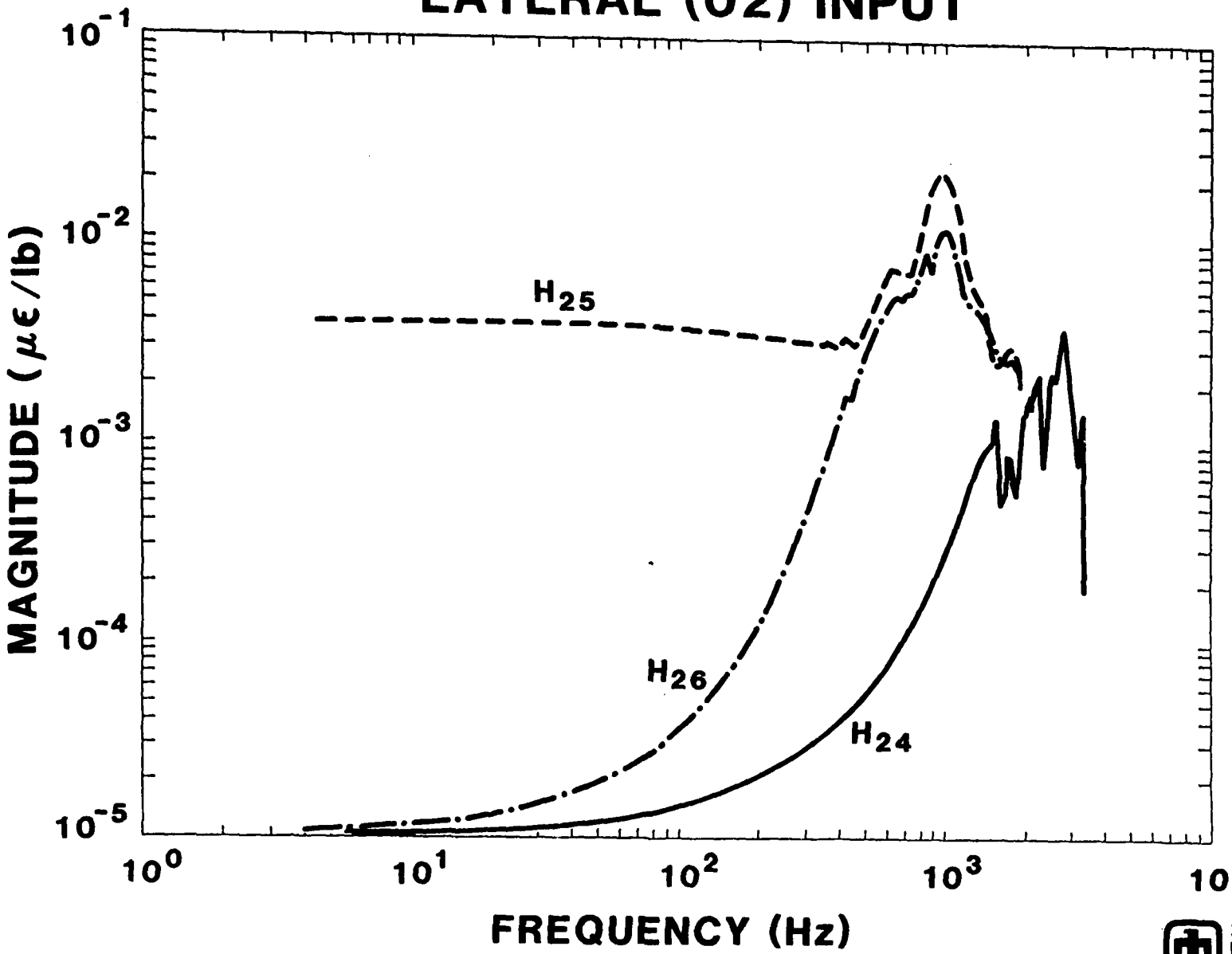


Sandia National Laboratories

# FREQUENCY RESPONSE FUNCTIONS FOR LATERAL (13) INPUT

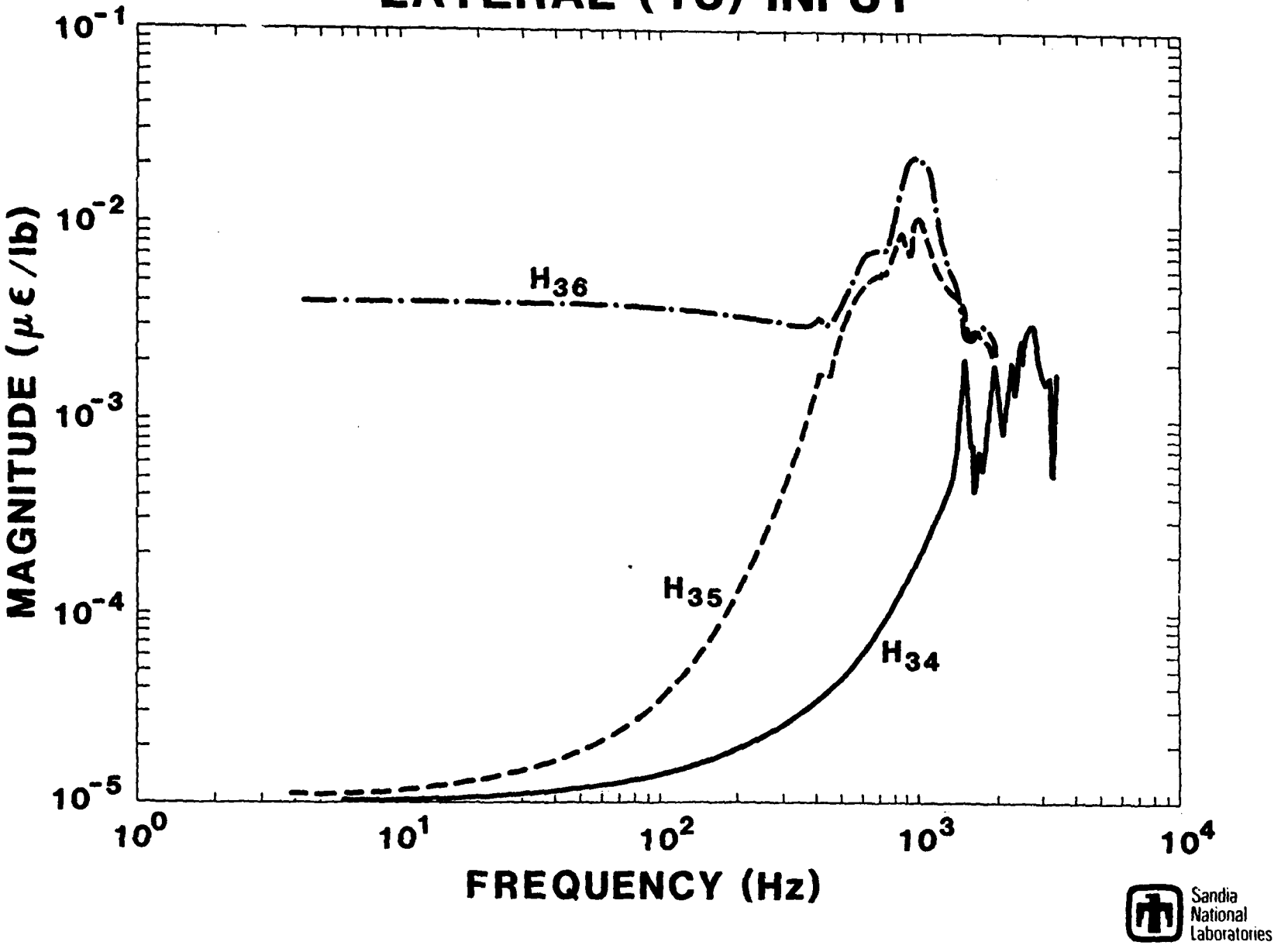


Sandia National Laboratories

VG-13-15:Frequency Response Functions

Each viewgraph represents a column in the frequency response function matrix.

# THE INVERSE OF THE AXIAL FREQUENCY RESPONSE FUNCTION FOR AN AXIAL INPUT FORCE ($h^{-1}_{11}$)

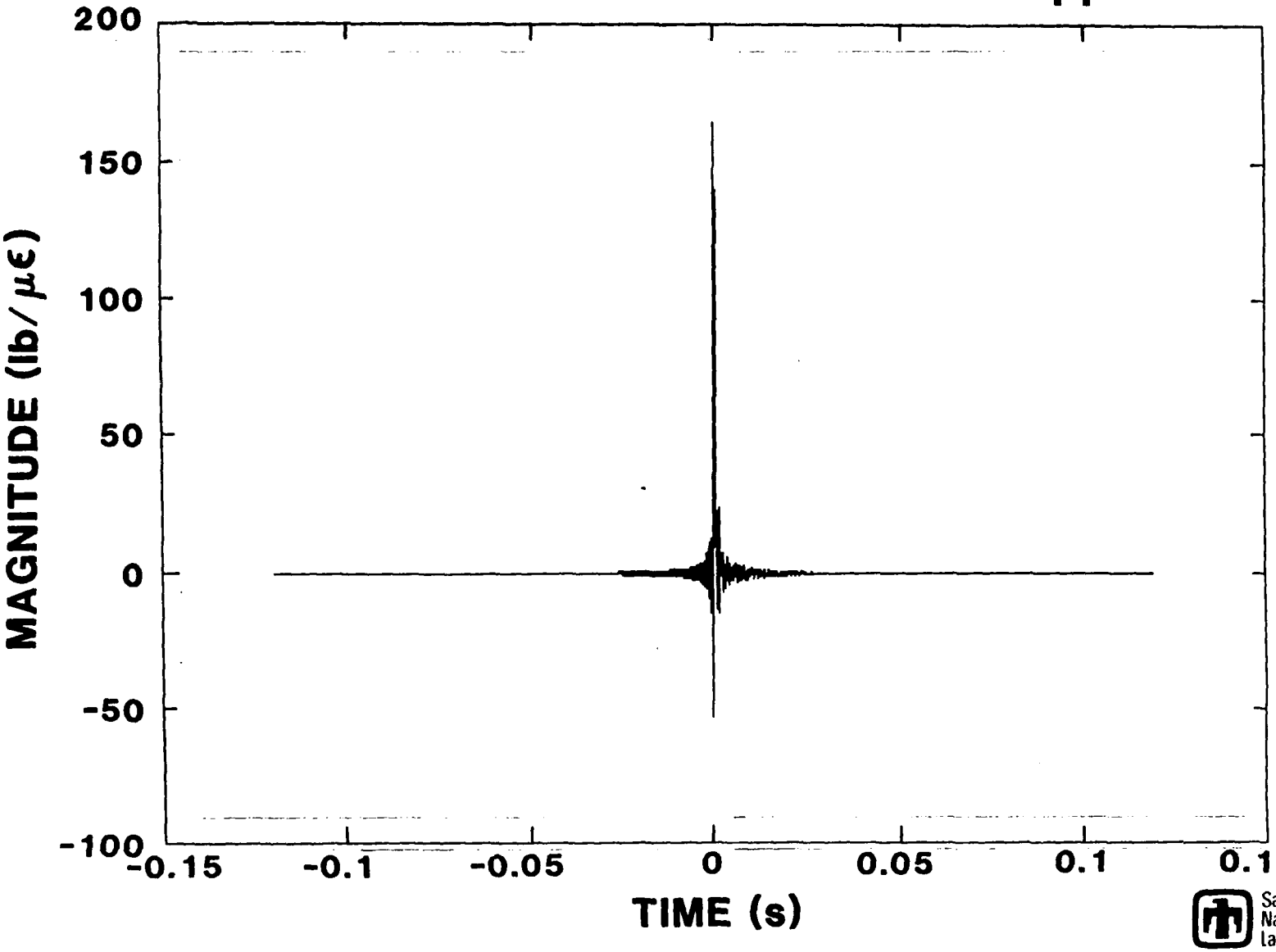


Sandia National Laboratories

# THE INVERSE OF THE LATERAL FREQUENCY RESPONSE FUNCTION (02 plane) FOR AN AXIAL FORCE INPUT ($h_{12}^{-1}$)

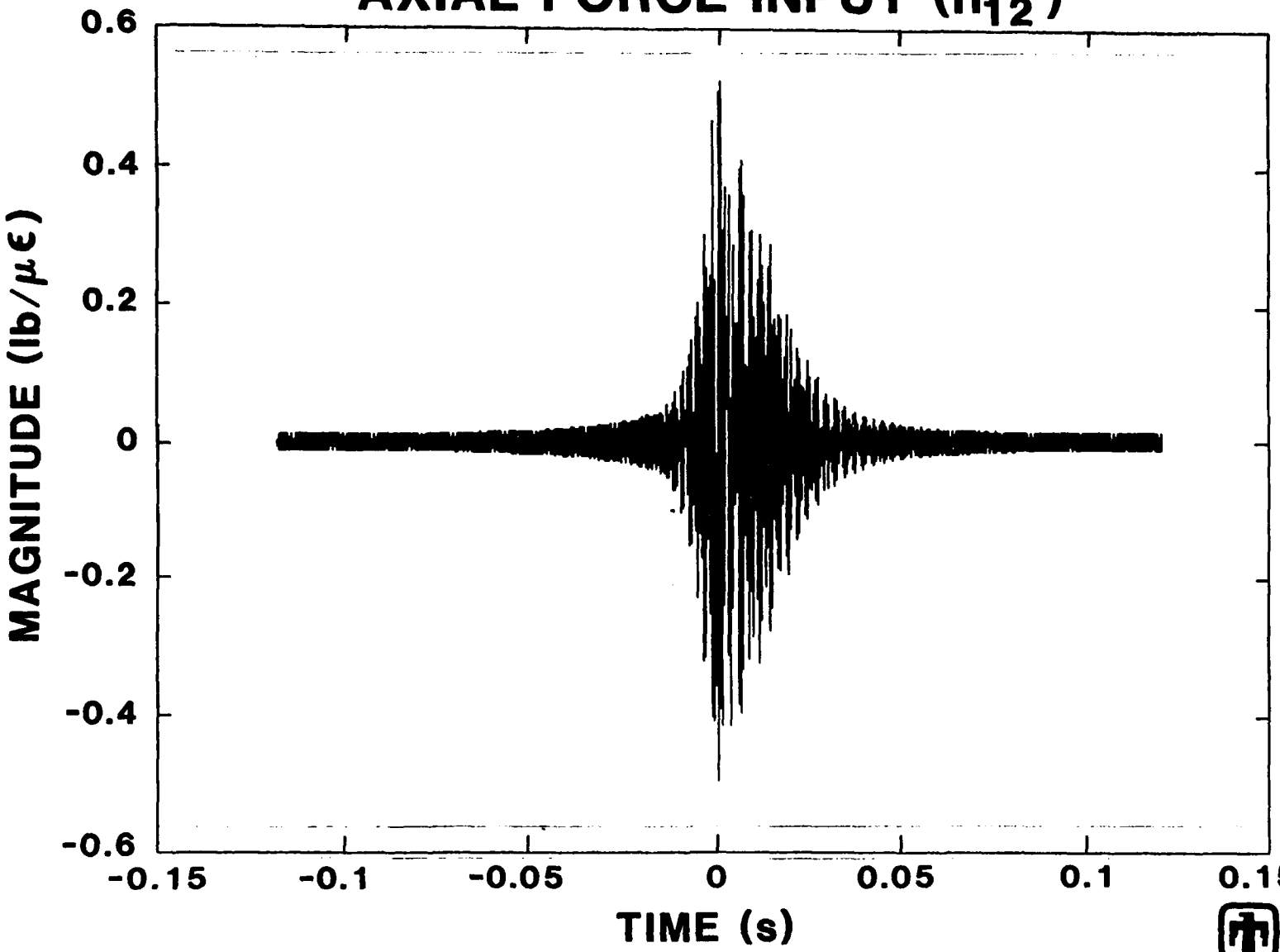


Sandia National Laboratories

VG-16-17:Inverse Frequency Response Function Matrix components

These graphs show the non-causal nature of the functions which is caused by the delay between the input and the response. The in-axis (16) function shows much less noise and much higher magnitude than the off-axis (17) function as expected.

# GM118 AXIAL STRAIN RESPONSE

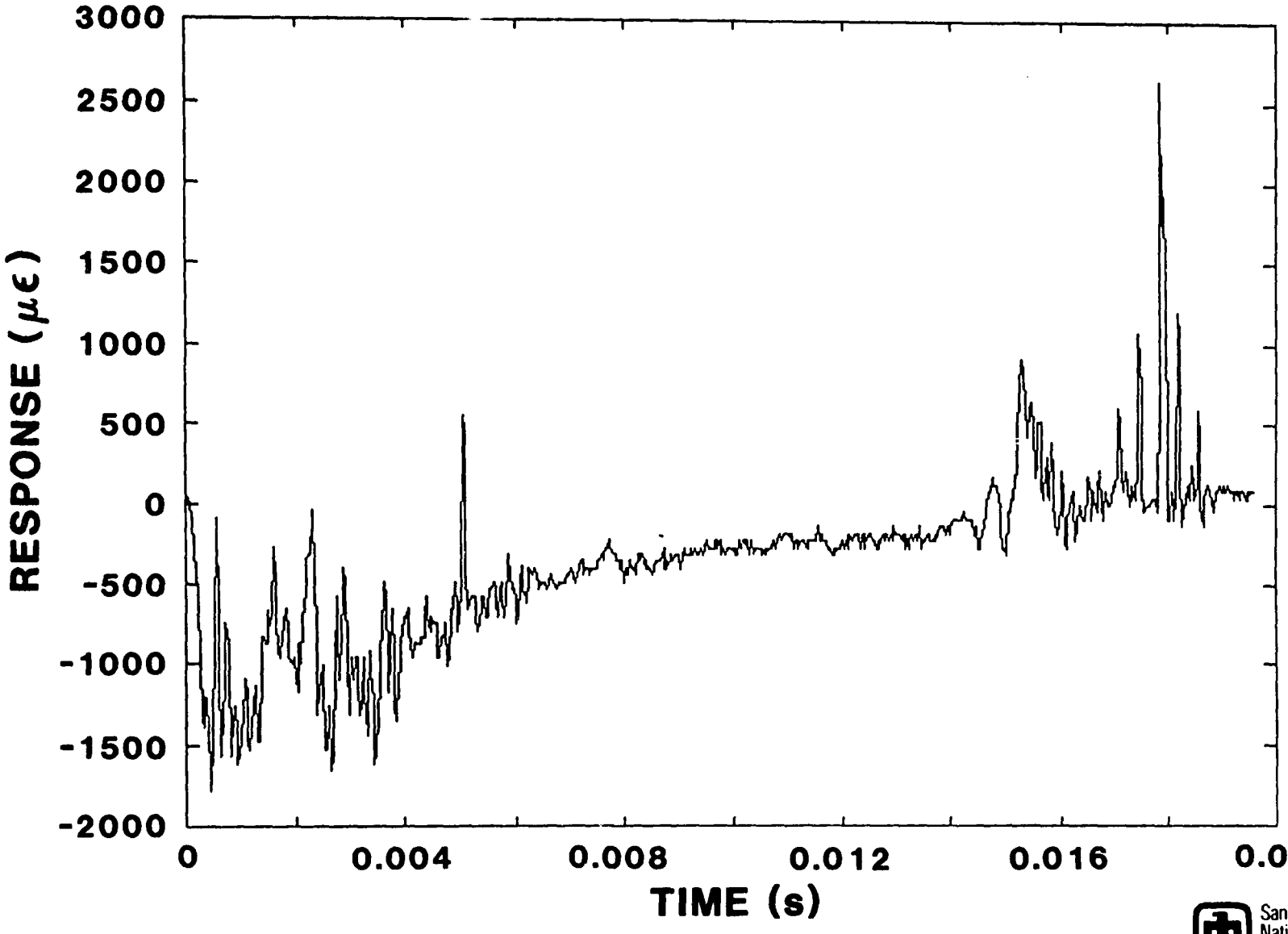


Sandia National Laboratories

# GM118 AXIAL FORCE RECONSTRUCTED FROM THREE ORTHOGONAL STRAIN RESPONSES

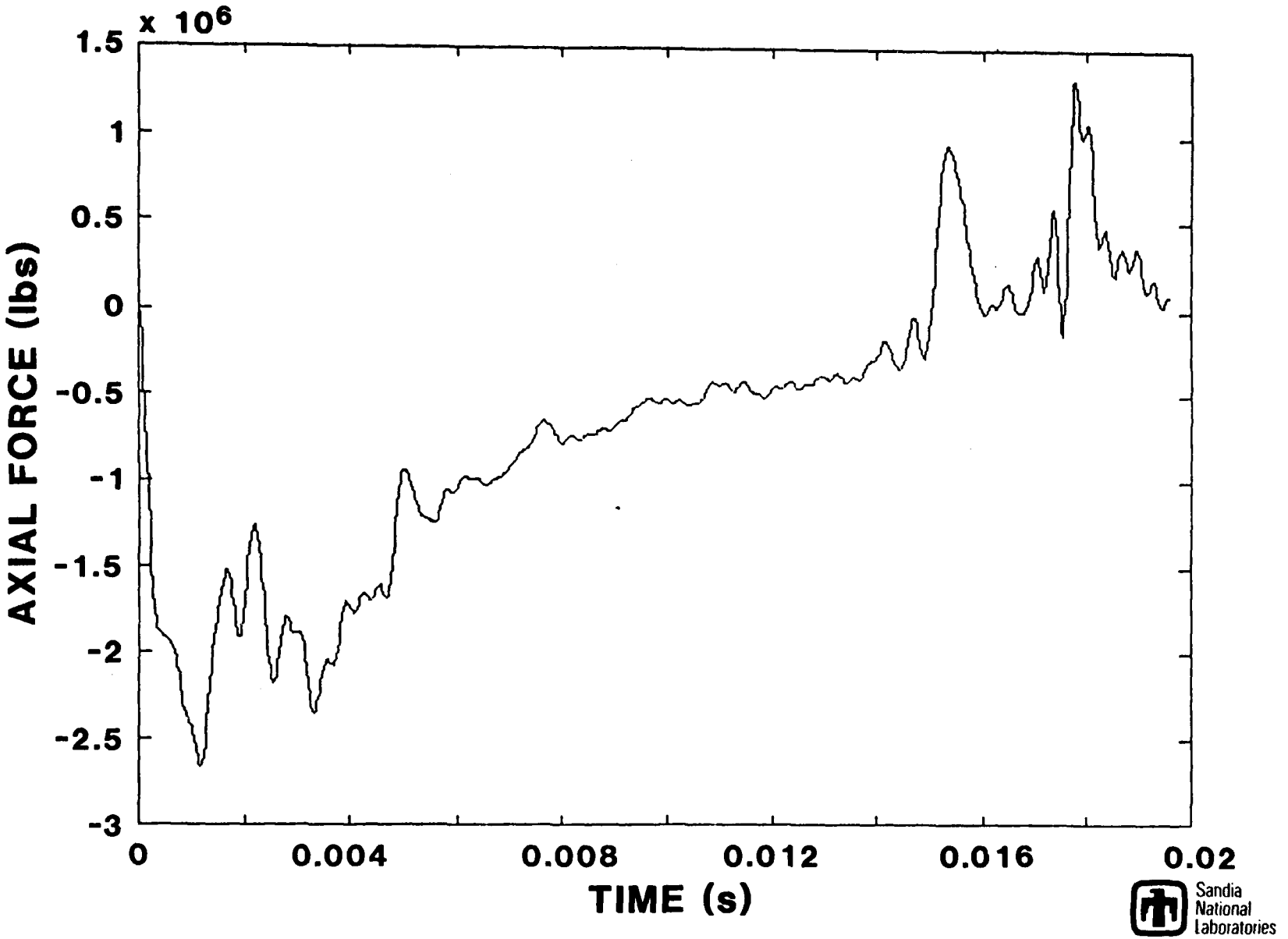


Sandia National Laboratories

# COMPARISON OF MEASURED AXIAL STRAIN AND RECONSTRUCTED AXIAL FORCE FOR GM118

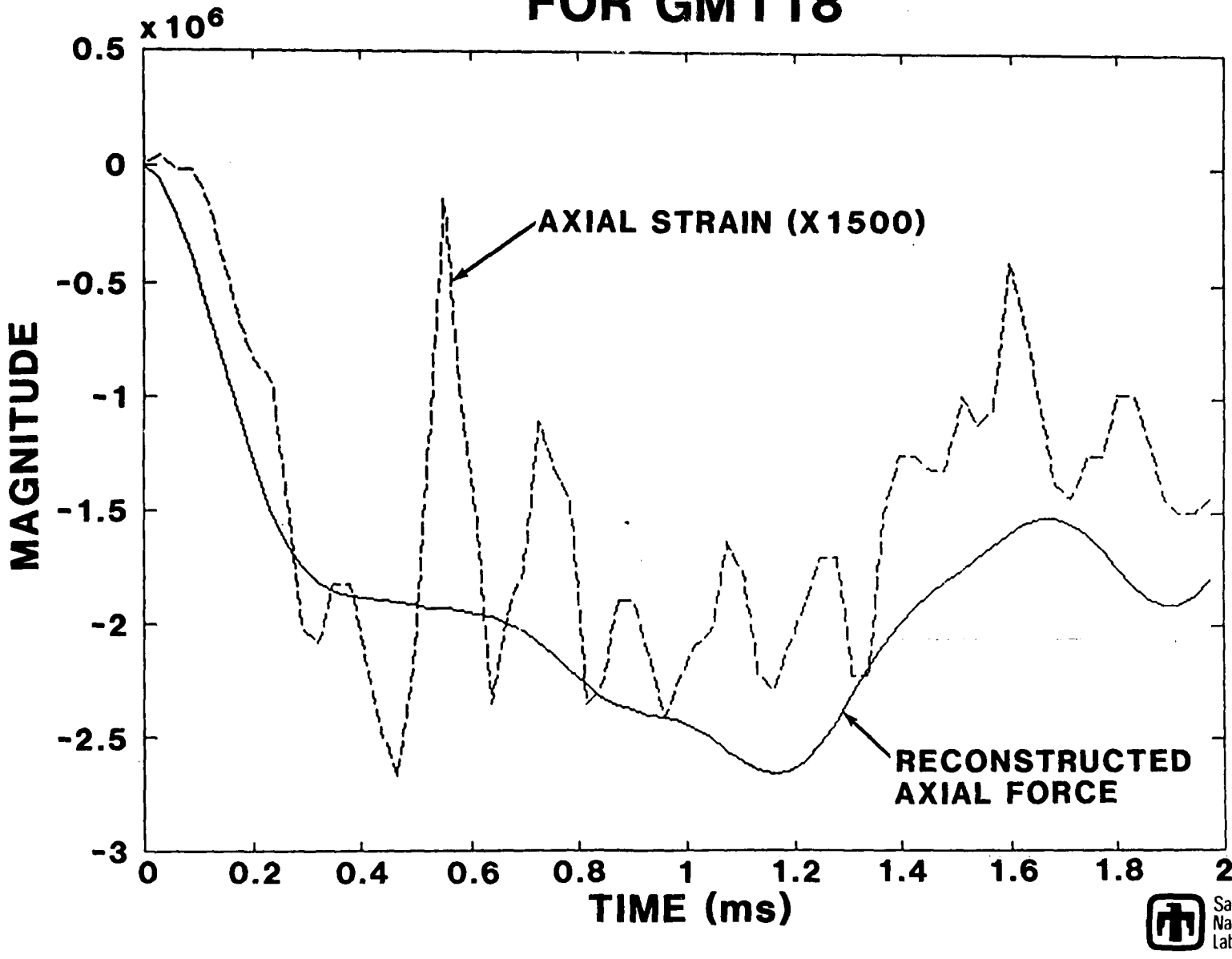


Sandia National Laboratories

VG-18-20:GM118 Axial Strain and Reconstructed Force

The structural response has been removed from the measured strain, and the reconstructed force reflects the difference between the nose force and the tail force. The rise time in the force has been preserved in the process as shown in the comparison of the force and the strain for 2 ms.

# MEASURED LATERAL (02 plane) STRAIN RESPONSE FOR GM118

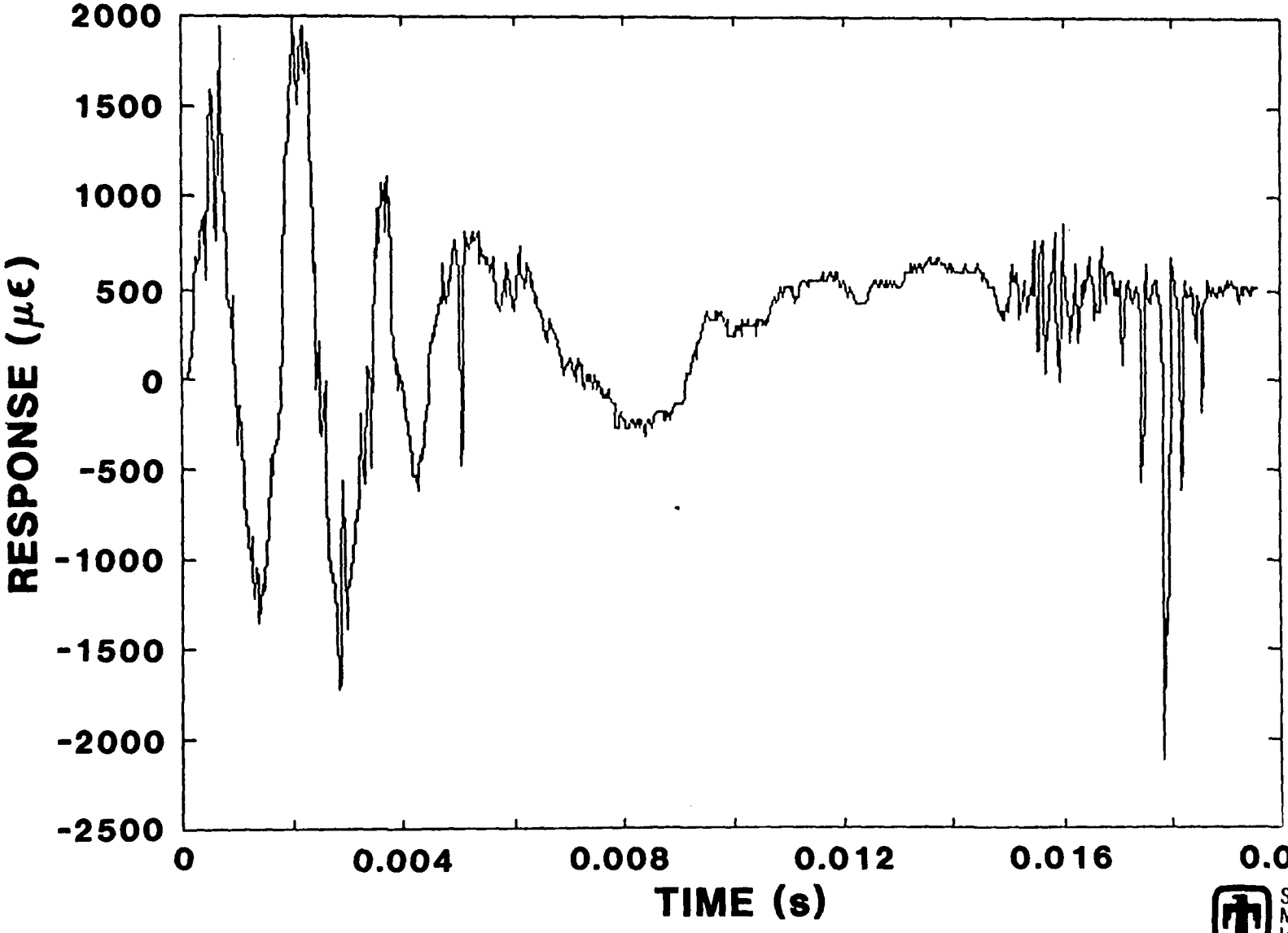


Sandia National Laboratories

# GM118 LATERAL (02 plane) FORCE RECONSTRUCTED FROM THREE ORTHOGONAL STRAIN RESPONSES

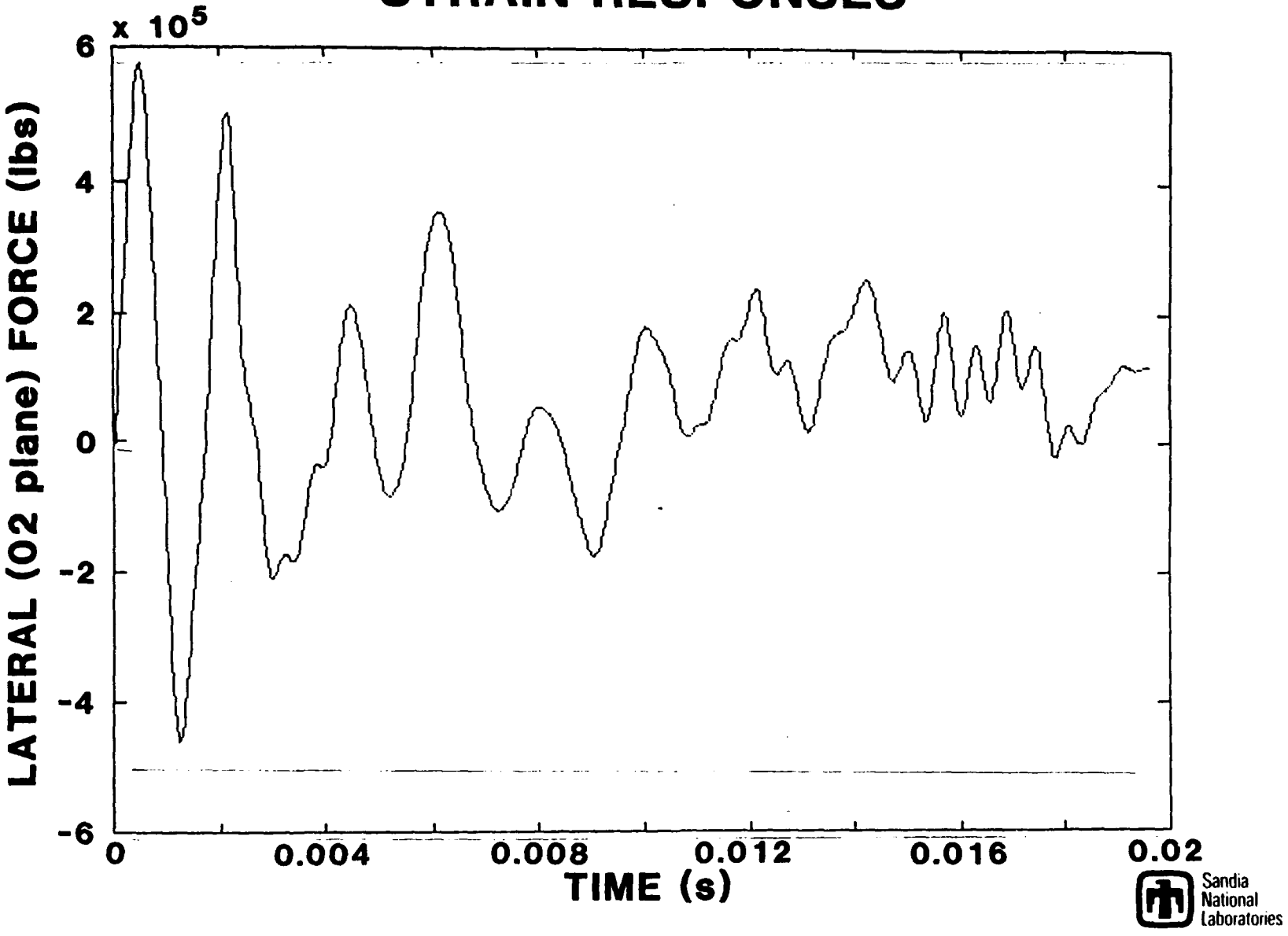


Sandia National Laboratories

# MEASURED LATERAL (13 plane) STRAIN RESPONSE FOR GM118

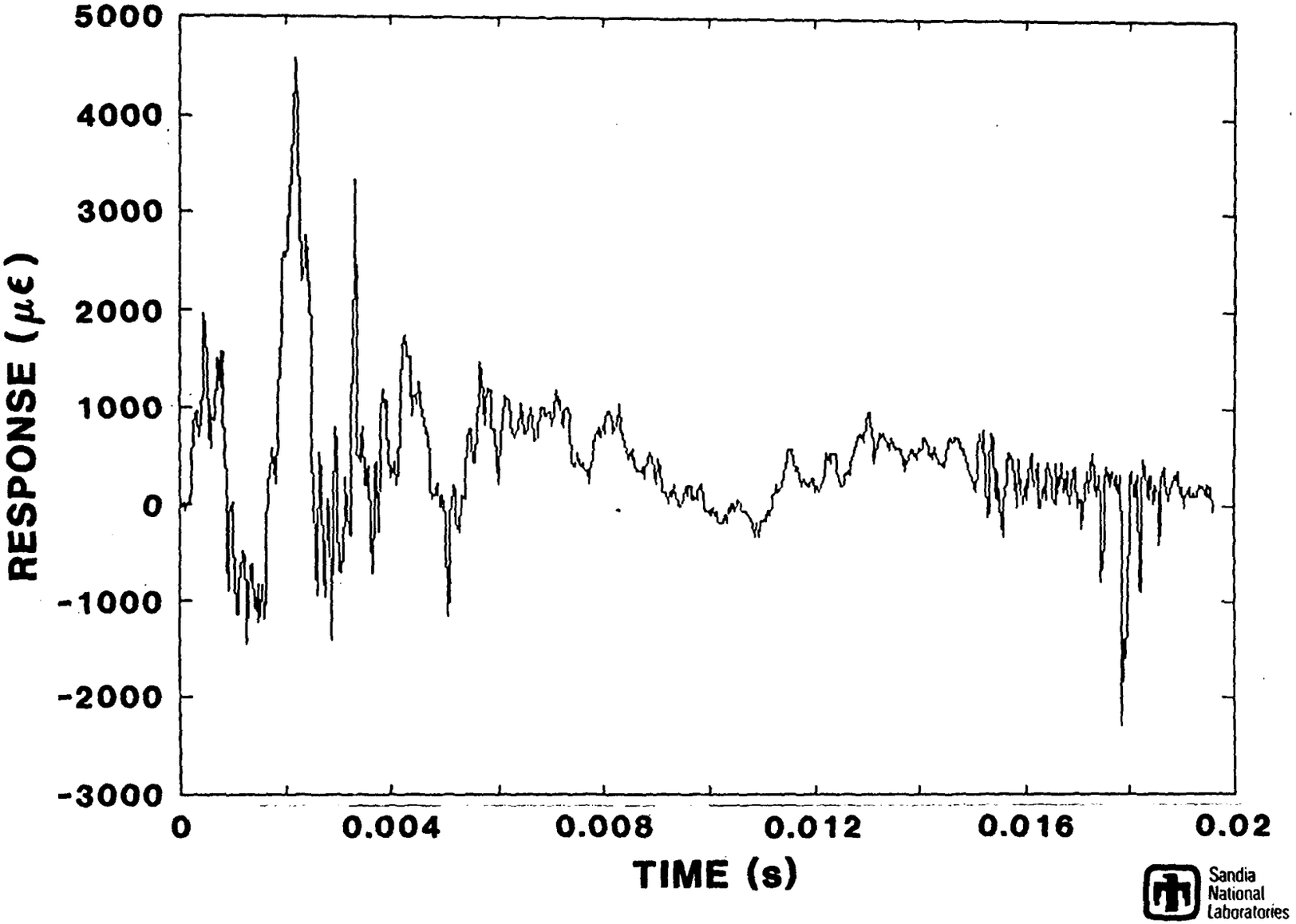


Sandia National Laboratories

# GM118 LATERAL (13 plane) FORCE RECONSTRUCTED FROM THREE ORTHOGONAL STRAIN RESPONSES

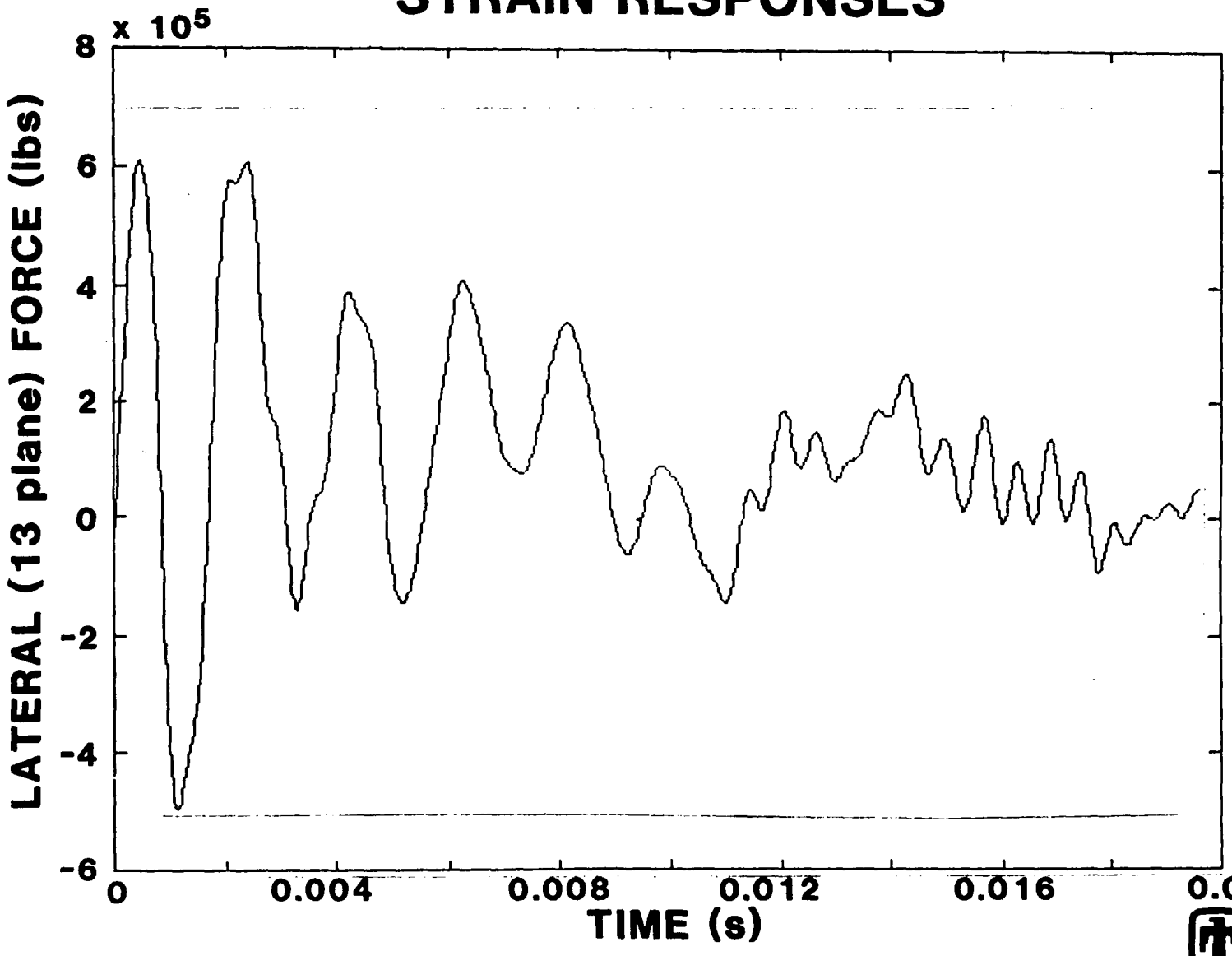


Sandia National Laboratories

VG-21-24:GM118 Lateral Strains and Reconstructed Forces

These are the first lateral forces reconstructed from penetrator field test data at Sandia and indicate the nose force and the tail force in the first 2 ms. After 2 ms, the penetrator is immersed in the medium.

# CONCLUSIONS

- AXIAL FORCES HAVE BEEN ESTIMATED FROM BOTH ACCELERATION AND STRAIN GAGE DATA TO 3300 Hz

- LATERAL FORCES HAVE BEEN ESTIMATED FROM STRAIN GAGE DATA TO 2000 Hz

- INSTRUMENTATION AND STRUCTURAL ANALYSIS TECHNIQUES ARE AVAILABLE TO ESTIMATE DISTRIBUTED FORCES AND MOMENT ABOUT THE CENTER OF MASS

Sandia National Laboratories

VG-25: Conclusions

Further information about this analysis may be obtained in SAND88-3046 of the same title which is available from NTIS.

# WEIGHT REDUCTION EFFECTS
# ON
# EARTH PENETRATING WEAPON CAPABILITIES (U)

(AIAA-88-C-1063)

NOVEMBER 1988

NED R. HANSEN

KEVIN R. EKLUND

SANDIA NATIONAL LABORATORIES
ALBUQUERQUE, NM

SNLA
NRH:5165, 10/88

# EPW WEIGHT TRADEOFFS

The motivation for the Earth Penetrating Weapon (EPW) weight reductions is to maximize the overall system (delivery and EPW) survivability envelope.

From the delivery system standpoint, a lighter EPW or system payload is most appealing. Generally, the lighter weight EPW gives the delivery system a greater range hence a greater standoff for the launch platform or more weapons per delivery vehicle for the same total weight. Rigorous tradeoffs or optimizations can only be done using a specific delivery system.

From the penetrator standpoint, a heavier EPW is best. The heavier EPW penetrates deeper with lower decelerations for the same frontal area and impact conditions. By not constraining the weight, the EPW designer is allowed greater flexibility and potentially a more robust EPW can be developed.

The presentation will be directed at methods for reducing the EPW weight while minimizing the reduction in the EPW operational capabilities.

# EPW WEIGHT TRADEOFFS

| Delivery System Standpoint | Penetrator Standpoint |
|---|---|
| "Lighter is Better" | "Heavier is Better" |
| Longer Delivery Range (Standoff) | Deeper Penetration |
| More Weapons per Vehicle | Lower Deceleration |
| Point Design Tradeoffs Required | More Design Flexibility |
| | Higher Capability |

Presentation Will Focus on Method for EPW Weight Reduction Consistant With Proper Penetrator Capabilities

SNLA

NRH:5165, 10/88

# DETERMINATION OF EPW CAPABILITIES

Before any comparisons of capability can be made, methods used to determine an EPW's capability must be defined. Testing and analysis are two complimentary methods used to determine an EPW capability.

A Davis Gun is used for the majority of the EPW testing. The Davis Gun is a recoilless gun that can give very precise impact conditions into "quality" geological targets. A "quality" in situ target is examined prior to testing by coring to determine if excessive weathering and nonhomogeneities exist. Impact conditions are generally selected to verify the predictions from analytical tools.

For scoping calculations, a modified version of the SAMPLL code is used to calculate survivability limits. The basis for the code is a set of empirical penetration equations which use S numbers to characterize the target hardness. A rigid body 2-D trajectory is calculated assuming a homogeneous semi-infinite target. From the rigid body loadings, case bending stresses and lateral accelerations are calculated using a very simplified response model.

# DETERMINATION OF EPW CAPABILITY

- Testing
  - Full and 3/4 Scale Davis Gun Tests Into "Quality" Geological Targets
  - Verify Performance Limits

- Calculational Method - SAMPLL
  - Empirically Based (S Numbers)
  - Rigid Body Trajectory Code
  - Assumes Homogeneous Semi-Infinite Targets
  - Simplified Case Bending Stress And Lateral Acceleration Responses

SNLA
NRH:5165, 10/88

# PENETRATOR PERFORMANCE CRITERIA

Four different failure criteria are used to evaluate the survivability envelope of the EPW. The presented criteria are assumed capability limits and actual levels will be determined as the design matures.

The assumed axial deceleration failure criterion is g's peak at the CG and the assumed lateral acceleration limit is g's peak at the aft surface of the EPW. The reason these limits are assumed different is because the axial deceleration spectra will contain more lower frequency modes and these modes contain higher energy levels. A case failure occurs when permanent deformation of the case is visually significant. This is determined calculationally by integrating the stress time history above the yield strength and when this integral exceeds an empirically based value the failure occurs. The minimum velocity requirement guarantees that the EPW will not ricochet out of the target and that it will penetrate to minimum of 1.5 body lengths vertically.

# PENETRATOR PERFORMANCE CRITERIA

## Assumed Baseline Penetrator Capabilities

- **Axial Deceleration Limit**
  **(  Gs Peak @ CG)**

- **Lateral Acceleration Limit**
  **(  Gs Peak @ AFT Surface)**

- **Case Stress Limit**
  **(Significant Bending or Destruction of Case)**

- **Minimum Velocity Requirement**
  **Ricochet (Broach of Target Surface)**
  **Or Vertical Depth (Minimum of 1.5 Body Lengths)**

SNLA
NRH:5165, 10/88

# EPW WEIGHT REDUCTION STUDY

Using the described calculational method and failure criteria, the limits for the baseline 880 lb EPW (defined later) are shown for two different impact conditions. It should be noted that the impact angle is defined from horizontal to the velocity vector and angle of attack is defined from the velocity vector to the EPW centerline (Nose up negative).

For case stress, lateral acceleration, and axial deceleration limits, any velocity greater than indicated will cause a system failure. The EPW must also impact at a velocity greater than defined by the minimum velocity curve. The penetrator survival is defined by a wedge shape region. Lower impact angles and higher angles of attack both reduce the survivability region.

# EPW WEIGHT REDUCTION STUDY

## 880 lb Baseline Design

### -2.0 degrees Angle of Attack

50 degree Impact Angle

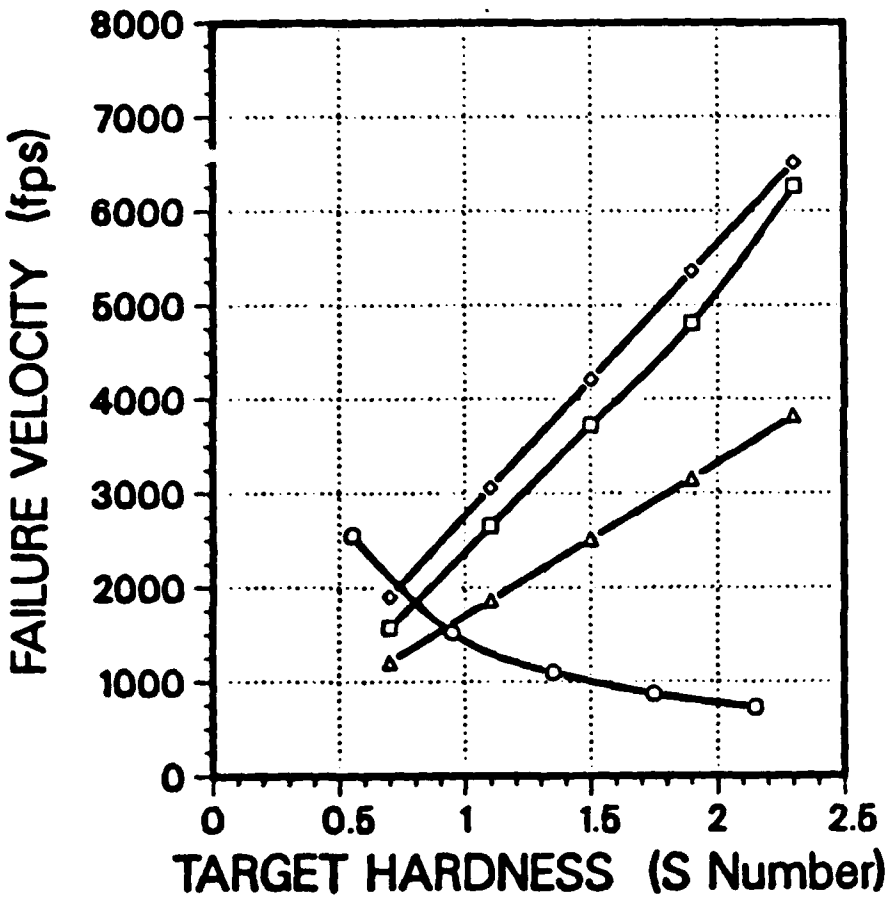


70 degree Impact Angle

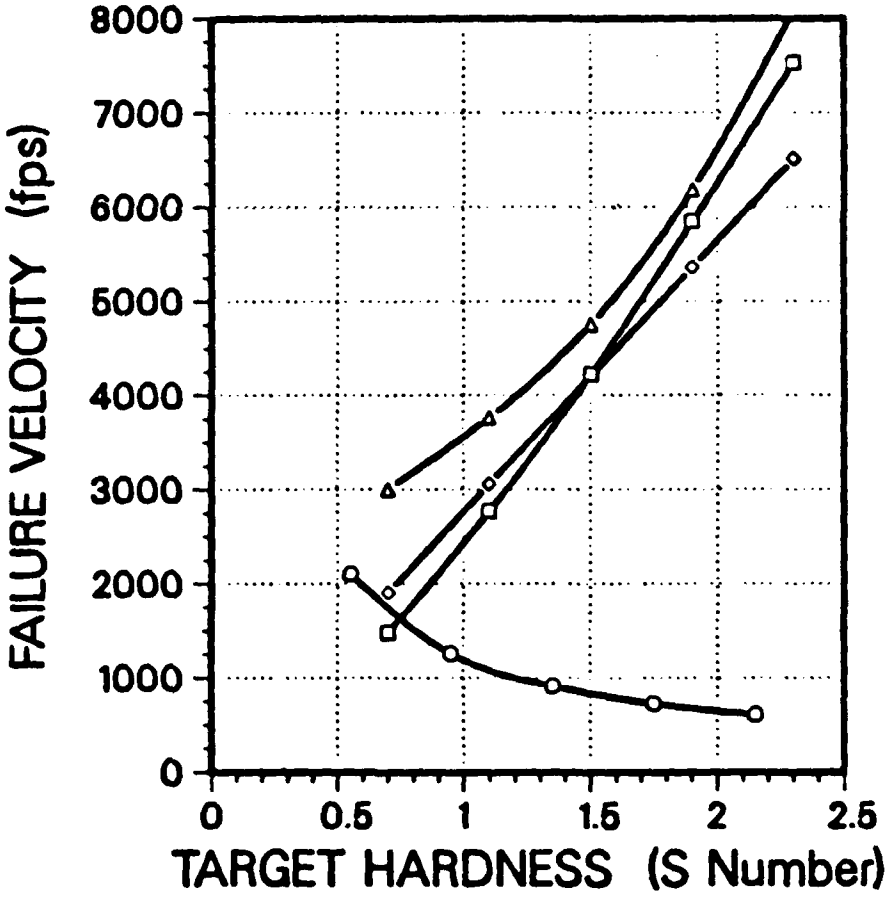


□ — Case Stress Limit ▵ — G Lateral Limit

○ — Minimum Velocity ◇ — G Axial Limit

SNLA

NRH:5165, 10/88

# V-GAMMA PRESENTATION FORMAT

In an effort to reduce the number of curves needed to define the survivabilty envelope of an EPW, an alternate presentation format is introduced. This format plots the composite failure velocity verses impact angle (Gamma) for a fixed angle of attack and target (S Number). Some of the detail is lost, such as which failure criteria is controlling, but the simplified format more graphically shows how the survivability envelope changes with design excursions.

For the remainder of this presentation, the V-Gamma format will be used to define the capability of various EPW designs. A medium (S=1.0) and a low (S=1.8) strength target will be presented throughout. U C S is an abbreviation for Unconfined Compressive Strength.

# V-GAMMA PRESENTATION FORMAT

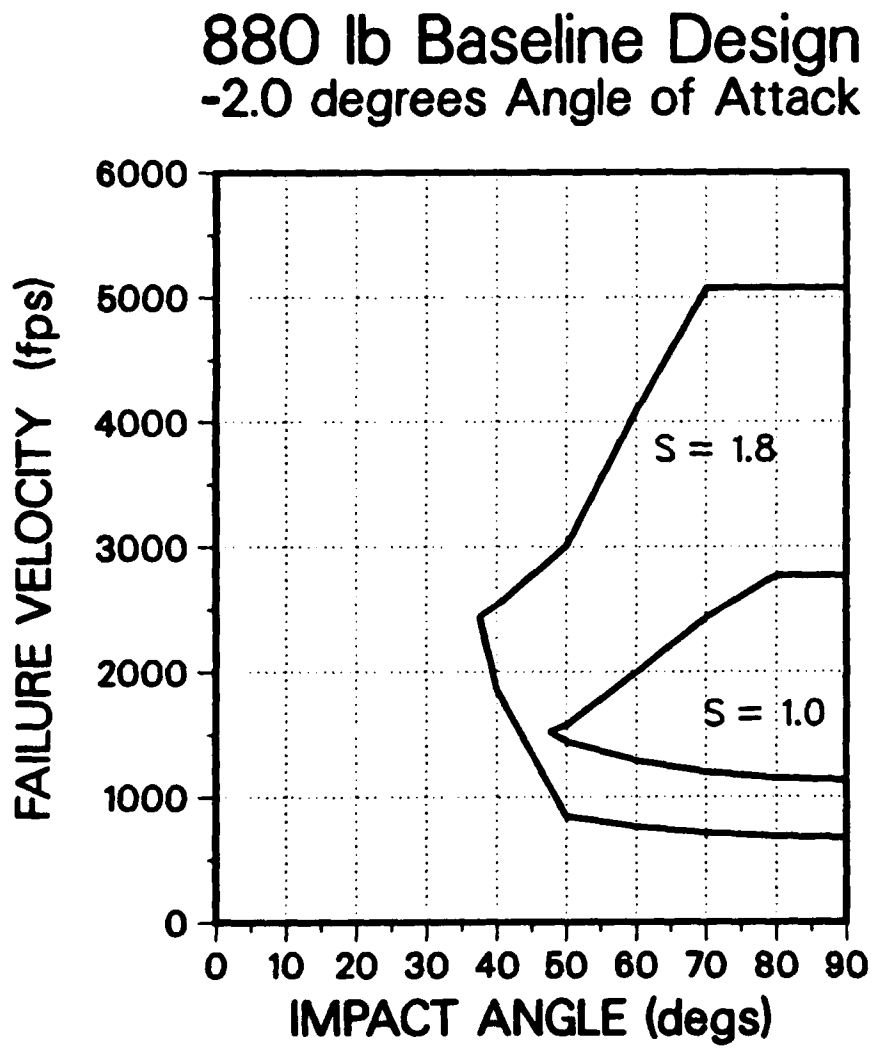


- **Condenses Large Number of Curves to a Simple Format**
- **Some Details Lost (Controlling Failure Criterion)**
- **Two Targets**
  - **Medium Strength Rock**
    - **S = 1.0, U C S = 8 ksi**
  - **Low Strength Rock**
    - **S = 1.8, U C S = 4 ksi**

SNLA
NRH:5165, 10/88

## WHERE CAN WEIGHT BE REMOVED FROM AN EPW?

To determine where weight can be removed from an EPW, let's examine a breakdown of the Baseline system weight. The case weighs 410 lbs, and the warhead (nuclear package plus AF and F) weighs 470 lbs. The AF and F represents such a small portion of the total system weight that no significant weight savings can be realized here. The nuclear package does make up a very significant portion of the total system weight but the removal of any weight here will result in a reduction in nuclear yield and a probable reduction in structural survival limits. Because the nuclear yield should not be sacrificed, the reduction in nuclear package weight will not be considered. Therefore, significant weight savings can only be accomplished by removing weight from the EPW case.

# WHERE CAN WEIGHT BE REMOVED FROM AN EPW?

- **Baseline Penetrator System Weight Breakdown**

| | |
|---|---|
| **Case** | **410** |
| **Warhead** | **470** |
| **Nuclear Package + AF&F** | **___** |
| | **880 lbs.** |

- **Significant Weight Savings Can Only Be Accomplished By Removing Weight From The Case**

SNLA

NRH:5165, 10/88

## SCHEMATIC FOR CASE WEIGHT VARIATIONS

Two methods are schematically represented for removing weight from the EPW case. The first, labeled case geometric variations and represented as moving vertically down on the schematic, is accomplished by removing material from the outside diameter of the EPW case. The case geometric variations will obviously reduce the overall EPW capabilities. The second method, labeled as case material variations and represented as a horizontally right movement on the schematic, is accomplished by changing the baseline case material to a material of either higher strength or lower density. The goal of the case material variations is to determine a material which has an equal case stress failure limit but produces a case of lesser weight.

Examples of these weight variation methods will be presented.

# SCHEMATIC FOR CASE WEIGHT VARIATIONS

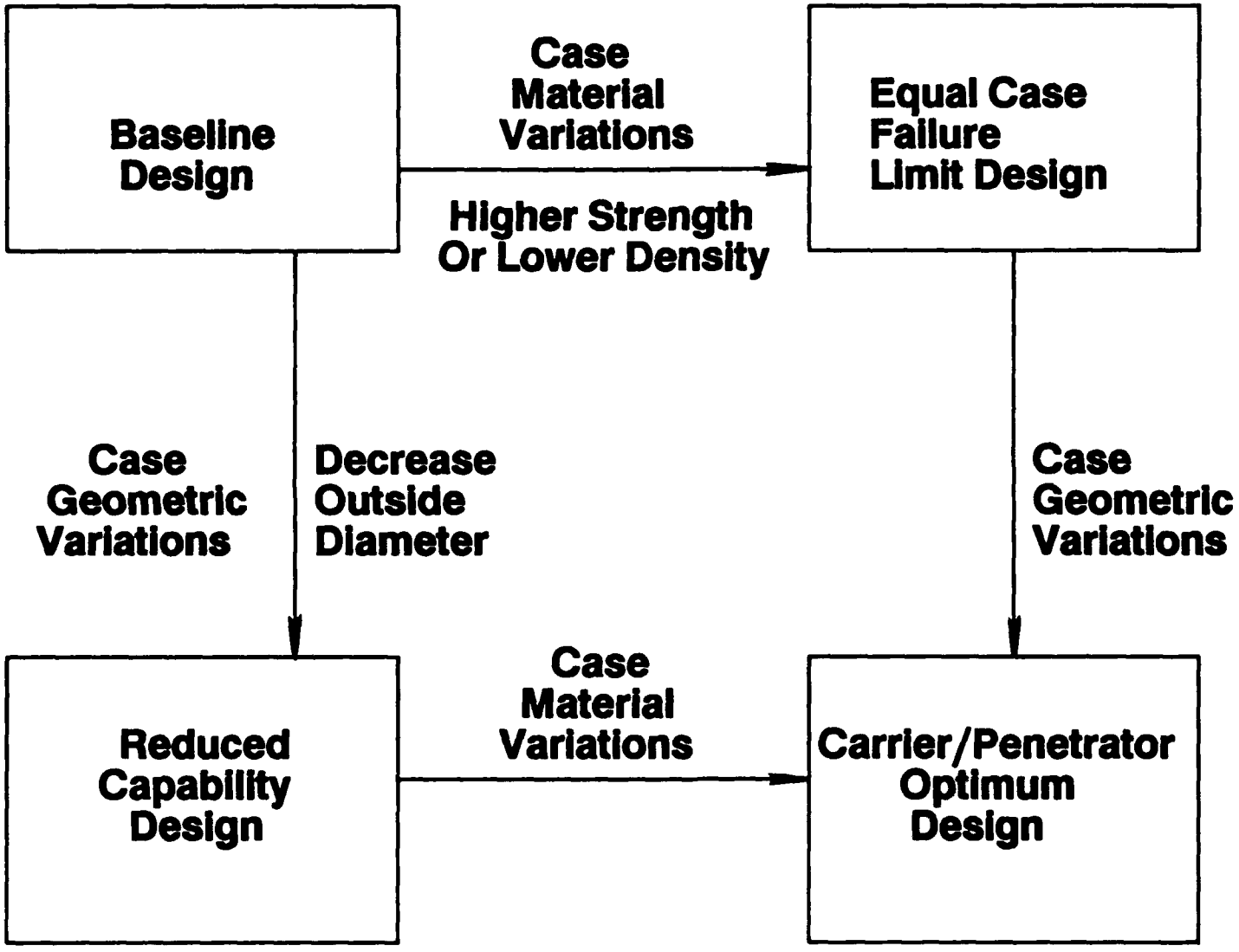


SNLA

NRH:5165, 10/88

# GEOMETRIC VARIATIONS DESIGN SUMMARY

To illustrate how the survivability envelope decreases by geometric case variations, two reduced weight EPW designs are given. Note the corresponding reduction in outside diameters as listed in the table. The unaltered parameters are also given for reference purposes.

# GEOMETRIC VARIATIONS DESIGN SUMMARY

| EPW Weight (lbs.) | Case Weight (lbs.) | Outside Diameter (in.) |
|---|---|---|
| 880 (Baseline) | 410 | 10.75 |
| 750 | 280 | 10.25 |
| 650 | 180 | 9.80 |

**Unaltered Design Parameters:**

- Case Material (HP 9-4-20, 180 ksi)
- Inside Diameter (8.9") and Contour
- WES Weight
- Physic Package Design (Weight)
- Case Length (55.5")
- Nose Shape (3 CRH)

SNLA

NRH:5165, 10/88

# BASELINE VS. 750 LB EPW

The reduction to 750 lbs reduces the operational window by approximately a third as is illustrated in a comparison of V-Gamma maps.

# EPW WEIGHT REDUCTION STUDY

## 880 lb Baseline Design
-2.0 degrees Angle of Attack

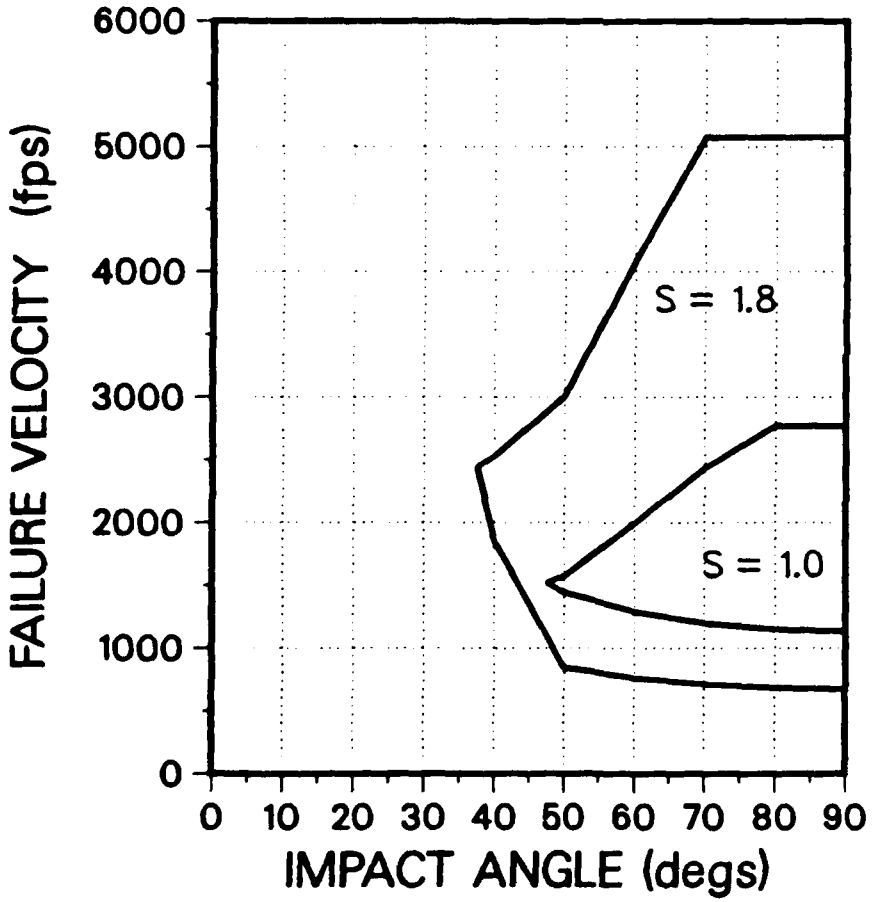


## 750 lb EPW Design
-2.0 degrees Angle of Attack

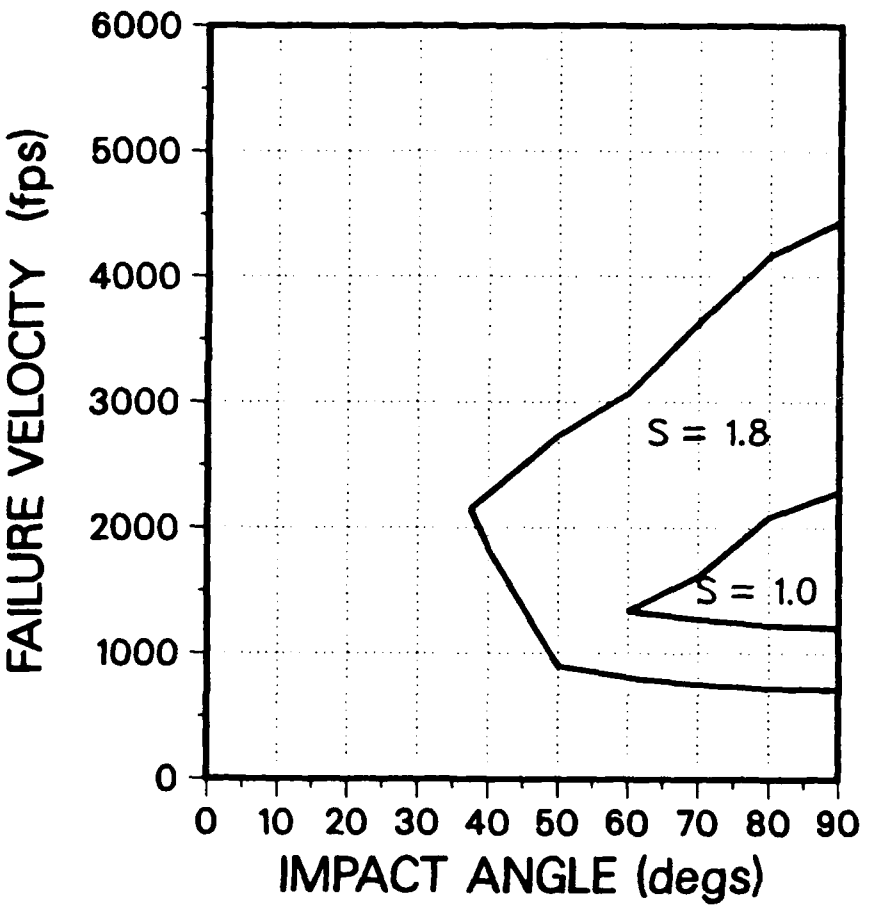


SNLA
NRH:5165, 10/88

# BASELINE VS 650 LB EPW

The reduction to 650 lbs reduces the operational window quite dramatically. The ability to attack medium strength rock targets is almost eliminated.

# EPW WEIGHT REDUCTION STUDY

## 880 lb Baseline Design
-2.0 degrees Angle of Attack

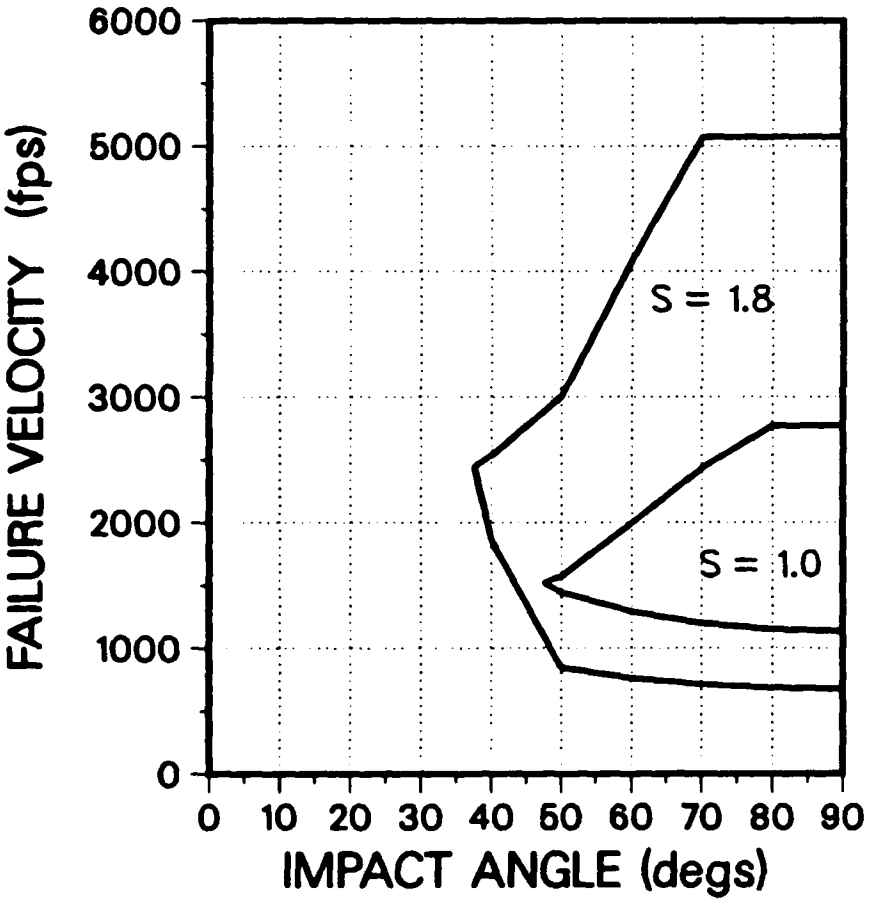


## 650 lb EPW Design
-2.0 degrees Angle of Attack

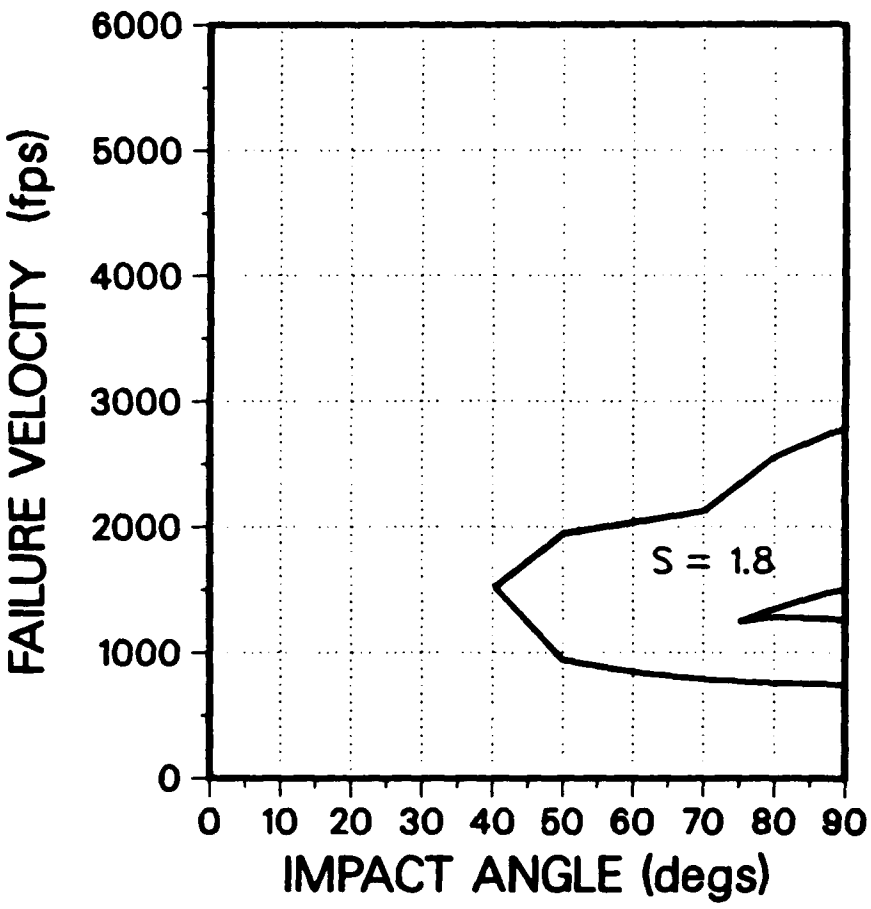


SNLA
NRH:5165, 10/88

# MATERIAL VARIATIONS DESIGN SUMMARY

From past penetrator programs at Sandia. HP 9-4-20 steel evolved as the best steel for penetrator cases due to its high strength and high fracture toughness. For the case material variations three alternate materials were considered in an attempt to produce a lower weight case with equal capability.

Aluminum (7075-T6) was considered for its low density but its low strength produces an equal weight case with inferior capability. Note also the large outside diameter which decreases the penetration depth and increases the decelerations.

For titanium, the alloy of choice is 10-2-3. Based on a ratio of yield strengths and densities it appears that a case of equal capability could be made with a 60 lb weight savings. The lower fracture toughness indicates a possible problem but penetration tests must be conducted to understand the problem. The larger outside diameter also has the same effect on penetration and decelerations as it does for aluminum.

Since the the earlier penetrator programs at Sandia, a new steel alloy (AF1410) has been developed which has higher yield strength and fracture toughness than the baseline HP 9-4-20. A case of equal capability could be made from AF1410 with the same 60 lb weight savings as Titanium. The smaller outside diameter also helps increase penetration and decrease the decelerations

Let's compare the V-Gamma maps for these alternate materials relative to the baseline design.

# MATERIAL VARIATIONS DESIGN SUMMARY

| | Material Spec. | Yield Strength (ksi) | Fracture Tough. (ksi$\sqrt{in}$) | Density (lb/in$^3$) | EPW Weight (lb) | Outside Diameter (in) | Length (in) | Comments |
|---|---|---|---|---|---|---|---|---|
| Baseline (HP 9-4-20) | AMS 6525 | 185 | 135 | .283 | 880 | 10.75 | 55.5 | Evolved From Past Programs |
| Aluminum (7075-T6) | QQ-A -367 | 65 | 50 | .098 | 880 | 13.7 | 61.2 | Shown For Completeness |
| Titanium (10-2-3) | AMS 4987 | 135 | 80 | .164 | 820 | 11.6 | 56.3 | Anisotropic Properties |
| New Steel AF1410 | AMS 6527 | 225 | 140 | .283 | 820 | 10.5 | 55.5 | Relatively New Material |

SNLA

NRH:5165, 10/88

# BASELINE VS ALUMINUM

As stated, the aluminum design is a significant reduction in capability relative to baseline. This is due to the increased diameter along with its inferior case strength.

# EPW WEIGHT REDUCTION STUDY

## 880 lb Baseline Design
-2.0 degrees Angle of Attack

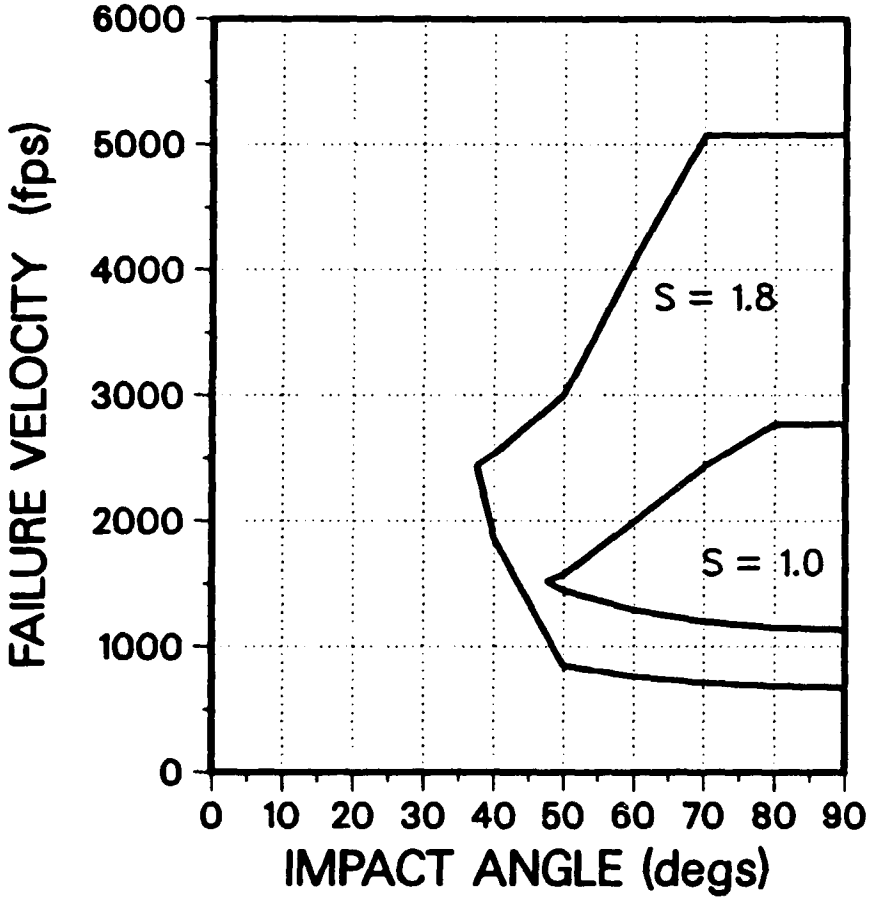


## 880 lb Aluminum EPW Design
-2.0 degrees Angle of Attack

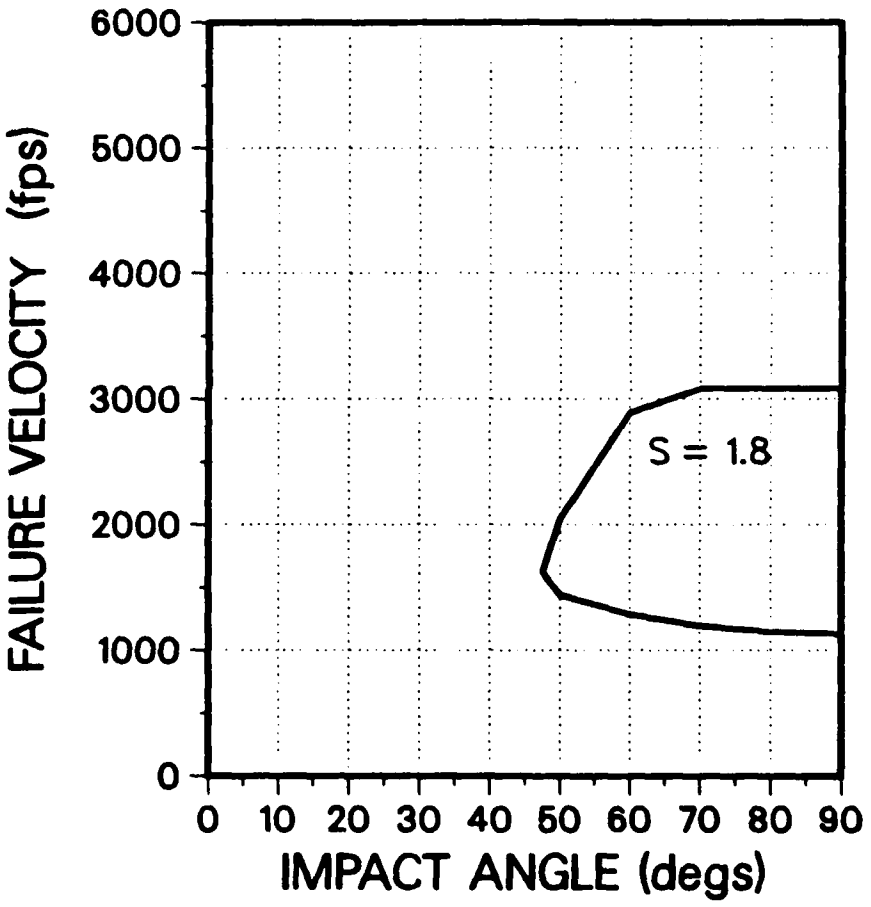


SNLA
NRH:5165, 10/88

# BASELINE VS TITANIUM

Although the titanium case is of equal capability based on yield strength, the operational window is still reduced because the increased outside diameter increases the deceleration levels for the same impact conditions. This window is of approximately the same size as the thinned down 750 lb HP 9-4-20 steel case design presented earlier.

# EPW WEIGHT REDUCTION STUDY

## 880 lb Baseline Design
-2.0 degrees Angle of Attack

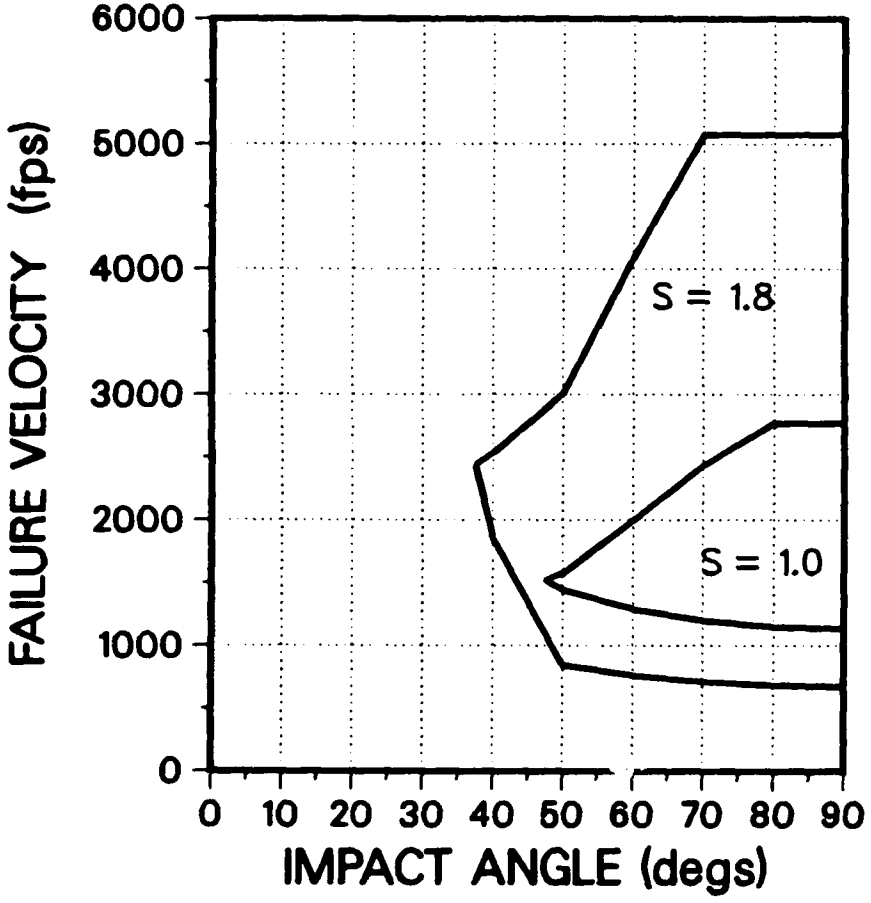


## 820 lb Titanium EPW Design
-2.0 degrees Angle of Attack

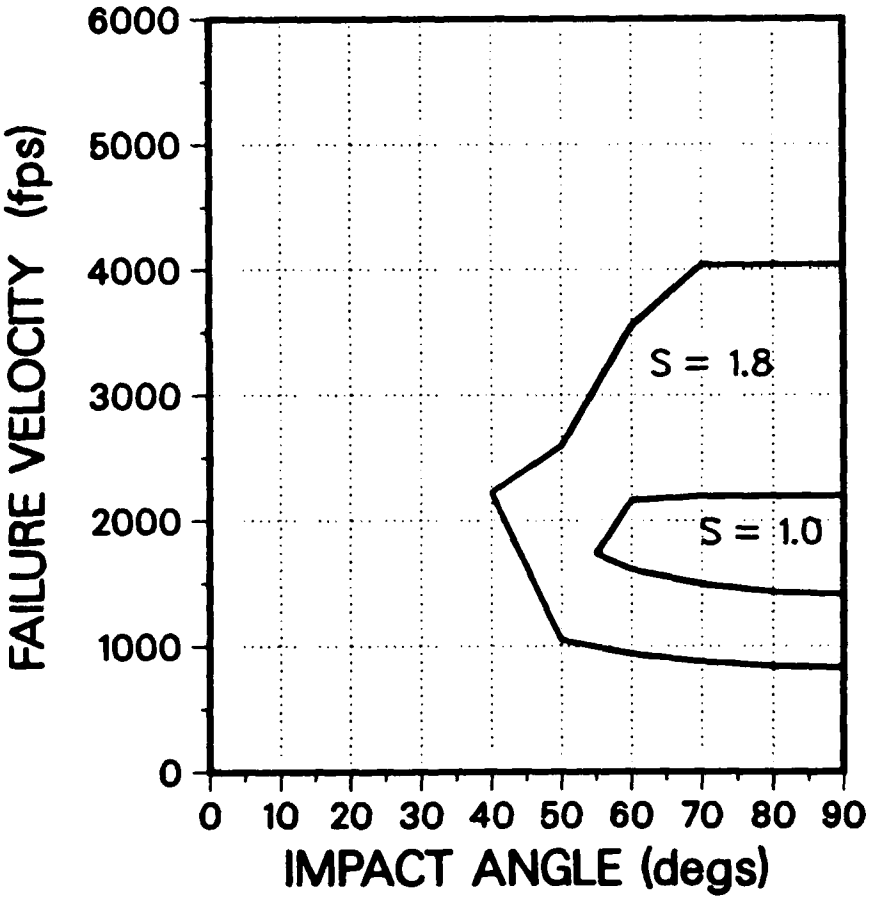


SNLA
NRH:5165, 10/88

# BASELINE VS AF1410 STEEL

The case made of the higher strength AF1410 steel appears to provide an equivalent operational window to the baseline design with a 60 lb weight savings. The decreased loading caused by the smaller diameter is counterbalanced by the reduced weight which causes the deceleration levels to increase.

# EPW WEIGHT REDUCTION STUDY

## 880 lb Baseline Design
-2.0 degrees Angle of Attack

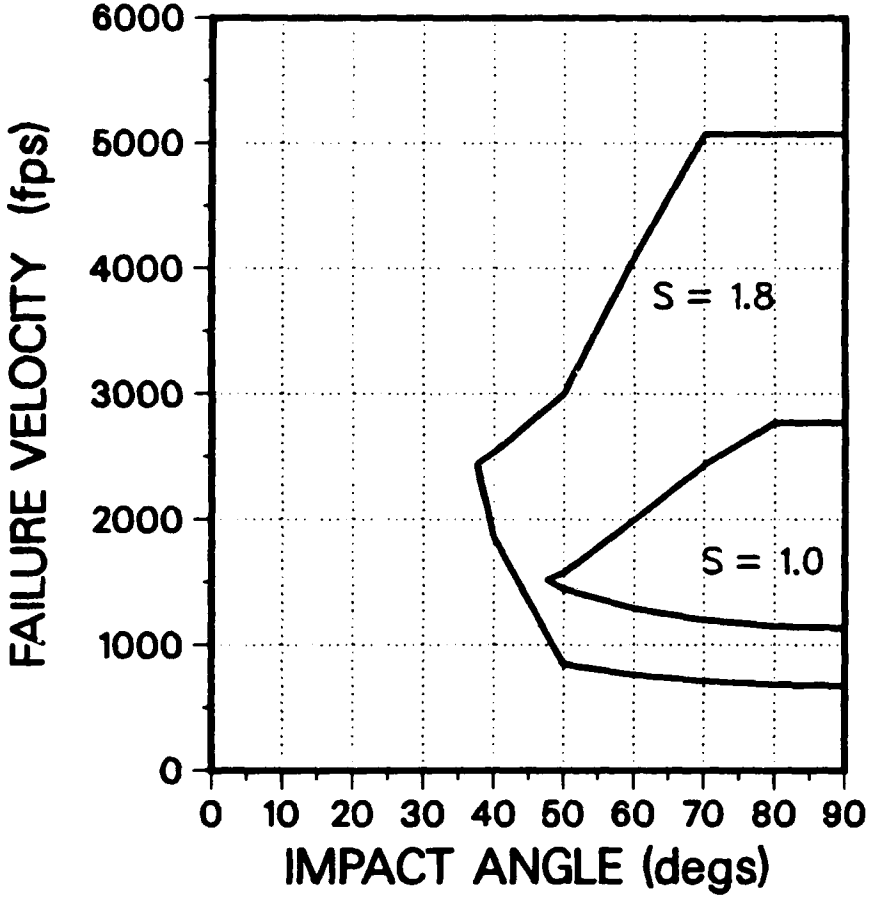


## 820 lb AF1410 Steel EPW Design
-2.0 degrees Angle of Attack

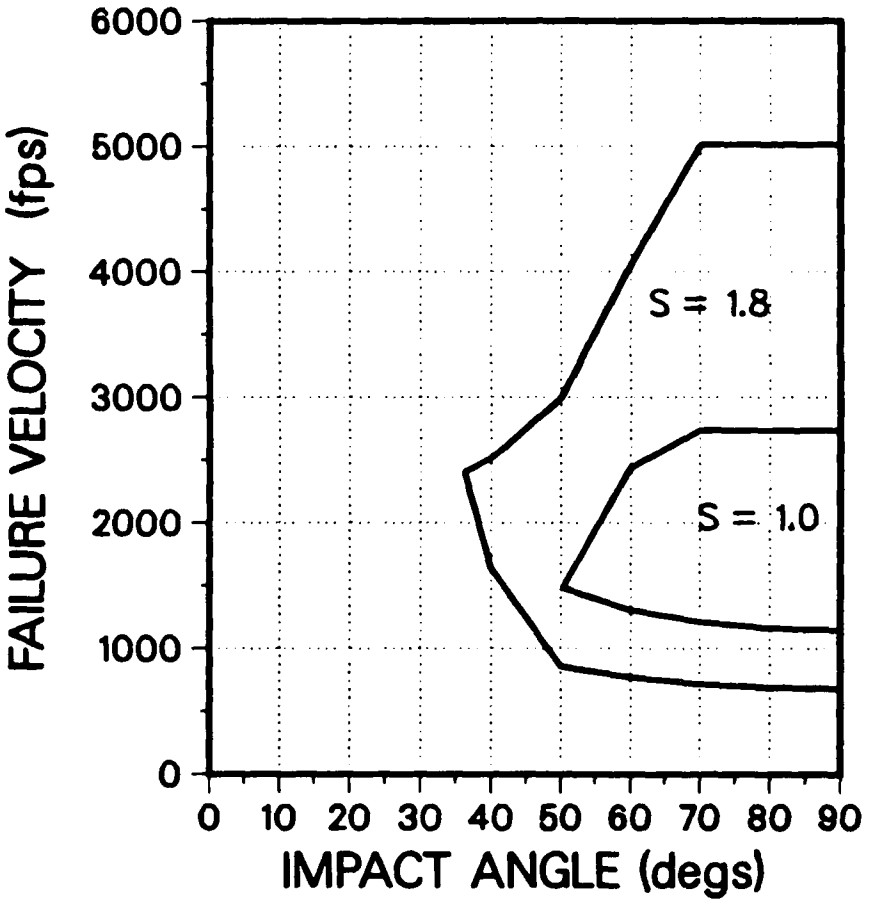


SNLA
NRH:5165, 10/88

# MATERIAL VARIATIONS TEST PLAN

As stated earlier capability is determined by a combination of testing and calculations. An alternate case material test series was conducted to verify the results of the presented calculations.

The goal of the material variations tests is determine which if any is the optimum penetrator candidate material for reducing weight while maintaining capabilities.

A 3/4 scale model of each of the designs was tested at the same impact conditions of 2400 fps, 50 degree impact angle, 0 degree angle of attack into a medium strength rock. This impact condition is very close to the case failure limit for the baseline and equivalent designs.

# MATERIAL VARIATIONS TEST PLAN

- Goal is to Filter the Candidate Alloys To Determine Best Case Material

- Same Impact Condition for Each Material:

  3/4 Scale Models
  2400 fps
  50° Impact Angle
  0° Angle of Attack
  Medium Strength Rock

- Calculationally Close to Case Failure

SNLA
NRH:5165, 10/88

# MATERIAL VARIATIONS TEST RESULTS

Before we considered a material variations test plan, a test had been conducted using an E4340 steel penetrator case which resulted in a bent case. Those test parameters were used as the benchmark for further testing and are defined under Test 1. From past experience, HP 9-4-20 out performs E4340, therefore we assumed that a test with HP 9-4-20 would have been no worse than the Test 1 results.

An unfortunate occurrence that makes direct comparison of test results difficult, is that sometime between Tests 2 and 3 the baseline design evolved from a MOD I to a MOD III design which has a different internal contour. Therefore, only test results of the same MOD design should be directly compared.

Test 2 was of the aluminum case and resulted in a catastrophic failure of the penetrator. approximately 50 pieces were located which amounted to less than 20 percent of the total weight. This was a MOD I design which can be directly compared to the Test 1 results.

Test 3 was of the titanium and the new MOD III design. The case broke into approximately 5 pieces, which were all located.

Test 4 was of the AF1410 steel and the MOD III design which can be directly compared with Test 3 results. The AF1410 steel case cracked circumferentially approximately 180 degrees. This result implies that the AF1410 steel case is better than the titanium case. The difference may be attributed to the superior mechanical properties of the AF1410, specifically the fracture toughness.

# MATERIAL VARIATIONS TEST RESULTS

**Test 1:** MOD I Design E4340 Steel Case
(From Past Experience HP 9-4-20 Out Performs E4340)
900 lb. Full Scale Equivalent Weight

Result: Bent Case

**Test 2:** MOD I Design 7075-T6 Aluminum Case
Designed to be Equal Weight but Calculations Showed Inferior Capability
900 lb. Full Scale Equivalent Weight

Result: Catastrophic Failure
(Disintegrated)

**Test 3:** MOD III Design 10-2-3 Titanium Case
820 Full Scale Equivalent Weight

Result: Broken Case (~5 Parts)

**Test 4:** MOD III Design AF1410 Steel Case
820 Full Scale Equivalent Weight

Result: Bent And Cracked Case

SNLA
NRH:5165, 10/88

# TEST RESULTS PHOTOGRAPHS

Shown are photographs of the results presented from the previous chart. Of special interest are the aluminum and titanium results. The aluminum failed so catastrophically that only a small percentage of the total case could be located following the test. The parts were scattered up to 1.5 miles form the impact point. The titanium case, although it did also break into parts, was all located near the impact point.

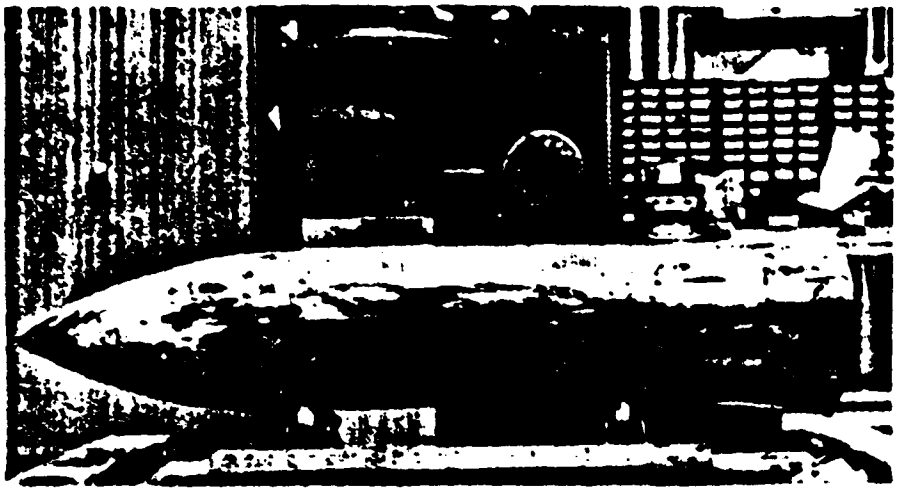

TEST 1 (E4340)

TEST 2 (Al 7075-T6)

TEST 3 (TI 10-2-3)

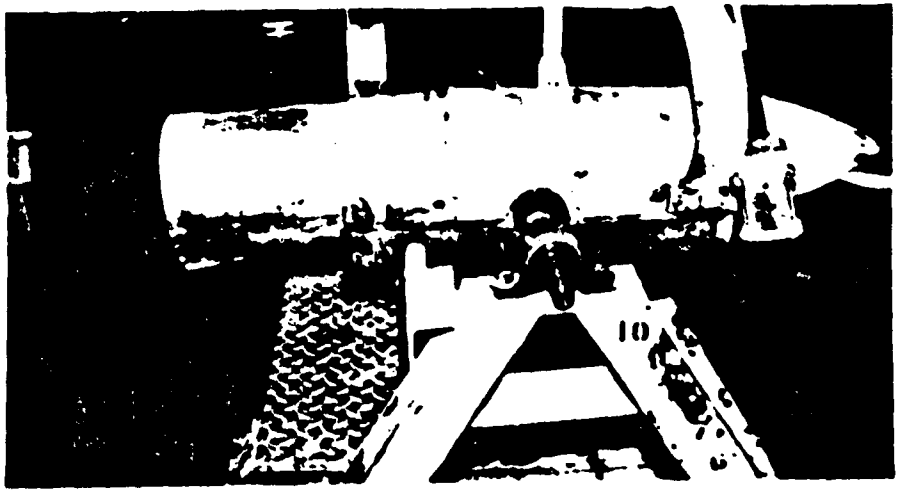

TEST 4 (AF1410)

SNLA

NRH:5165, 10/88

## MATERIAL VARIATIONS TEST CONCLUSIONS

As a result of the material variations test conducted to this point, aluminum has been completely eliminated as a viable weight reduction candidate for EPW designs. It also appears that AF1410 steel is better than the 10-2-3 titanium tested and no further testing of titanium will be done. AF1410 has not been eliminated as a weight reduction candidate and further testing is merited.

# MATERIAL VARIATIONS TEST CONCLUSIONS

- Aluminum Has Been Eliminated as a Viable Weight Reduction Candidate
- AF1410 Appears to be a Better Weight Reduction Candidate than Titanium
- Further Testing of AF1410 is Merited

SNLA

NRH:5165, 10/88

# EPW WEIGHT REDUCTION SUMMARY

In summary,strictly removing case material from the baseline EPW design tends to degrade the penetrator capabilities. Also, AF1410 steel appears to be the best alternate case material available for reducing case weight while maintaining EPW system capabilities. When the time comes to evaluate the tradeoffs between EPW capabilities and delivery system capabilities, using the best case material, as determined in the case material variations analysis, as the starting point for removing case material tends to maximize the weight savings and minimize the reduction of penetrator capability.

# EPW WEIGHT REDUCTION SUMMARY

- **Strictly Removing Case Material as a Weight Reduction Scheme Degrades Penetrator Capabilities**
- **AF1410 Steel Appears to be the Best Candidate to Reduce Case Weight While Maintaining Capabilities**
- **Using The Best Case Material as a Starting Point for Removing Weight from the Case Tends to Maximize the Weight Savings and Minimize the Reduction of Penetrator Capability**

SNLA

NRH:5165, 10/88

# WEIGHT REDUCTION EFFECTS ON EARTH PENETRATING WEAPON CAPABILITIES (U)

Portrait and Landscape PRESTIGE ELITE fonts are ready for use with MASS-11:

Printer ID: 21 ELITE

Fonts:

| | |
|---|---|
| 1 | Prestige Elite 12 pitch Regular and Bold |
| 2 | Prestige Elite 12 pitch Italic |
| 3 | Prestige 16.66 pitch Regular |

To print Sandia memohead or letterhead automatically, embed the command

FILE=MEMO.SNL
or
FILE=LETTER.SNL

as appropriate, on the first line of your document. Enclose the command in angle brackets; end the line with a hard return.

# ATTACKING STRATEGIC RELOCATABLE TARGETS: AN ARTIFICIAL INTELLIGENCE APPROACH

H. W. Edgorf
Los Alamos National Laboratory
Los Alamos, NM

J. S. Denelsbeck
Strategic Air Command Liaison Office
Los Alamos National Laboratory
Los Alamos, NM

## Introduction

Strategic Relocatable Targets (SRT) represent a significant problem to strategic target planners. Operational concepts that heretofore were adequate to hold fixed targets at risk are no longer valid. The problem is now a multidimensional one that forces inclusion of timely, accurate $C^3I$ in any technical solution to the relocatable problem. $C^3I$ is essential for accurate tracking, cuing, and attacking SRTs such as the rail mobile SS-24 and road mobile SS-25. The integration of $C^3I$ and weapon systems acting in concert with National Security Policy lends itself to the application of artificial intelligence methods. A knowledge engineering environment allows the rapid prototyping of new capabilities in arenas of interest including policy, decision processes, sensors, weapon systems, or warhead and effects. To effectively determine both optimal and sub-optimal solutions to the problem, evaluations of system capability must be made in the context of tactics, standard and non-standard weapon effects, targeting methodology and $C^3I$ integration. The Strategic Engagement Analysis Tool (SEAT) is a model that performs such an integration.

## Background

In examining the multi-dimensional environment of the relocatable target problem, one must consider the integration of technology, doctrine, and tactics with an order of battle.

SEAT is a simulation of a number of different, interacting systems in the strategic warfare arena. The SEAT model includes representations of strategic relocatable missile launchers, target acquisition systems, air defense systems, offensive attack systems such as ICBMs and manned bombers, and the associated Command and Control Systems.

Traditionally, military simulations have focused on physical process representations such as weapons effects. SEAT attempts to balance this with explicit representations of $C^3$ and decision-making processes. Our attempt to enhance the behavioral and decision making aspects of military simulations brings with it a set of unique challenges. We meet these challenges by blending traditional software engineering methodologies with an advanced computing development environment that includes tools and techniques developed by the Artificial Intelligence Community. This paper addresses some of the distinctions and advantages of our approach to simulations in the context of the SEAT development.

The simulation presented in this paper was implemented using Common Lisp, Common Windows, and KEE* running on a Symbolics** 3600. SEAT also incorporates existing modules which have been written in procedural languages such as FORTRAN. KEE is an expert system shell based upon a frame system that provides a variety of modern programming paradigms.

## Model Requirements

SEAT is designed to assist in the determination of which factors can affect combat involving systems that employ $C^3$ and decision-making as well as the more normally modeled physical aspects of the objects under analysis. The requirements of such a system include those normally associated with large simulation models, as well as some new requirements associated with the $C^3$ representations.

1. SEAT allows modeling $C^3$ and decision-making activities of organizations associated with the SRT problem in a form that is intuitive to the analyst. The analysis to be performed with SEAT will often deal with the $C^3$ representations more than the physical process representations. We attempt to make these $C^3$ representations explicit and easy to access by the analyst rather than burying such representations in the model's computer code.

2. SEAT is flexible from the viewpoint of the analyst in allowing different configurations and scenarios to be used with SEAT.

*KEE is a trademark of Intellicorp, Mountain View, CA.

**Symbolics is a trademark of Symbolics Inc., Cambridge, MA.

3. SEAT also provides the normal statistics, history, pre- and post-processors, etc., provided by simulation models used for analysis of physical systems.

## Software Engineering

The software engineering used in SEAT and the design of the SEAT analysis tool have been driven primarily by the model considerations just discussed. These considerations have led to a design with the following major characteristics:

1. An Actor-based specification technique is used. This technique characterizes each object upon which analysis is to be performed as an Actor. Each Actor in the simulation has both physical capabilities (as are normally modeled in a more traditional simulation systems) and cognitive capabilities that represent the decision-making and associated $C^3$ capabilities of the object.

2. An Object-Oriented design technique is used that characterizes the exercise of any capability of an Actor as an event associated with an object representing that Actor. The events representing the exercise of a physical capability of an Actor are methods of the associated object usually written in a procedural programming language (Lisp and FORTRAN in the case of SEAT). The events representing the exercise of a cognitive capability of an Actor are methods of the associated object usually written using a forward-chaining rule system.

The use of the forward-chaining rule system to represent the decision-making and $C^3$ capabilities of the Actor provides an explicit representation of these decision-making processes.

## The Actors of SEAT

SEAT is an Object-Oriented model that makes use of multiple inheritance to define the behavior of actors in the simulation.

The structure of SEAT is a directed graph of classes with a distinguished root node called SEAT-Objects. The classes farther along the graph inherit characteristics and abilities from those classes earlier in the graph, and may specialize or augment those characteristics and abilities to create more specialized sub-classes.

An analyst creates a scenario for a SEAT analysis task by indicating that specific instances of these classes will be created with specific initial values. These instances then represent the actors with whom the simulation operates.

An example of this is the creation of two different sorts of aircraft to participate in a simulation task. The first will represent a reconnaissance aircraft with flight characteristics similar to an SR-71 and a Synthetic-Aperture-Radar (SAR). The second will represent an attack bomber similar to a B-1, with the same SAR as the SR-71 reconnaissance aircraft and four SRAMs. The B-1 will also include the capability for a crewman to visually sight targets in addition to whatever the SAR sees.

These two actors involve several different classes of objects. (The classes listed here are those used for this example. SEAT contains many more classes of objects than those listed here.)

1. Aircraft in SEAT are objects that follow flight plans provided by the analyst. This class provides the basic simulation event procedure that steps the aircraft along its flight plan.

   This class is specialized in two areas. Different aircraft performance characteristics can be provided by different subclasses. This might be used to provide subclasses B-1b and SR-71 with the two example actors above each being an instance of its special class. (Aircraft performance characteristics are similar enough that this is often not done. It is sufficient for the analyst to provide different operational parameters such as speed, fuel use, etc. to the single class Aircraft.) This is illustrated in Fig. 1.

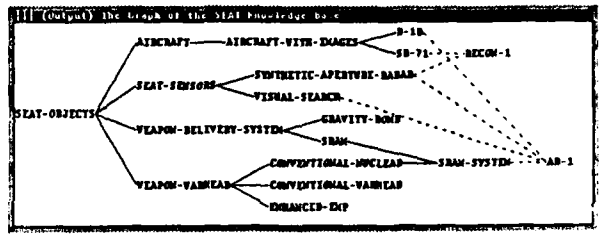


Fig. 1.

   A different specialization is used to perform housekeeping chores for the simulation. For example, those aircraft that wish to be seen on a graphic display can be made an instance of the class Aircraft-With-Images rather than the class Aircraft. Aircraft-With-Images is a subclass of Aircraft that provides an appropriate graphic image, and specializes the behavior of the basic simulation step of the aircraft to include moving the graphic image on the display as needed.

2. Sensors in SEAT are objects that provide the ability for a SEAT actor to detect other SEAT actors. This class is specialized into subclasses that provide different types of area coverage, different detection probabilities, and other operational parameter differences.

3. Weapon Systems in SEAT are objects that provide the combined functionality of a Weapon-Delivery-System object and one or more Weapon-Warhead objects.

   The Weapon-Delivery-System object provides the policy regarding use of that weapon system, and the events for the simulation that deliver the associated Weapon-Warhead to its

detonation location. Weapon-Delivery-System objects range from simple gravity bombs (that must be released at the detonation location) that fall for a period of time and then detonate, to SRAMs and cruise missiles that have relatively complex behavior independent of the launching aircraft.

The Weapon-Warhead object provides a weapon effects algorithm used when the delivery system has delivered the warhead to its detonation point.

In order to construct a Reconnaissance Aircraft actor, the analyst creates an instance that is a member of the SR-71 and SAR-sensor classes. The aircraft will follow the analyst's provided flight plan and the associated sensor will detect potential targets according to the sensor's capabilities, and cause the reporting of sensor detections to a central $C^3$ actor.

To construct the Armed Recce actor, an object is constructed in a similar way to the Reconnaissance Aircraft actor with the addition of membership in a Sensor class that represents a crew member looking out of the aircraft, and the addition of membership in the class of SRAMs with a nuclear warhead. Making the actor an instance of the weapon system class causes the basic simulation step event of the aircraft to be modified with decision-making procedures regarding the use of that weapon system against detected targets. Such behavior modification is automatic, and requires no assistance by a programmer to the analyst.

Policy, Decision-Making, and $C^3$ in SEAT

A major characteristic of SEAT is its treatment of decision-making and $C^3$. Objects in SEAT can explicitly represent a doctrine or policy set and make decisions based upon that policy. This decision-making process is represented using a Forward-Chaining rule system.

An example of the use of this decision-making representation is given using the two aircraft actors described above.

The Reconnaissance Aircraft actor detects a potential target during one of its step events. An event is created for the controlling $C^3$ actor representing the receipt of a message from the Reconnaissance Aircraft actor.

The receipt of the message causes the rule system to examine the perceptions of the $C^3$ actor regarding targets and attacking systems. This decision-making procedure may cause the controlling $C^3$ to schedule a new event for an Armed Recce actor in the region of the perceived target directing that actor to attack the target.

The receipt of that message by the Armed Recce aircraft causes a modification of the aircraft's flight plan (initially provided by the analyst via scenario description) to enter an attack mode, fly to an appropriate release point, and attack the target.

At the end of this modified flight segment, the target is attacked, and the aircraft communicates the results of the attack to the controlling $C^3$ by way of posting an event for that actor so that the $C^3$ actor can update its perceptions and continue the cycle.

This sort of explicit representation of the $C^3$ and Decision-Making has several benefits.

1. The main benefit is a rather subtle but pervasive change in the way a simulation is designed. Many existing simulation designs put an emphasis on the physical activities in the situation being modeled. Representation of $C^3$ and Decision-Making is added at a late stage of the design as decisions in the procedural code representing the physical activities in the situation.

   An early split between physical and cognitive capabilities of an actor in the simulation encourages the simulation designer to make a distinction between the perceived state of a situation as viewed by the actor and the actual, or ground truth, situation that is the reality of the situation at that moment. It is this clear distinction between the physical reality and the perception that forms the basis of the modeling of $C^3$ and decision-making in SEAT.

2. The emphasis on physical activities in the situation being modeled leads to a sequence of events of the form Physical-event-1→Physical-event-2→...→Physical-event-n. The ability to model cognitive processes as well as physical processes leads to a refined picture of an activity that includes an initial assessment of the current situation (based on the perceived situation) followed by the physical activity decided upon (based on the actual; or ground truth, state) followed by another assessment. This sequence of decide what to do, do it, assess the results of your actions repeats throughout the simulation, with the assessment at the end of one activity usually connected with the decision on the next thing to do. This leads to an event sequence of the form Assessment-and-decision-event-1→Physical-event-1→Assessment-and-decision-event-2→Physical-event-2→...→Physical-event-n.

3. The split between cognitive and physical activities assists the designer in building $C^3$ representations into the model. Each actor builds perceptions based on what it can determine about the situation, and acts on those perceptions. The $C^3$ structure of the system under study is naturally built as the major factor affecting the perceptions of some of the actors.

4. The existence of a forward-chaining rule system provides a natural tool for the description and implementation of the

cognitive activities in the simulation. The benefits of the use of such a system are that the policy of the situation becomes an explicit object rather than an artifact of the flow of control within some program, and that such an explicit object becomes another target upon which analysis can be performed. Many existing and planned analysis tasks for SEAT involve modeling of effects of changes to the $C^3$ and decision-making aspects of the situation rather than the effects of changes to the physical characteristics of the actors.

## Model Outputs

SEAT provides two main interactions with the analyst. The construction of the system with an object-oriented design allows easy integration of graphics which provide near real-time visualization of the systems under analysis. Also, the system produces a history trace of all events executed by the system along with statistics generation detailing the behavior of the systems under test. These history mechanisms allow a variety of post-processors to be used for data reduction and report generation.

## Analysis Capabilities

The model as currently structured permits the evaluation of the search and attack scenarios for holding SRTs at risk. We model the search, identification, reporting, and strike phases of the mission. This is all accomplished in an air defense environment that can be varied in both quality and quantity.

For the example analysis, given as part of this paper. The altitude, speed, sensor suites, and search patterns were varied to determine the optimum search mode. The following represents the variation in parameters used in this sample analysis.

Armed Reconnaissance Aircraft (air speed 800 km/hr):

Search Patterns:

1) Geometric,

2) Probable SRT deployment areas with cueing.

Altitudes:

1) 200 meters

2) 500 meters

3) 800 meters.

Sensors:

radar

1) 1 in. 25 slope

2) 1 in. 50 slope

3) 1 in. 75 slope.

Air Defense systems (ground based):

search radar--

1) 1 in. 25 slope

2) 1 in. 50 slope

3) 1 in. 75 slope.

Both the probability of detecting the SRT and the probability of surviving to strike the target are indicated for three altitude regimes.

TABLE I.

| PATTERN: CUED | ALTITUDE | | |
|---|---|---|---|
| | 200 | 500 | 800 |
| Sensor A | 1.31 | 1.31 | 3.92 |
| Sensor B | 1.31 | --- | 6.52 |
| Sensor C | 2.61 | 6.52 | 9.14 |
| **PATTERN: GEOMETRIC** | | | |
| | 200 | 500 | 800 |
| Sensor A | --- | 0.72 | 0.72 |
| Sensor B | -0- | 2.17 | 5.88 |
| Sensor C | 0.72 | 5.07 | 11.02 |

Valves shown are # contacts/hour

Summary:

The cued search yielded a higher number of contacts on the brigade in all cases with the exception of Sencor C at 800 meters. The exception in this case is due to the extremely large viewing area. At this sensor-altitude combination. While this analysis remains rudimentary in nature, the flexibility of the model has been demonstrated.

## Future Directions

SEAT was initially implemented as a proof of concept prototype incorporating all of the aspects discussed. This prototype was successful in demonstrating the feasibility of both the utility of the model (even in its prototype/demonstration form) and the power of the $C^3$ representations used.

SEAT is currently being re-implemented as a production analysis tool with additional emphasis on the reliability, maintainability, and corrections of its operation. Major elements to be added are:

1. Different mobile targets. The prototype and the initial production version of SEAT only model SS-24s on a rail network. Target systems such as SS-25s on road networks are being added.

2. Additional sensing capabilities. The prototype includes only simple sensor capabilities. The production version will include much more accurate and specific models of sensing devices.

3. Expanded and enhanced air defense systems, environments, and capabilities.

4. Enhanced terrain and environmental representations. The prototype employs a simple node and edge representation of the target rail network. An enhanced terrain representation is being incorporated into the production model to allow other environmental conditions such as trees, elevation, smoke, dust, weather, and cloud conditions.

5. Additional environmental aspects such as generators for background rail traffic, and the associated cognitive capabilities required to characterize SRT targets.

6. Additional $C^3$ aspects. The structure for $C^3$ is in place, but details will be added over time. Of particular interest is the use of additional operational information regarding the deployment and employment of the mobile targets as such information becomes available, and the addition of a more detailed model of the $C^3$ structure, the SRT system and of the Soviet air defense system.

## Summary

SEAT provides the capability to perform sensitivity analysis. Dynamic creation of actors and easy scenario specification facilitate this requirement. The actor's physical and cognitive capabilities as well as the number and type of actors can vary with simulation runs; thus, providing an extremely flexible analytical tool and analysis environment. By explicitly modeling both physical and cognitive capabilities, the real world system is more accurately portrayed within the simulation.

We view SEAT as the first step in developing a library of objects (e.g., planes, sensors, weapons, etc.) which can be reused as necessary in future simulation developments. It is easy to visualize a reconnaissance plane in SEAT, modeled as an object, which could be reused in a simulation of the conventional battlefield in Europe. The capability provided by advanced computing environments such as KEE to create and modify objects, encapsulate the object's capabilities and data structure in the object definition, and to confine the interface with the object to a well-defined protocal provided by the object oriented system forms a solid foundation for our simulation developments. Our ultimate goal is to be able to respond quickly to analysis needs by tailoring new simulations quickly to the analysis task at hand. Libraries of reuseable objects are essential to our capability to do this.